PULLOUT BEHAVIOR OF HORIZONTAL SQUARE PLATE ANCHOR IN REINFORCED CLAY

THESIS SUBMITTED IN PARTIAL FULFILLMENT

FOR THE AWARD OF THE DEGREE

Of

MASTER OF CIVIL ENGINEERING

In

SOIL MECHANICS AND FOUNDATION ENGINEERING

By

RATUL ROY

*UNIVERSITY REGD. NO. –**140639 of 2017-18***

*CLASS ROLL NO. **-001710402012***

*EXAM ROLL NO. –**M4CIV19016***

Under The guidance of

Dr. Sibapriya Mukherjee
Professor
Civil Engg Dept.
Jadavpur University

Dr. Sumit Kumar Biswas
Associate Professor
Civil Engg Dept.
Jadavpur University

Dr. Pritam Aitch
Associate Professor
Civil Engg Dept.
Jadavpur University

JADAVPUR UNIVERSITY
CIVIL ENGINEERING DEPARTMENT
MAY 2019

JADAVPUR UNIVERSITY

FACULTY OF ENGINEERING AND TECHNOLOGY

DEPARTMENT OF CIVIL ENGINEERING

MAY, 2019

DECLARATION OF ORIGINALITY AND COMPLIANCE OF ACADEMIC ETHICS

I hereby declare that this thesis contains literature survey and original research works by the undersigned candidate, as part of his Master of Civil Engineering in Soil Mechanics & Foundation Engineering studies.

All the information in this document have been obtained and presented in accordance with academic rules and ethical conduct.

I also declare that, as required by these rules and conduct, I have fully cited and referenced all material and results that are not original to this work.

Name – RATUL ROY

University Regd. No. – 140639 of 2017-18

Class Roll No. - 001710402012

Exam Roll No. –M4CIV19016

Thesis Title – **Pullout Behavior of Horizontal Square Plate Anchor in Reinforced Clay**

_____

Singanature with Date

JADAVPUR UNIVERSITY

FACULTY OF ENGINEERING AND TECHNOLOGY

DEPARTMENT OF CIVIL ENGINEERING

CERTIFICATE OF RECOMMENDATION

I hereby recommend that the thesis prepared under my supervision by Ratul Roy (Exam Roll No.: M4CIV19016) entitled "**Pullout Behavior of Horizontal Square Plate Anchor in Reinforced Clay**" be accepted in partial fulfillment of the requirements for the Degree of Master of Civil Engineering with specialization in Soil Mechanics and Foundation Engineering from Jadavpur University during the year 2018-2019.

In-Charge of thesis :

Dr. Sibapriya Mukherjee ***Professor*** ***Civil Engg Dept.*** ***Jadavpur University***	***Dr. Sumit Kumar Biswas*** ***Associate Professor*** ***Civil Engg Dept.*** ***Jadavpur University***	***Dr. Pritam Aitch*** ***Associate Professor*** ***Civil Engg Dept.*** ***Jadavpur University***

Countersigned by :

Dean ***Faculty of Engineering and Technology*** ***Jadavpur University***	***Head of the Department*** ***Department of Civil Engineering*** ***Jadavpur University***

JADAVPUR UNIVERSITY

FACULTY OF ENGINEERING AND TECHNOLOGY

DEPARTMENT OF CIVIL ENGINEERING

CERTIFICATE OF APPROVAL

The foregoing thesis is hereby approved as a creditable study of an Engineering subject carried out and presented in a manner satisfactory to warrant its acceptance as a pre- requisite to the degree for which it has been submitted. It is understood that by this approval the undersigned do not necessarily endorse or approve any statement made, opinion expressed or conclusion drawn therein, but approve this thesis only for the purpose for which it is submitted.

Board of Thesis Examiners:

1……

2……

3……

4……

JADAVPUR UNIVERSITY

FACULTY OF ENGINEERING AND TECHNOLOGY

DEPARTMENT OF CIVIL ENGINEERING

ACKNOWLEDGEMENT

I would like to express my special thanks and gratitude to the professor of Civil Engineering Department, Jadavpur University who gave me the golden opportunity to do this wonderful study on the topic "Pullout Behavior of Horizontal Square Plate Anchor in Reinforced Clay". I am really thankful to them. I am extremely grateful to Prof. S. P. Mukherjee, Dr. P. Aitch and Dr. S. K. Biswas for their persistent and valuable guidance, vigilant supervision, critical evaluation, constant support and encouragement throughout my work. Again, I am indebted to Prof. R. B. Sahu, Prof. G. Bhandari & Dr. N.Roy for their precious advice and guidance.

I express my thanks to all the staff members of Civil Engineering Department, Jadavpur University for providing me timely assistance in the course of this study.

I am also thankful to my friends for their help, moral support, constant encouragement and quality discussion on geotechnical concepts.

Place : Kolkata

Date :

RATUL ROY
UNIV. REGD. NO- 140639 of 2017-18
CLASS ROLL NO-001710402012
EXAM ROLL NO-M4CIV19016
FACULTY OF ENGINEERING & TECHNOLOGY
JADAVPUR UNIVERSITY
KOLKATA - 700032

Table of Contents

LIST OF FIGURES

LIST OF TABLES

LIST OF SYMBOLS

SYMBOL		DESCRIPTION OF SYMBOL
Φ	=	Angle of Shearing Resistance
δ	=	Angle of Wall Friction
C_u	=	Undrained Cohesion of Soil
γ	=	Bulk Unit Weight of Soil
γ_d	=	Dry Unit Weight of Soil
K_p	=	Coefficient of Passive Pressure
W	=	Weight of Soil
W_a	=	Weight of Anchor Plate
F_c	=	Breakout Factor
β	=	Inclination of Anchor
Q_g	=	Gross Ultimate Load
Q_u	=	Net Ultimate Load
H	=	Depth of embedment of Anchor
B	=	Width of Anchor Plate
H/B	=	Embedment Ratio
H'	=	Distance of Geotextile from bottom of Anchor Plate
B_g	=	Width of Geotextile
W_L	=	Liquid Limit
P_L	=	Plastic Limit
E	=	Young's Modulus
μ	=	Poisson's Ratio
UR	=	Unreinforced
RE	=	Reinforced

ABSTRACT

Different types of anchors are used for offshore and onshore structures to resist uplift. In case of soft clay the uplift capacity may be increased by using geotextile reinforcements. In the present study an attempt has been made to find uplift capacity of model plate anchors of sizes 50 mm X 50 mm, 75 mm X 75 mm, 100 mm X 100 mm, embedded both in reinforced and unreinforced soil with embedment ratios of 1, 2 and 3. Properties of clay and geotextile have been appropriately considered by carrying out relevant laboratory tests. The laboratory model anchor tests have been carried out for all the above mentioned plate in reinforced and unreinforced clay using a 1m X 1m X 1m foundtaion tank. The monotonic loads have been applied by means of a pulley system and the displacements have been recorded using Linear Variable Differential Transformer (LVDT). To supplement the experimental results, numerical analysis has been carried out by ABAQUS version 6.14, simulating experimental models for all the plate sizes, for embedment ratios of 1, 2 and 3. The geotextile layer has been considered for an extent of four times the anchor width at a distance of 0.25 times the embedment depth above the top of the anchor. It has been observed that the pullout capacity increases with increase of plate size on an average by 113% for unreinforced clay when plate size increases from 50 mm to 75 mm. It has been observed that for embedment ratio 2 and 3 the increase in pullout capacity compared to embedment ratio 1 for 50 mm plate in unreinforced condition is 33% and 61% respectively. It has also been observed that the ultimate uplift capacity increases by 25% on an average for 50 mm plate, with inclusion of geotextile layer.

Chapter 1

INTRODUCTION

1.1 General

The foundations of many civil engineering structures are subjected to vertical or inclined tensile loads. To withstand such loads, horizontal plate anchors are widely used both in onshore and offshore structures. Different types of anchorages are used in the field depending on the size and type of loading, the type of structure to be supported, the importance of the structures and the conditions of the subsoil. An excellent description and use of different type of anchors in field are reported by **Dutta and Singh (1984)**. Anchorage by horizontal plate anchor, of different shapes like square, circular, rectangular is one of the most common types of anchors used in civil engineering constructions. The ultimate strength of these anchors depends on the shape and size of the anchor, the depth of anchorage, the characteristics of the coating soil, the inclination of the tensile loads, etc. However, when the depth of anchor is shallow, excavation costs less to accommodate the anchor, and control of pit placement is easier and safer. However, in order to withstand the tensile load, the anchor plate size or depth of penetration, or both, must be increased depending on the size of the excavation area and the depth of the excavation. This not only leads to an increase in the area and cost of excavation work, but also problem of excavation below possible existing water table and compacting fill material below water table at great depths. In such condition it will be worthwhile to search alternate cost effective method to improve the resistance capacity of a shallow anchor by adopting suitable method as suggested by **Khatun and Chattopadhyay (2010)**. Over the past four or five decades, researchers have presented theoretical and experimental studies on the behavior of plate anchors in different types of soils under different conditions (**Rowe and Davis (1982), Dickin (1988), Merifield et al. (2001)**). It is known that the capacity of the anchor plate can be increased by grouping the anchors, increasing the unit weight of the embedded soil, increasing the embedment depth and the size of the anchor plate. But, in present days one of the possible alternative for such kind of problem is use of geosynthetics. **Subba Rao et al. (1988)**, **Krishnaswamy and Parashar**

(1994), Bhattacharya et al. (2008), Ravichandran et al. (2008) studied the pull-out behavior of the anchors in various types of soils with reinforcement and obtained the capacity considering the effects of embedment, size and shape of the anchor, reinforcement and density of soil under different loading conditions. Without changing the embedment depth and the size of the anchor plate, the pulling capacity of these anchors can be increased by introducing a coaxial geotextile sheet onto the anchor plate and then compacting the fill over it. The increase in the tensile load-carrying capacity of such a combination will depend on the relative size of the coaxial geotextile laid, relative to that of the anchor plate, the depth of anchorage, the characteristics of the geotextile layer and the properties of the filling material.

.A plate anchor embedded in the ground, when it experiences a pullout load, a part of the mass of the soil along the plate tends to separate from the rest of the soil mass and the failure occurs in the final load that depends on the depth of the embedment, the geometry of the plate and eccentricity of pulling, as well as the shear resistance of the surrounding soil. The prediction of the pullout capacity depends on the failure surface and the corresponding load and the axial movement of the anchor. Now, with the inclusion of geotextile as reinforcement, the pullout capacity is improved in the embedded soil, due to its interaction with the soil.

The present study is aimed to understand the pull-out behavior of anchor plates in reinforced soft clay by using experimental and numerical methods for different sizes of anchors under monotonic loading. A detailed review of available literature in relevant field is presented in Chapter 2 and the research gap is mentioned there. Based on these the objectives and scope of work for the present research have been arrived at.

1.2 Objectives

The main objective of the thesis was to study the pullout behavior of horizontal square plate anchors of different width embedded in soft clay reinforced with geotextiles and to compare the same for unreinforced soil.

Hence the determination of pullout capacity for different sizes of square anchor plates has been envisaged with different embedment depths in both unreinforced and reinforced soil. With the above in view, the following objectives have been identified for the present study :

i) To study the effect of inclusion of geo-synthetic reinforcement in soft clay on pullout behavior of horizontal plate anchors by experimental and theoretical investigation under central vertical pull.

ii) To study the effect of shape and size of anchors and embedment depth on such pullout of plate anchors in soft clay with and without reinforcement adopting experimental and numerical methods.

iii) To compare the results obtained from experimental and Numerical Analyses.

1.3 Scope of Work

To achieve the above mentioned objectives experimental and numerical investigations have been carried out for the square anchor plates for different embedment ratio and placing the geotextile, having width four times the width of plate, at a height 0.25 times the embedment depth from the bottom of plate. The extent and position of reinforcement is chosen based on the study conducted by **Bhattacharya et al. (2008)**, where they concluded that the above mentioned ratios would yield maximum increase in pullout capacity as discussed in Chapter 2 (Ref: page -18).

For experimental investigation, pullout tests have been carried out with model plate anchors to estimate the ultimate pullout capacity from load vs axial movement behavior. For numerical analysis of the anchor plates, the finite element software ABAQUS v6.14 has been used to estimate vertical pull-out capacity of the anchor plates. The simulations have been carried out for different sizes of square anchor plates with different embedment depth in both unreinforced and reinforced condition.

For the following section scope of work has been divided into experimental and numerical investigation as illustrated below

1.3.1 Experimental Investigation

Model tests have been carried out to find out the pullout load vs axial movement behavior for square anchor plates of three different sizes in unreinforced and reinforced bed of clay with variation of embedment depth. For the ongoing investigation width and location of geotextile has been kept in a fixed ratio with the width of plate and depth of embedment respectively. For all the tests Load vs Displacement values have been recorded up to a prescribed displacement of 10% plate dimension.

1.3.2 Numerical Investigation

To obtain vertical pull-out capacity of the anchor plate finite element software ABAQUS v6.14 has been used for both unreinforced and reinforced soil. For discretization of soil a 4-noded quadrilateral plane strain elements has been adopted for the analyses. Material non-

linearity has been taken in to account by considering the Mohr-Coulomb plasticity model. The anchor plate and geotextile has been modeled as 2-D wire elements. In case of geotextile material a linear elastic model has been adopted with the compressive strength reduced to zero as it cannot take any compressive loads. A prescribed displacement of 10% plate dimension has been applied in order to get the load displacement behavior of the anchor plate and this continued for all the sizes of plates and different embedment ratio values. The load displacement curves have been developed from which the breakout factors have been computed.

1.4 Organization of Thesis

This thesis is organized in to total six chapters;

Chapter 1 presents an INTRODUCTION to the background of the present investigation followed by defining the objectives and scopes available to achieve the same.

Chapter 2 presents LITERATURE REVIEW, and exhibits the various studies involved in the behavior of anchor plates in cohesive soils and cohesion less soils with and without geosynthetic reinforcement. Although a considerable research available in this field but there is a need for further research in the cohesive soils with reinforcement under monotonic loading through experimental investigations followed by numerical modeling of the same, and comparison of the obtained results.

Chapter 3 focuses on EXPERIMENTAL STUDY, that depict the aspects of model anchor tests followed by presentation of results of the same.

Chapter 4 deals with the NUMERICAL STUDY, with the description of ABAQUS model and finite element formulation used for analyses. It discusses the Mohr-Coulomb plasticity model used in the software. The results obtained from numerical analyses are also presented in this chapter.

Chapter 5 contains the DISCUSSION ON RESULTS, obtained from the experimental and numerical studies presented in Chapter 3 and 4 respectively, with effects of considered parameters on the pull-out capacity of the anchor plates.

Chapter 6 presents SUMMARY COMCLUSIONS AND SCOPE OF FUTURE STUDY., It presents brief summary of the present research and conclusions drawn from the obtained results and also suggests scope of future study in the related field.

Chapter 2

LITERATURE REVIEW

2.1 General

Behavior of plate anchors of different geometry with different embedment depth has been studied by many researchers through experimental and theoretical investigation for both non cohesive as well as cohesive medium. With the initial study by **Balla (1961)** for soil anchor required in supporting transmission tower in non cohesive medium, majority of the research work has been carried out in non cohesive medium afterwards by **Turner (1962), Ireland (1963), Baker & Kondner (1966), Adams & Hayes (1967)** and **Matsuo (1968)** based on field model tests or analytical methods developed using predefined slip surface. Although much effort has been made to find anchor behavior in non cohesive medium, limited research has been conducted over cohesive medium and also in view of the effect of geosynthetic reinforcement on pullout capacity of plate anchors. In this chapter a brief review of the studies referring to horizontal plate anchors in cohesive and non-cohesive medium also in reinforced soil has been carried out. The overall review has been carried in the following parts;

A. Unreinforced Soil
    i) Experimental Investigation
    ii) Numerical Investigation
B. Reinforced Soil
    i) Experimental Investigation
    ii) Numerical Investigation

2.2 Unreinforced Soil

2.2.1 Experimental Investigation

Among various failure surfaces, there are primarily three distinctive failure modes proposed by several researchers, as shown in Fig. 2.1. The first type of failure surface is a frictional cylinder method that was first proposed by **Majer (1955)**, as shown in Fig. 2.1(a). The

pullout capacity is computed from the weight of the soil within the cylindrical failure surface directly above the anchor plus the frictional resistance along this surface. Because the failure mass mobilized by an anchor is normally larger than the cylinder above the anchor, the pullout capacity tends to be underestimated on the basis of this type of failure surface **(Ilamparuthy et al. 2002)**. The second type of failure surface was first proposed by **Mors (1959)**, which is a truncated cone that extends from the anchor with an apex angle of 90° + ϕ, where ϕ is the friction angle of soil, as shown in Fig. 2.1(b). The pullout capacity is calculated to be only the weight of the soil on the truncated cone. The Mors method is usually too conservative for shallow anchors because it ignores the frictional force along the failure surface. However, it overestimates the pullout capacity for deep anchors where the failure surface normally does not extend to the ground surface and will be smaller than the assumed truncated cone. The third type of failure surface is a circular failure surface that extends from the edge of the anchor and intersects with the ground surface at an angle of approximately (45° - ϕ/2), as shown in Fig. 2.1(c). This type of failure surface was observed by **Balla (1961)** and **Baker** and **Kondner (1966).**

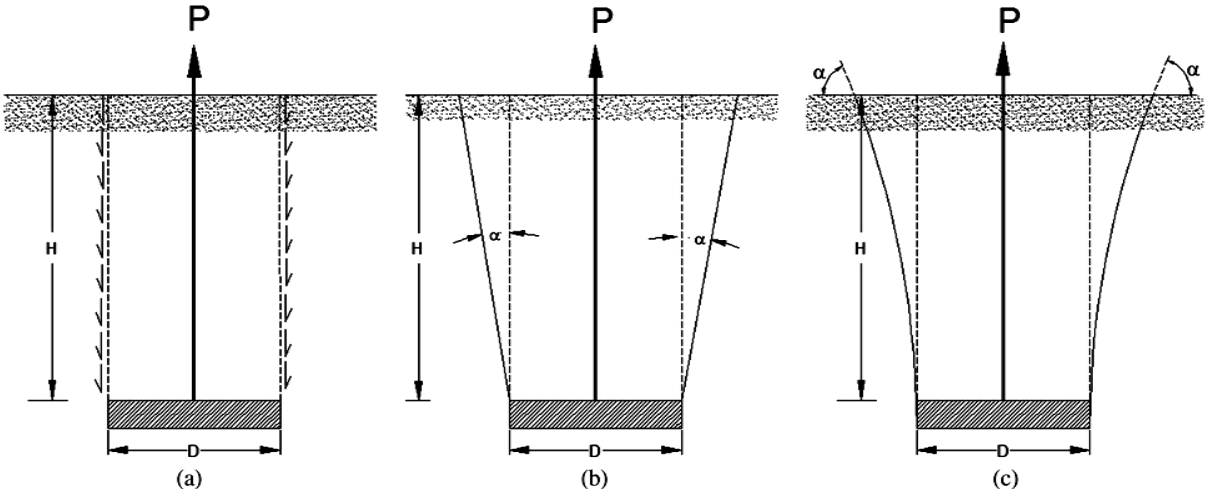

Fig. 2.1: Three different failure modes of a soil anchor: (a) Frictional cylinder; (b) Truncated cone; (c) Circular failure surface

Balla (1961) showed that in dense sand the failure surface for shallow-footings was approximately circular in elevation, and that the tangent to the surface of ground contact was at an angle of approximately (45° - Φ/2) to the horizontal. Assuming a circular failure path he obtained a reasonable correlation between theory and the results of full-scale tests on shallow footings. Using model tests in sand, **Macdonald (1963)** showed that for shallow depths the failure surface was approximately parabolic and for greater depths the failure plane was approximately vertical, the diameter of the cylinder formed being about 1.75 times the base diameter of the footing. Macdonald developed two theories to account

approximately for this behavior. For the shallow case, failure was assumed to be conical, with angle of inclination equal to one-half the angle of internal friction; for the deep case, failure was assumed to be cylindrical with a cylinder diameter of 1.75 times the base diameter. The results of model tests were in reasonable agreement with this theory.

Meyerhof & Adams (1968) noticed that there is lack of agreement on uplift-capacity theories of foundations based on slip surface mainly due to the difficulty of predicting the geometry of the failure zone. Based on model tests, they proposed a semi-theoretical relationship for strip, circular & rectangular footings in sand and clay soils. They observed very distinct failure pattern in sandy soils, whereas the failure pattern was complicated in clayey soils due to the formation of tensile cracks. The theory is derived for a strip footing and is then modified for circular and rectangular footings and for group action. The same theory can be applied to plate anchors. The proposed relationship for ultimate pullout capacity of strip footings is:

$$Q_u = 2cH + \Upsilon H^2 K_P \tan\delta + W \qquad \text{.....(2.1)}$$

where $\delta = Ø/2$ to $2Ø/3$, K_P = coefficient of passive earth pressure, and W = weight of soil above the footing.

Das (1978, 1980) and **Das et al (1985)** have suggested procedures, based on model laboratory tests, to estimate the ultimate uplift capacity of square, rectangular and strip anchors vertically or horizontally in clay. . These tests were mainly carried out on soft clays, with a limited number of tests carried out on stiff clays. The critical embedment ratio expressed as the ratio of embedment depth to plate size was given as a function of shear strength. This critical depth was found to be between 3 and 7 for circular and square plates over an undrained shear strength range of 5 kpa to 30 kpa, and for rectangular anchors the critical embedment ratio increased approximately linearly to a maximum value of 1.55 times the square for an aspect ratio of 3 or more

Das & Puri (1989) investigated the pullout capacity of inclined anchors embedded in compacted clay. Pullout tests were performed on anchors with inclinations between 0° (horizontal) and 90° (vertical) for embedment ratios up to 4. They proposed an empirical relation of breakout factor for different inclination of pullout load based on model tests. Fig 2.2(a) shows the nature of failure of soil mass for horizontal, inclined, and vertical plate anchors in clay subjected to ultimate pullout load. The net ultimate holding capacity can also be expressed as given by

$$Q_u = (Q_g - W_a \cos\beta) = AC_uF_c + W\cos\beta \quad \text{..... (2.2)}$$

Where, Q_g = Gross ultimate load, W_a = Self weight of the Anchor

Q_u = Net Ultimate Load, A = Area of Anchor Plate

C_u = Undrained Cohesion, F_c = Breakout Factor

W = Weight of Soil immediately above the anchor plate

β = Inclination of anchor with the horizontal as shown in fig 2.2(b)

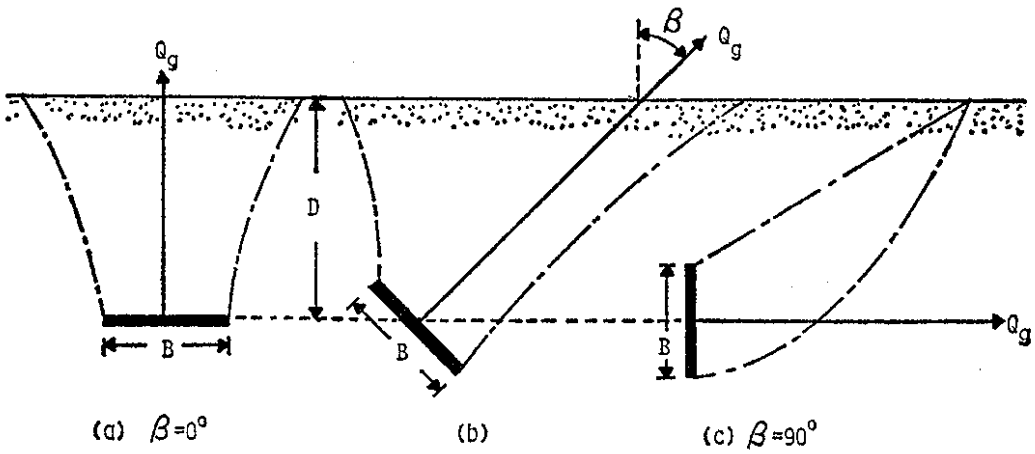

Fig. 2.2(a): Nature failure surface in soil at Ultimate load after (Das & Puri, 1989)

Now based on model test they derived breakout factor for horizontal, inclined and vertical plate anchors with the help of Eq. 2.2 given above. They observed that for a given inclination of anchor the breakout factor increases with average embedment ratio up to a maximum value afterwards remains constant as exhibited in fig 2.3.

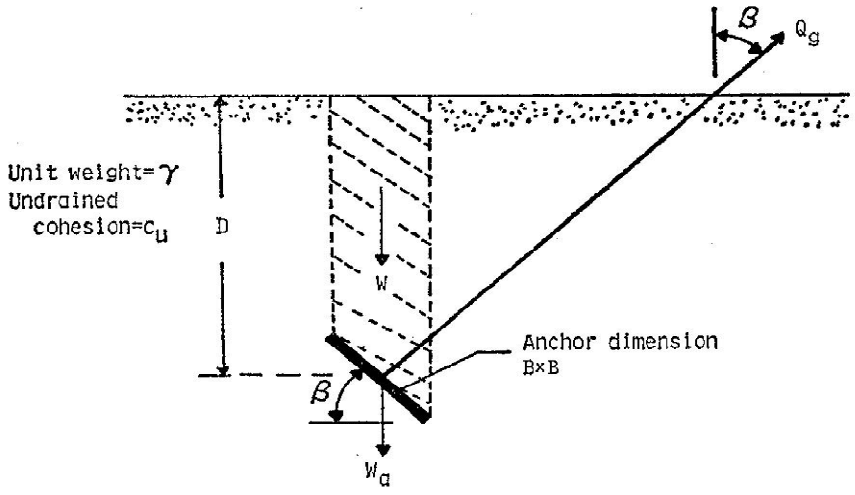

Fig. 2.2(b): Geometric parameter of an Inclined Square Anchor in Clay after (Das & Puri, 1989)

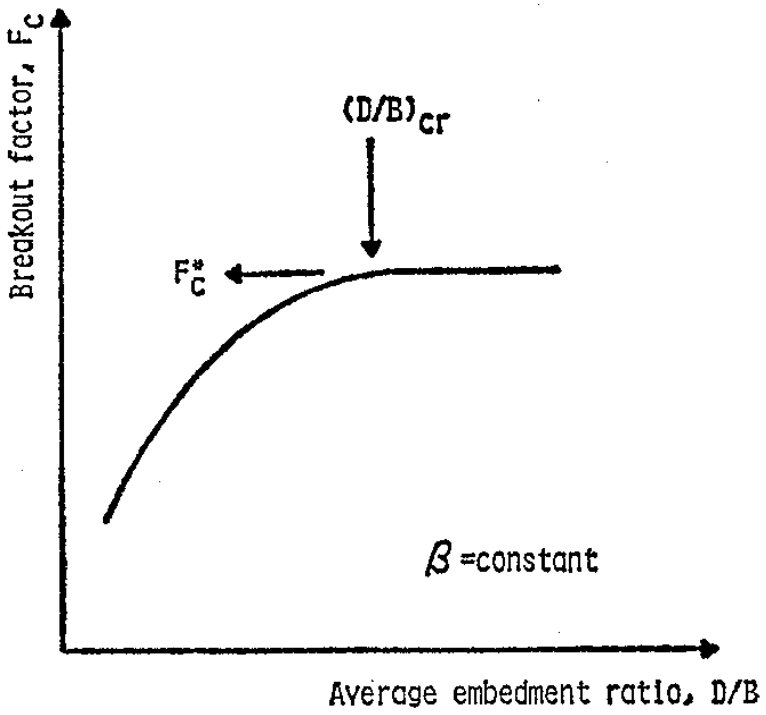

Fig. 2.3: Nature of variation of F_c with D/B for a given anchor inclination after (Das & Puri, 1989)

Ghaly et al (1991) presented an experimental and theoretical analysis on the behavior of spiral screw anchors in non-cohesion soils. A mathematical model was developed using the limit equilibrium method based on the failure mechanism observed in the experimental work. It was found that the theoretical model was in agreement with the results of the experimental and field tests, in which the pullout capacity depended on the depth of embedment of the anchor and the angle of shearing resistance of the sand.

Das et al (1994) conducted a number of laboratory tests on circular anchors in soft clay to determine the breakout factors and the variation of suction force with embedment ratio.

2.2.2 Numerical Investigation

Rowe and Davis (1982) reported results from two dimensional finite element analysis of continuous vertical and horizontal plate anchors. Behaviour of plate anchors in relation to embedment ratio, friction angle, angle of dilatancy, initial stress state, anchor roughness and the orientation of the anchor were examined. It was observed that anchors with horizontal axis exhibited higher collapse load than vertical anchors for similar conditions. Soil dilatancy was found to have a significant effect on the pull out capacity of both types of anchors.

Chattopadhyay et al. (1986) proposed a theoretical model assuming a curved axisymmetric failure surface to predict the ultimate break out capacity of horizontal circular plate anchors embedded in sand .The proposed theory indicates that the existence of a characteristic relative depth, beyond which breakout factor approaches a constant value. The value of characteristic relative depth depends on the angle of shearing resistance of the soil as shown in Fig.2.4.

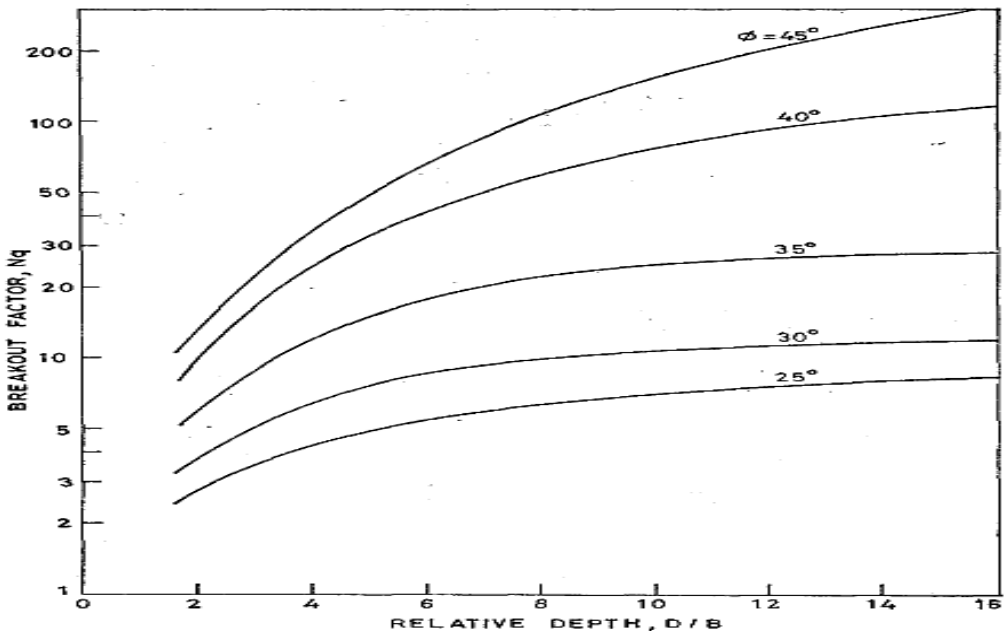

Fig. 2.4: Theoretical values of break out factor N_q in sand after (Chattopadhyay et al., 1986)

Tagaya et al. (1988) proposed formulae to estimate the uplift capacities of plate anchors in medium to dense sandy soil. Results of elasto plastic finite element method analysis using the constitutive model proposed by Ladd (1972,1975) were compared with the results obtained from centrifugal model tests and the solution by Meyerhof (1973). Good agreement among the theories and experimental values was observed by them

Merifield et al. (2001) evaluated the stability of vertical and horizontal strip anchors in undrained clay. A rigorous analysis of the limits of the ultimate extraction capacity was obtained using two numerical procedures based on finite element formulations of the upper limit and the lower limit analysis theorems. These formulations followed standard procedures assuming a rigid plastic clay model with a Tresca Yeild criterion and generated linear programming problems. By obtaining estimates of the upper and lower limits of the shrinkage capacity, the actual tensile strength was bracketed from above and below. The results obtained for both homogeneous and inhomogeneous clay were presented in terms of

avoidance factors, as shown in Fig.2.5 (a & b) and Fig.2.6 (a & b) for Horizontal and vertical bands and a single parametric equation for avoidance factors for horizontal and vertical anchors have been suggested.

The bound solutions were compared with existing numerical solutions as well as with published results from small scale laboratory tests. Based on their analysis they concluded

a) The related solutions are able to predict the exact anchorage capacity within ± 5% and compare well with the results of small scale laboratory tests.

b) Existing digital solutions can differ by up to ± 25% with bonded solutions in homogeneous soil, with a slight reduction of the error for homogeneous soil whose resistance increases with depth. For a H / B integration rate> 4, the existing solutions are usually the ones that make the biggest mistake.

c) The ultimate capacity of all anchors increases linearly with the overburden pressure up to a limiting value. This limiting value reflects the transition from shallow to deep anchor behavior.

d) It was found that anchor roughness affected the ultimate capacity of vertical anchors as it increased, while the ultimate capacity of horizontal anchors was less affected.

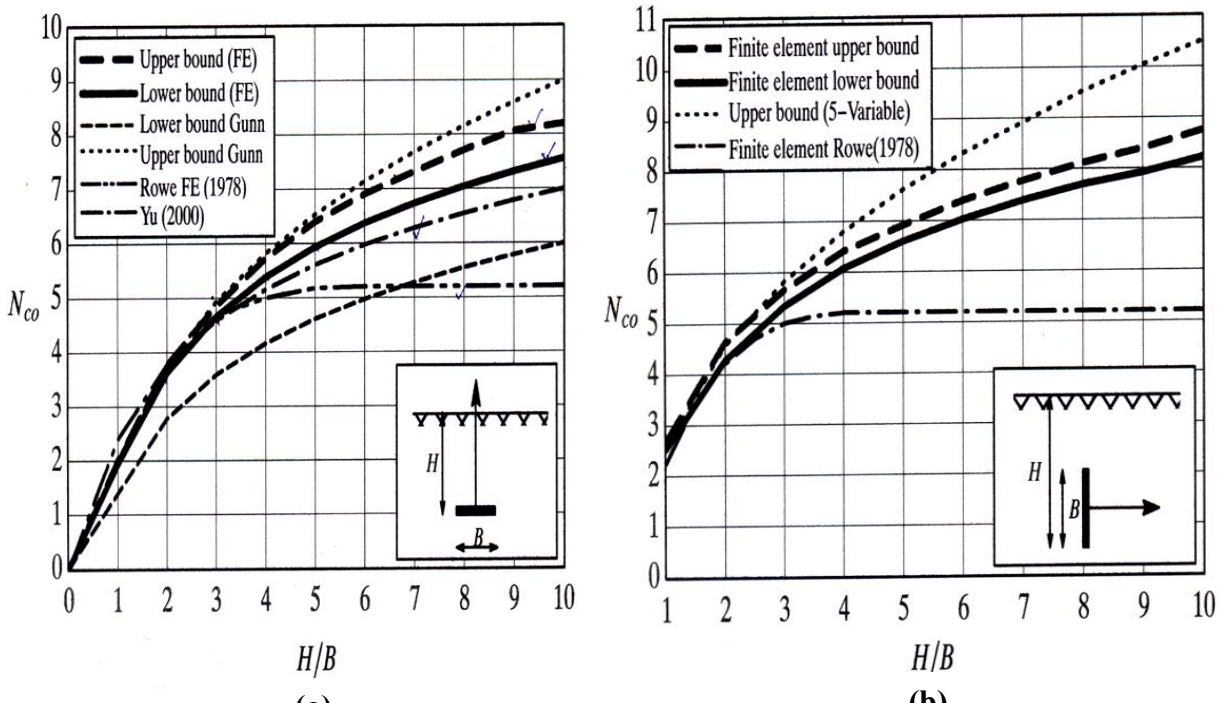

Fig 2.5: Break-out factors for horizontal and vertical anchors in homogeneous soil after (Merifield et al., 2001)

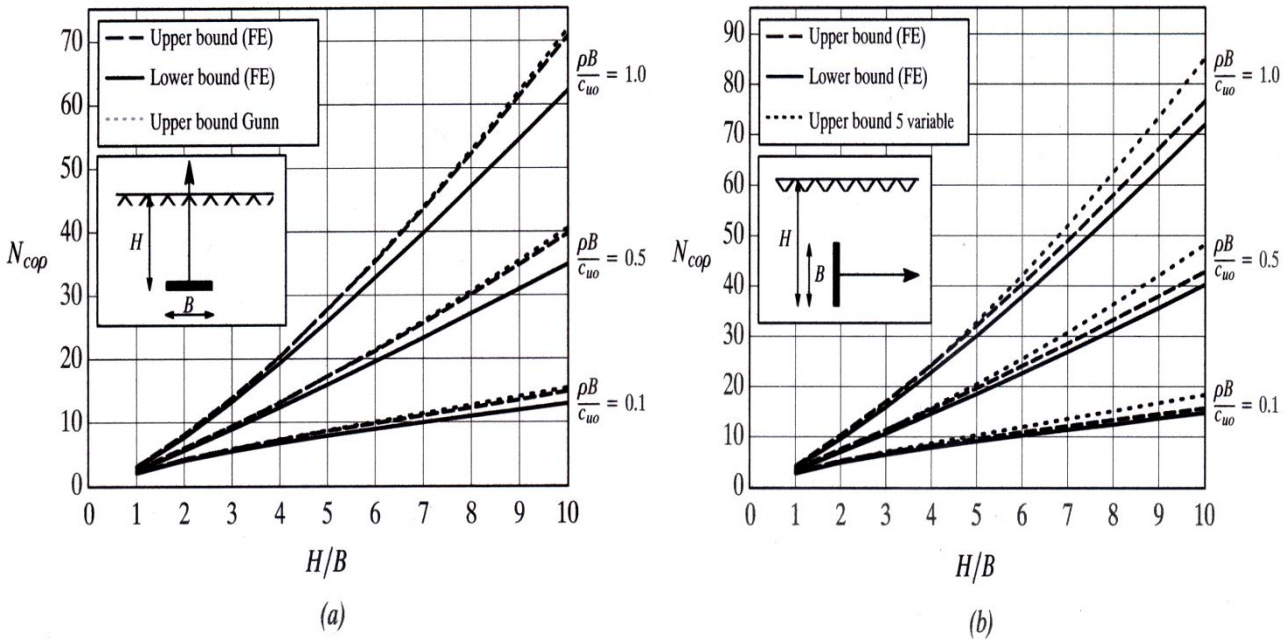

Fig 2.6: Break-out factors for horizontal and vertical anchors in non-homogeneous soil after (Merifield et al., 2001)

Merifield et al. (2003) estimated the ultimate pullout capacity of different shapes of anchor in clay using a new three-dimensional numerical procedure based on finite element formulation of the lower bound analysis theorem. From the analysis, an estimate of the lower limit of anchor failure factor (N_C) was obtained for square, circular and rectangular anchors, as shown in Fig.2.7 (a, b and c). The estimated capacities have been encouraging compared to the results of published and available laboratory tests. Similar to **Merifield (2001)**, it was found that the anchoring capacity of strip anchor increased when overburden pressure reached a limiting value reflecting the change from shallow to deep anchoring behavior. In addition, according to them, at a given depth of anchorage, an anchor may behave as shallow or deep, depending on the dimensionless overload ratio H / Cu. From their analysis, simple parametric equations for avoidance factors, as indicated below, have been suggested to determine the capacity of square and circular anchors in a homogeneous soil profile for different anchoring depths.

$$N_{co} = S\,[2.56 \ln (2\,H/B)] \qquad \text{.....(2.3)}$$

Where, N_{co} = breakout factor

S = shape factor for square or circular anchor

H/B = embedment ratio

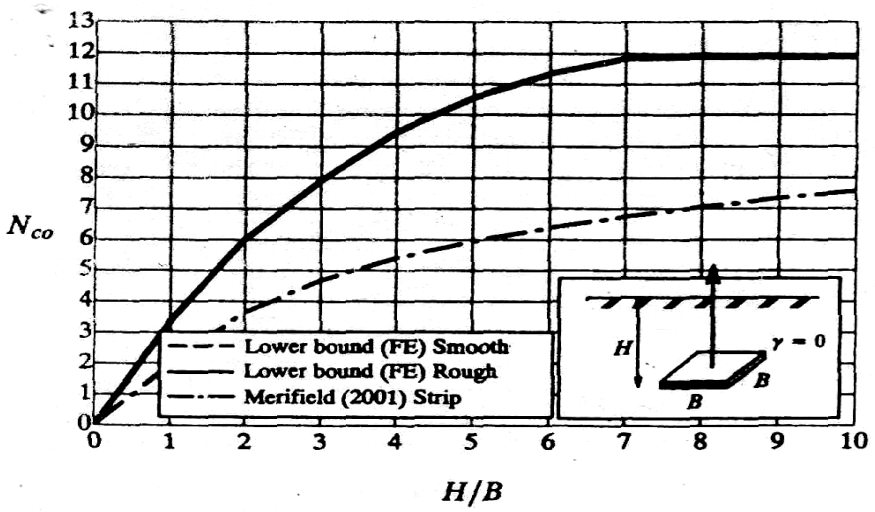

Fig. 2.7(a): Breakout factor for square anchor in clay after (Merifield et al, 2003)

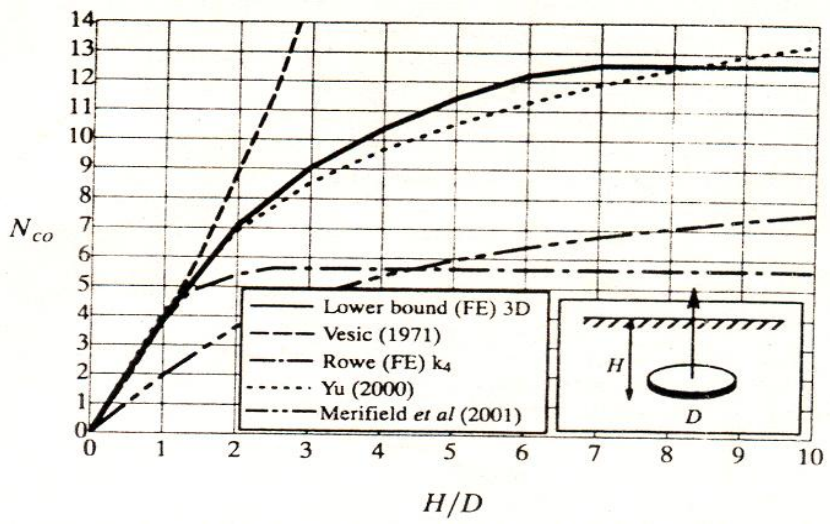

Fig. 2.7(b): Breakout factor for square anchor in clay after (Merifield et al, 2003)

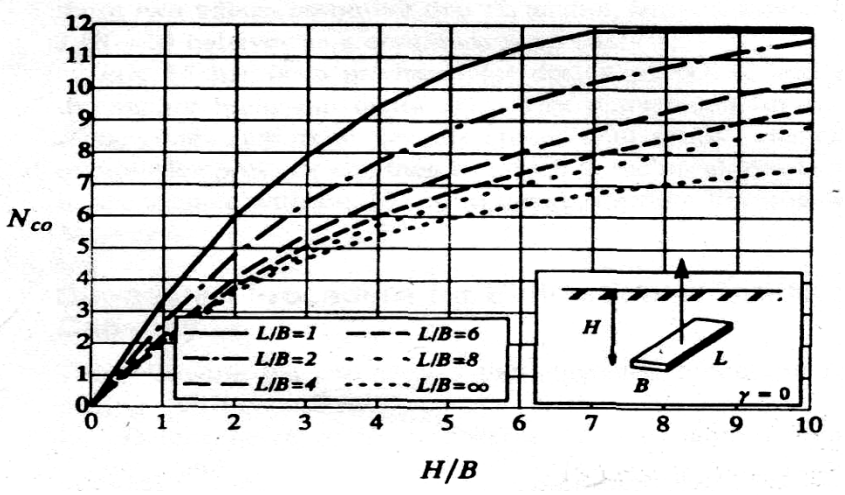

Fig. 2.7(c): Breakout factor for square anchor in clay after (Merifield et al, 2003)

Thorne et al. (2004) studied the uplift behavior of horizontal strip anchors in clay under fast loading. The possible failure mechanisms were reviewed, including failure due to shear and traction in the soil and the development of suction in the porous fluid. The analysis was made using the finite element program AFENA (Carter and Ballaam, 1995) of the problem of large deformation and an assumption of progressive displacement. Based on their findings the following conclusions were drawn :

a) The behavior of the strip anchors in the pullout capacity are functions of the non-dimensional parameters H/B, ϒH/C, U_c/C ,where H is the embedment depth, C is the cut resistance without drainage, Uc is the magnitude of the maximum tensile stress of the pore water in the soil and ϒ and B are the unit weight and width of plate.

b) Shallow anchors in relatively strong soil tend to fail due to the development of a tensile failure in the soil that is above the anchor and the ultimate capacity is a function of the undrained shear strength of the soil, its own weight and the tensile capacity of the porous fluid

c) The failure mechanism of the deep anchors where the initial vertical total stress in the plate exceeded seven times the resistance without draining involved only one cut fault located around the anchor. The ultimate capacity in such a case becomes a function only of the resistance without draining the soil.

Merifield et al. (2005) conducted a rigorous numerical study on the pullout capacity of the inclined anchors in clay. Finite element methods of numerical merged solution and displacement were used. The effect of anchor inclination on the pullout capacity was investigated and a simple empirical equation was proposed which, on average, provided an estimate of the collapse load within ± 5% of the actual values. The results of the finite element displacement method were compared favorably with the numerical bonded solutions and it was found that the final capacity increased linearly with the overload pressure up to a limit value that reflected a transition from surface to deep anchor behavior.

Randolph et al. (2005) investigated the behavior of inclined strip plate anchors using finite element analysis of high deformation. The rotation behavior of the anchor plates during continuous extraction in clay was introduced by the finite element method. They observed that the extraction capacity increased with increasing insertion depth and inclination with a final extraction capacity factor Nc = 12 at an embedment ratio of 3 for the anchors attached to the ground. But for the anchors that were allowed to separate from the ground, a

limiting value of the uplift capacity factor was not obtained until an embedment ratio of 8 in soil without weight. They also concluded that for the analysis of the pullout capacity of small deformation, the factor increased with increase in the depth of embedment and before the limiting capacity factor for a given embedment was reached, the vertical plate anchor showed pullout capacity smaller than that of the horizontal anchor.

2.3 Reinforced Soil

2.3.1 Experimental Investigation

Subba Rao et al. (1988) reported for the first time the improvement in pullout capacity using the geotextile as anchoring loops embedded in the sand. In this regard, model tests were performed on two types of anchors reinforced in sand. One was a cylindrical pile of 100 mm in diameter and the other a flared anchor of 75 mm in diameter of the stem and 190 mm in diameter of the base with geotextile ties of 650 mm and 350 mm in length, respectively. Based on the experimental results, they indicated that the geotextile ties provided a much higher resistance to lifting than unreinforced anchors. In addition, they concluded that the use of multiple geotextile layers was useful, but the increase in the number of layers did not offer a proportional increase in uplift resistance.

Nene & Garg (1991) investigated the behaviour of shallow plate anchors in reinforced cohesive soil using both woven and non woven geotextile. The breakout loads were computed by limit equilibrium method suggested by **Saran et al. (1986)** by considering the equilibrium of the wedge as shown in the Fig.2.8.

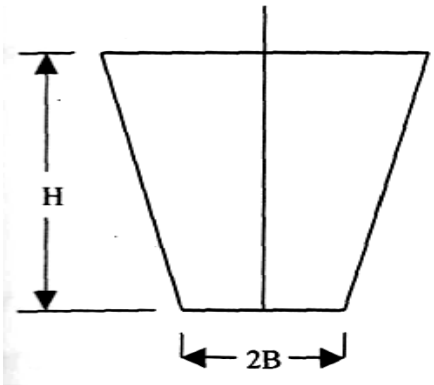

Geometrical symbols for anchor without Geo-synthetic

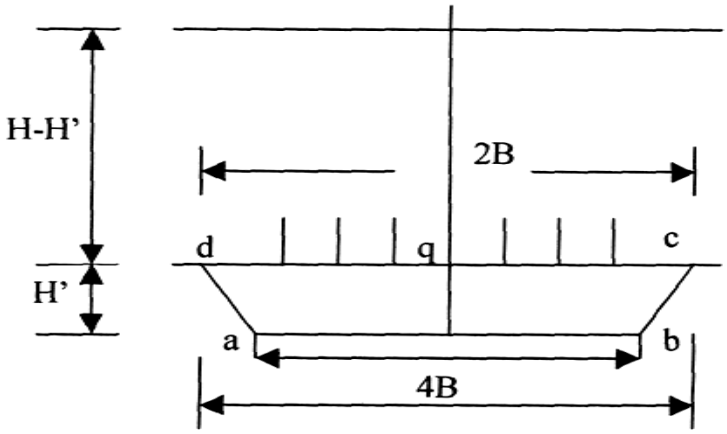

Geometrical symbols for anchor with Geo-synthetic

Fig.2.8: Failure mechanism for reinforced clay after (Nene & Garg, 1991)

The breakout load for square or circular anchor in reinforced soil was obtained as

$$q_r = C.\ F_{rc} + \gamma\ H\ F_{ry} + \gamma\ H\ F_{rq} + C\ F_{gc} + \gamma\ H\ F_{gy} \quad \text{.....(2.4)}$$

where C = unit cohesion

γ = unit wt. of soil

F_{rc}, F_{ry}, F_{rq}, F_{gc} and F_{gy} are the non dimensional load factors. Values of these non dimensional factors were obtained from the equilibrium analysis as given below :

$$F_{rc} = 4\ \lambda^{/}\ (1 + \lambda^{/} \tan \phi) \quad \text{.....(2.5)}$$

where $\lambda^{/} = H^{/} / 2\ B$,

$H^{/}$ being the height of geotextile from the top of plate and 2 B is the width of anchors

$$F_{ry} = 1 + 2\ \lambda^{/} \tan \phi + 4/3\ \lambda^{/\,2} \tan^2 \phi \quad \text{.....(2.6)}$$

$$F_{rq} = (1 + 2\ \lambda^{/} \tan \phi)^2\ (1 - \lambda^{/} / \lambda) \quad \text{.....(2.7)}$$

where $\lambda = H/2B$

$$F_{gc} = 2\ A\lambda^{/}\ \mu\ (1 - \lambda^{/} / \lambda) \quad \text{.....(2.8)}$$

where μ = adhesion factor at the interface of soil and geotextile

$$F_{gy} = F_{gc}\ (1 - \lambda^{/} / \lambda) \tan \phi \quad \text{.....(2.9)}$$

$$A_r = r^2 - (1 + 2\ \lambda^{/} \tan \phi) \quad \text{.....(2.10)}$$

where, r = L/B, L being the length of geotextile

To validate the analytical method, laboratory model tests were performed on cohesive soil with circular and square anchors with geo-synthetics placed at a distance of B / 2 and B from the top of the anchor of the plate and the width four times the width of the foot model. Based on a limited number of model tests at two different embedment depths, they concluded that the uplift capacity increased in both the woven geotextile and the nonwoven used, although a greater increase was observed for the woven geotextile. It was found that the experimental results were in agreement with the suggested analytical method.

Krishnaswamy and Parashar (1994) studied the uplift behavior of plate anchors embedded in a cohesive and non-cohesive soil, with and without geo-synthetics by testing small-scale models in the laboratory. It was found that the uplift behavior is affected by the depth of embedment, the type of geosynthetics used and the relationship of the geosynthetic

inclusion area to the anchoring area of the plate. Significant influences of the soil type were noted, as well as the deformation rate and the position of the water table in the lifting capacity. In both the cohesive and non-cohesive soils, it was observed that the uplift capacity increased with the inclusion of geosynthetics.

Garg (1997) predicted the ultimate uplift capacity of reinforced anchors with woven and nonwoven geotextiles and geogrid type reinforcements following the analytical procedure of **Nene and Garg (1991)**. They also performed laboratory model tests with shallow plate anchors of strips, circular and square with a width of 50 mm and 100 mm in diameter / width, respectively, in cohesive soils reinforced with geosynthetics. The relationship between the depth of insertion and the width was varied between 1 and 4 and the geo-synthetics were placed in a single layer with a size of 3 times the width of the plate and with a placement ratio of 0.25. It was found that the experimental results were in agreement with the analytical solution. Based on their findings, they concluded that there was a definite increase in uplift capacity due to reinforcement and it was found that the geo-grid reinforcement was better than woven or non-woven geotextiles. According to them, the increase was around 30 to 50% and this increase was due to the friction properties of geotextiles. In addition, it was found that the deformation of the reinforced anchor was less than that of the non-reinforced anchor for any uplift load.

Ilamparuthi et al. (2002) proposed that the uplift capacity of circular anchors is governed by their diameter, embedment ratio, and sand density. Two modes of failure develop within the soil mass depending on the anchor embedment ratio.

The surface anchoring behavior is characterized by a raised trunk of a soil cone extending from the anchor to the sand surface, with sloping sides approximately φ / 2 to the vertical, regardless of the density of the sand.

The behavior of the deep anchorage is characterized by a rupture zone in the form of a balloon in the mass of the ground on the anchor. The flat part of this rupture surface emerges from the upper edge of the anchor and is inclined at 0.8φ with respect to the vertical, it is also independent of the density of the sand. a three-phase behavior that characterizes the superficial case and a behavior of two phases the deep case.

Ravichandran et al. (2004) studied the behavior of rectangular plate anchors in the bed of unreinforced and reinforced sand (horizontal and vertical). The vertical reinforcement showed a greater increase in the lifting capacity of the anchors than the

horizontal reinforcement. According to them, this difference was due to the better interlocking arrangement attributed by vertical reinforcement than that of horizontal reinforcement.

Bhattacharya et al. (2008) reported on the response of lifting the square anchor plates in reinforced kaolin. The experimental tests were carried out with anchor plates of sizes of 7.5 cm x 7.5 cm and 5 cm x 5 cm for embedment (H / B) ratios of 2 to 4 with geotextile layers.

A single layer of woven geotextile was laid horizontally above the top surface of the anchor plate at variable distances of 0.25H, 0.5H and 0.75H, where H is the depth of embedment of the anchor. The length of geotextile was kept as four times the width of plates used in the test.

The typical load-displacement curves for 50 mm x50 mm anchor plate with an embedment ratio of 2 with and without reinforcement have been shown in fig. 2.4.Parametric study has been done in the form of relative failure displacement, breakout factors and ultimate load factor for plate sizes of 50mm and 75mm. They concluded that

(a)Unreinforced clay has more displacement with less ultimate uplift capacity compared to that of reinforced clay.

(b) The uplift capacity is dependent on embedment ratio H/B and the position of the geotextile with respect to the embedment depth. The capacity increases with the increase in embedment ratio but decreases with the increase in height of placement of geotextile above the plate.

(c) Maximum value of uplift capacity obtained when the geotextile layer is placed at a depth of 0.25 times the embedment depth.

Das et al. (2013) reported that with the use of a geotextile sheet of adequate diameter, the detachment capacity of the shallow anchors can be increased in many folds, according to the increase requirement. They presented a theoretical model to predict the breaking capacity of circular plate anchors covered by a coaxial geotextile sheet. The detachment capacity of said combination depends on the diameter of the anchor, the relationship between the diameter of the coaxial sheet and that of the anchor, the angle of friction between the geotextile sheet and the surrounding soil, the depth of the embedment and the properties of the soil surrounding.

2.3.2 Numerical Investigation

Rowe et al. (1982) examined the undrained behavior of the anchor plates with a vertical or horizontal axis, resting on saturated clay. The numerical solutions were obtained from an analysis of elasto-plastic finite elements using the theory of soil structure interaction described by Rowe, Booker and Balaam (1978). This substructure approach allows consideration of plastic failure within the soil, anchor breakaway from the soil behind the anchor, and shear failure at a frictional, dilatant soil structure interface without the introduction of special joint or interface elements. The anchor was assumed to be thin and perfectly stiff. It was assumed that the soil had a Mohr-Coulomb failure criterion. They proposed a critical depth beyond which the final anchoring capacity does not depend on the overburden pressure, the orientation of the anchor and any adhesion or suction developed between the anchor and the ground.

Mistri et al. (2011) presented the analysis of finite elements for the anchoring of plates in homogeneous and non-homogeneous soils using the PLAXIS 3D. In the initial stages, the final uplift capacity in homogeneous clay shows a rapid increase and can become almost constant at great depth. They proposed that such a change in the rate of increase occurs at the depth of transition where the behavior of the surface anchor changes to the deep anchor. However, such transitional behavior is not observed markedly in the clay when increasing the shear strength. As the consistency of the soil increases, the variation in the final uplift capacity also increases.

Makarchian et al. (2012) performed experimental and numerical investigation on behavior of uplift capacity of circular plate anchors of different diameter embedded in sand of different relative density in unreinforced and reinforced condition with multi-layers of geonet. A schematic diagram of experimental set up used for the above mentioned investigation is shown below in fig 2.9.

Based on laboratory test and numerical study they concluded that

- With increase in embedment ratio pullout capacity increases for both unreinforced as well as for reinforced condition.
- The ultimate uplift capacity in dense sand condition is more than in medium dense condition
- In experimental tests, the axial movement required to reach ultimate pullout load is larger than FEM approximately five times

The pullout vs displacement plot for both model test and numerical analysis for the above investigation is depicted below in fig 2.10(a) and fig 2.10(b).

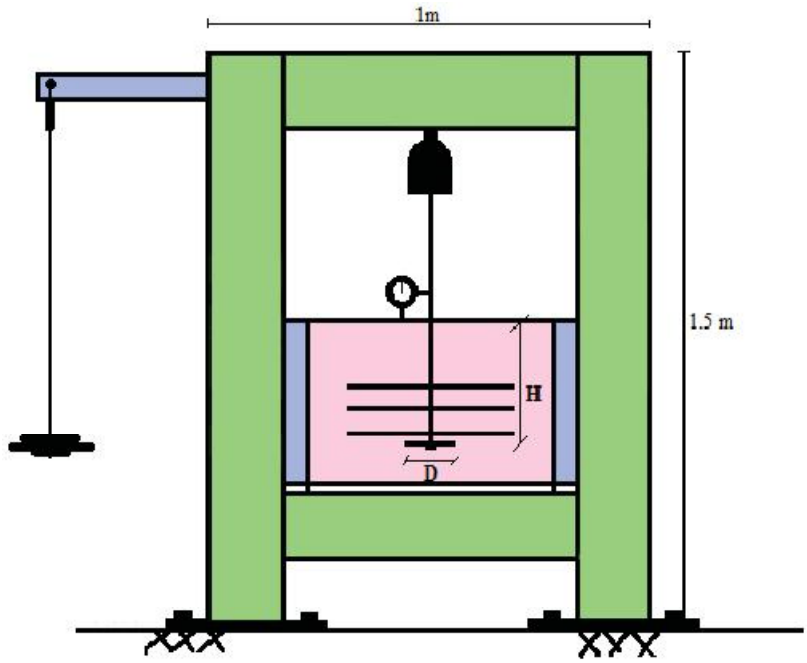

Fig.2.9: Schematic view of Experimental Set up after (Makarchian et al., 2012)

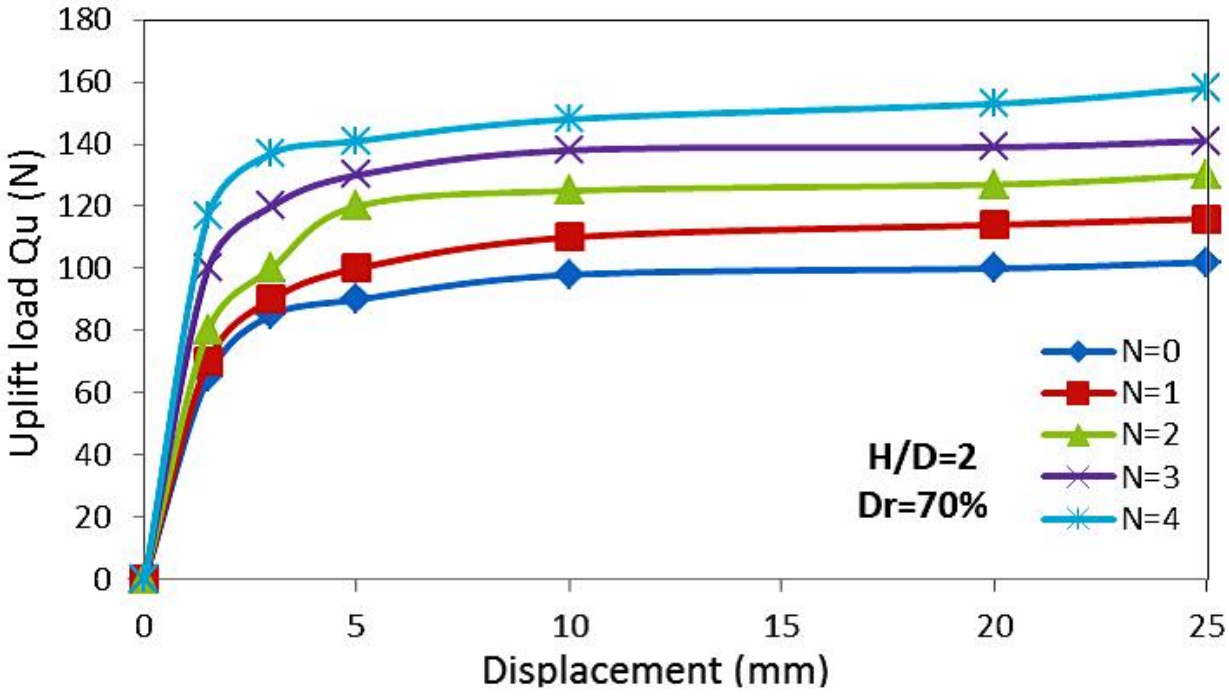

Fig.2.10(a): Load-displacement curve for Experimental Tests after (Makarchian et al., 2012)

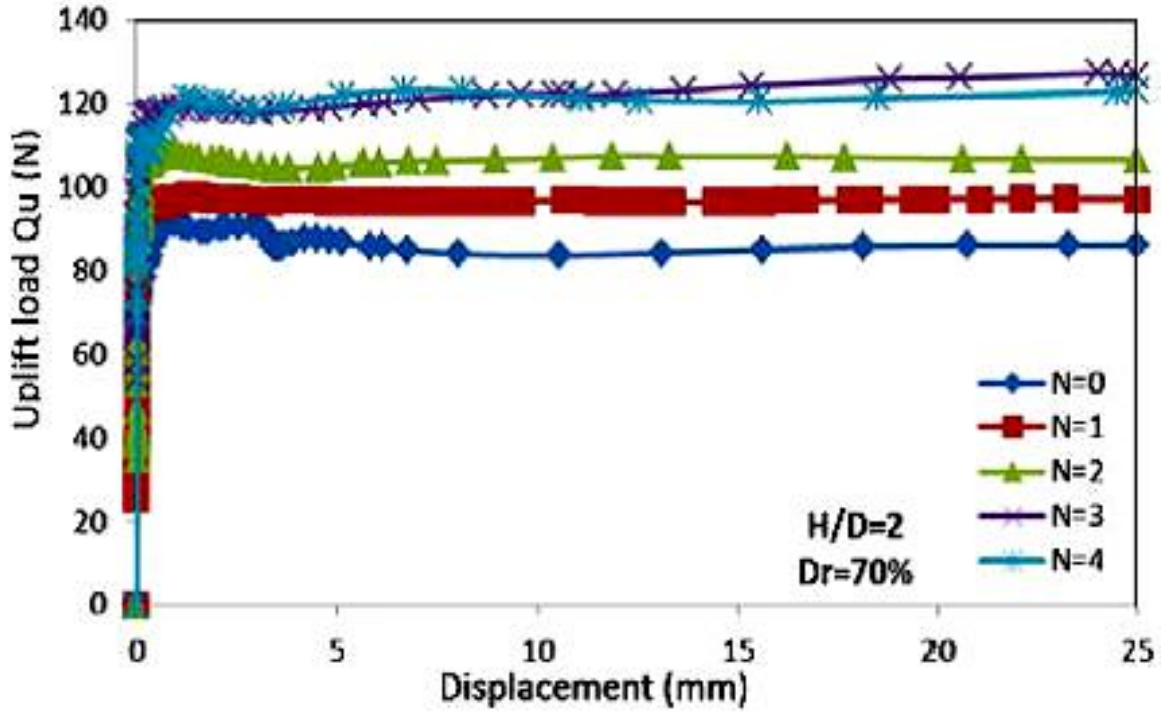

Fig.2.10(b): Load-displacement curve for FEM after (Makarchian et al., 2012)

Yu et al. (2015) were conducted 1 g model tests to investigate the strain softening behavior of the bearing capacity of plate anchors in clay under cyclic loading. Numerical analyses were conducted using FLAC to quantify the strain softening parameters.

Hegde and Roy (2017) carried out a comparative numerical study on soil-geosynthetic interaction using large scale direct shear test and pullout test. The analyses were carried out using finite element package PLAXIS^{2D} in two dimensional frameworks. Based on their study they concluded that the shear strength at the soil-geotextile interface was found to be less than that of soil-soil interface with the interaction ratio varying from 0.67 to 0.97 for different types of sand. The interface frictional angle tends to decrease with increase in fines content and the friction coefficient obtained from pullout load was about 50% of the value obtained from direct shear test.

2.4 Motivation of Work

The above review of literature shows that the pullout capacity of plate anchors in unreinforced cohesive soil has been predicted by some model tests or by a limited number of numerical or analytical methods. Comparative analyses of pullout capacity based on these methods are also limited in the case of unreinforced soil. In addition, very few experimental or analytical methods have been reported for the pullout capacity of square plate anchors in reinforced cohesive soil. Moreover, it seems that a few attempts have been made in the literature for numerical modeling or finite element modeling in reinforced soil for anchor breakout capability.

Therefore, considering all of the above, it is prudent to attempt in this investigation to conduct model testing with square plate anchors in reinforced cohesive soil and theoretical analysis according to the finite element technique, then to establish a comparison for the pullout capacity. In this perspective, the present study has been performed on the behavior of plate anchors in reinforced cohesive soil.

Chapter - 3

EXPERIMENTAL STUDY

3.1 General

The aim of this investigation is to find out uplift capacity of anchors embedded in both un reinforced and reinforced clay using square anchors. Reinforcement in clay has been provided with geotextile sheet placed at a position having a fixed ratio with the embedment depth within the embedded clay bed. From the observed capacity, the behavioral aspects of the anchors in reinforced clay have been studied in terms of various parameters involved.

Full scale tests generally yield very much reliable results. But variation of different parameters with full scale tests involves substantial expenditure, time and space, making such testing very much difficult to be executed.

Model study is one of the alternative means of fulfilling the objective mentioned in the beginning. Possibility of extending the results of model study through non-dimensional quantities encourages the investigator to pursue the same. The added advantage of the model study is that the pertinent parameters influencing the behavior of anchors in reinforced clay can be controlled as per requirement. In addition, the cost of carrying out model investigation is far less as well as the convenience is much more compared to field tests. In view of these, model study and consequent validation of the obtained results with numerical investigation was adopted in the present study.

3.2 Model Test Programme

The entire test programme was aimed and categorized to determine

a) Properties of foundation medium (clay) used in the investigation,

b) Properties of geotextile used as reinforcing material,

c) Interface adhesion between the geotextile and the clay bed and lastly,

d) Model anchor tests.

3.2.1 *Routine Tests for Clay*

Locally available clay collected from Jadavpur, West Bengal, India has been used in this study. In order to find out engineering properties of the Clay routine standard laboratory tests were conducted for index properties, compaction characteristics and undrained shear strength.

3.2.2 Tests for Geotextile

Woven geotextile of permeable polystron fabric has been used in the present investigation as reinforcing material. Standard tests have been conducted to find out the thickness, mass per unit area and tensile strength for geotextile.

3.2.3 Interface Adhesion between Geotextile and Clay

Adhesion between geosynthetic material and the soil plays a significant role when geosynthetics are used as reinforcing material. This adhesion also depends on the overburden pressure. In order to simulate the field condition modified direct shear test has been carried out under different appropriate normal stresses as per the methodology adopted by **Bhattacharya et al. (2008)**. The interface adhesion value has been found to be 0.17 from modified direct shear test and the same is used to define soil-geotextile interaction in numerical analyses.

3.3 Testing of Materials

a) Clay: The experimental procedure for routine tests on Clay used was followed according to IS specification in which tests like Grain Size Distribution (IS : 3104-1965), Atterberg Limit (IS : 2720 Part V, 1965), Standard Proctor Test (IS : 2131-1963) and Undrained Shear Strength were conducted. For undrained shear strength, the test was done with Clay compacted to a water content of 19.5% and dry density 16.5 KN/ m^3. For the present study water content for compaction was fixed at OMC+4 %, based on literature study done previously as it would resemble to the field condition that would require improvement through the use of plate anchors.

- ***Properties of Clay:-*** Laboratory test conducted over clay showed following results
  - Liquid Limit (W_L) = 37.7 %
  - Plastic Limit (P_L) = 23.8 %
  - Optimum Moisture Content = 14 %
  - Maximum Dry Density (Υ_d) = 1.70 T/m^3

- Average water content during testing = 18%
- Unit wt. of compacted soil during testing = 19.38 kN/m^3
- Undrained cohesion, C = 2.5 T/m^2
- Angle of internal friction, $\phi = 5^0$
- Grain size : Sand = 0%, Silt = 75%, Clay = 25%

Based on the test data, grain size distribution, Proctor compaction and Unconfined compressive strength ofclay used in the present investigation are exhibited in Figs 3.1(a) to 3.1(d) ``

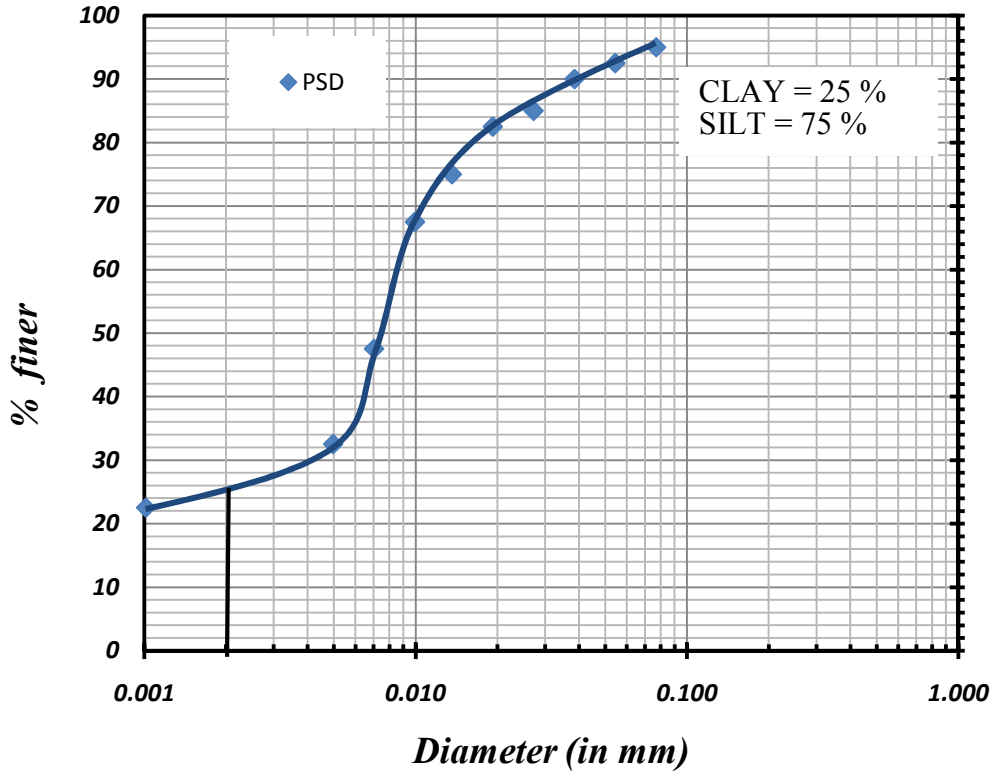

Fig 3.1(a): Particle Size Distribution through Hydrometer Analysis

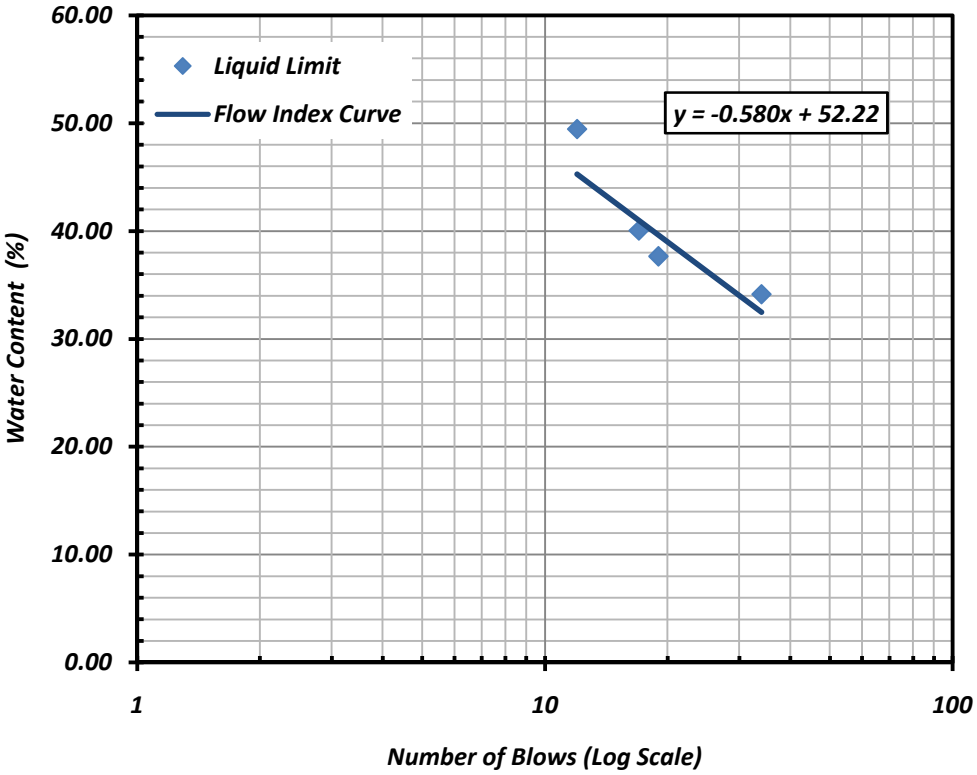

Fig 3.1(b): Liquid Limit Determination

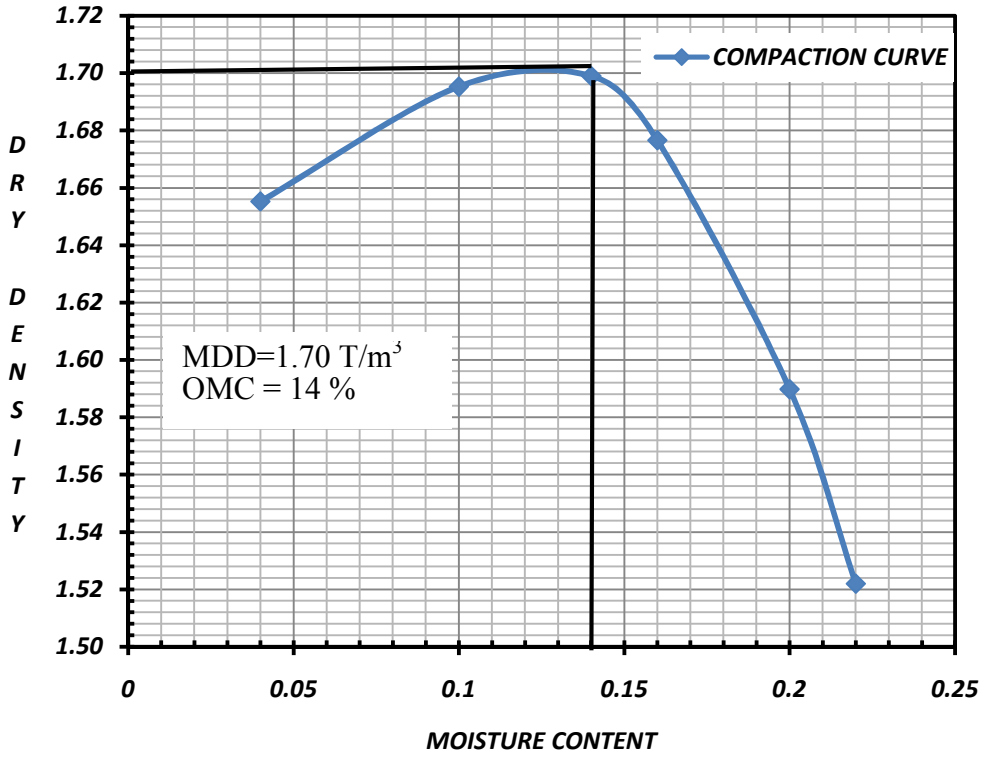

Fig 3.1(c): Determination of Proctor Density

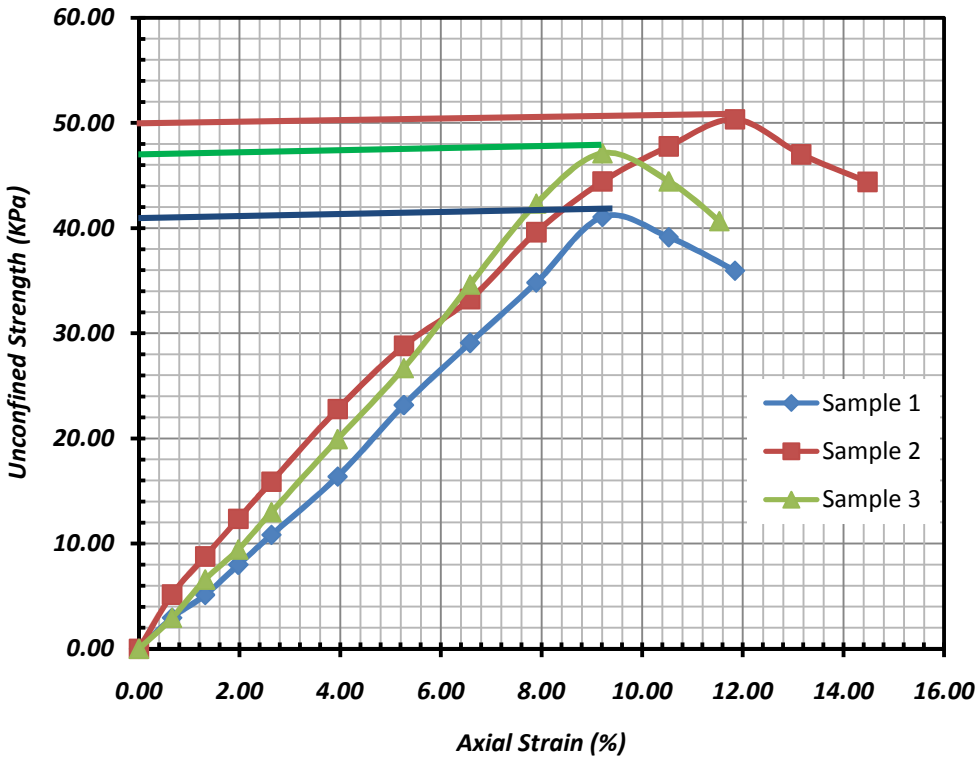

Fig 3.1(d): Determination of Unconfined Compressive Strength

b) Geotextile: Test were conducted on geotextile material to be used in the present study to determine the thickness (ISO 9863), mass per unit area (ISO 9864), Apparent opening size (ISO 12956). Tensile Strength at 10% elongation (ISO 10319) as well as the breaking load was estimated. The obtained results of the tests conducted over the geotextile material showed more or less similar values that are obtained from Manufacturer's manual.

- ***Properties of Geotextile:-*** Physical and mechanical properties of the geotextile obtained from the standard tests as discussed above are given below :
  - Thickness = 0.36 mm
  - Mass per unit area = 146 gm/m^2
  - Tensile strength = 27.6 KN/m
  - Elongation at maximum load = 28.6%
  - Load at 10% elongation = 15 KN/m
  - Interface friction between Soil and Geotextile = 0.17

The Tensile stress characteristics of the geotextile has been shown in Fig.3.2

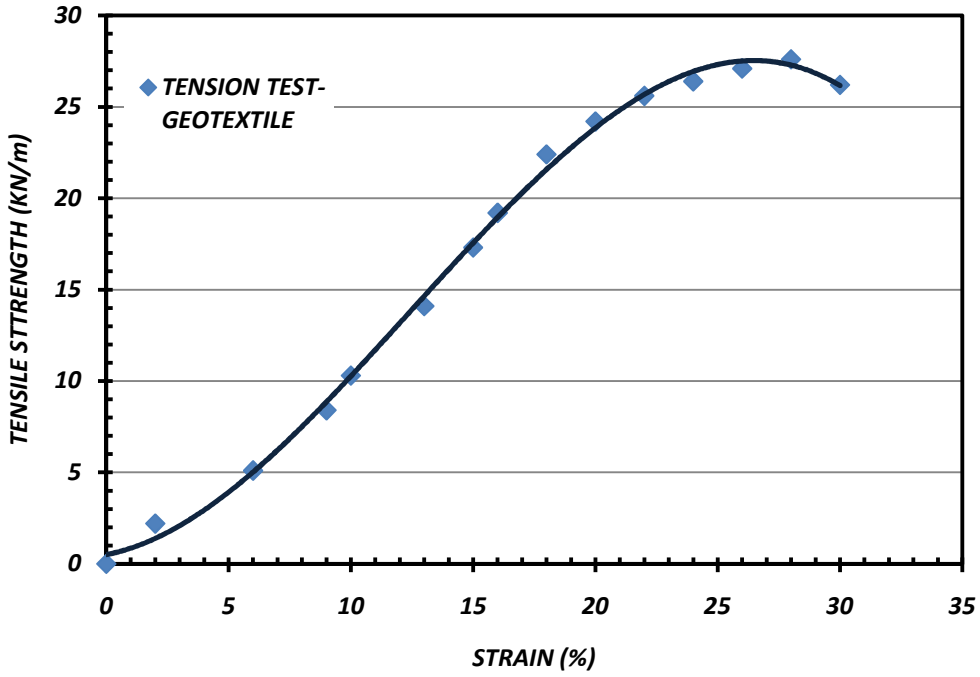

Fig 3.2: Tension Test of Geotextile

c) Anchor Plate: In the ongoing investigation square anchor plates made of mild steel has been used. To determine the properties of the mild steel plates to be used a Tension test was conducted with a round tensile specimen made from mild steel and tested in UTM at a strain rate of 0.05 mm/sec. Typical Stress Strain graph obtained from tension test of mild steel specimen has been exhibited in fig 3.3(a) to 3.3(d)

- ***Properties of Anchor Material:-*** Physical and mechanical properties of the Anchor material obtained from the Tension tests as discussed above are given below :
  - Young's Modulus (E) = 200 GPa
  - Mass per unit volume (Υ) = 7850 Kg/m^3
  - Poisson's Ratio (μ) = 0.33

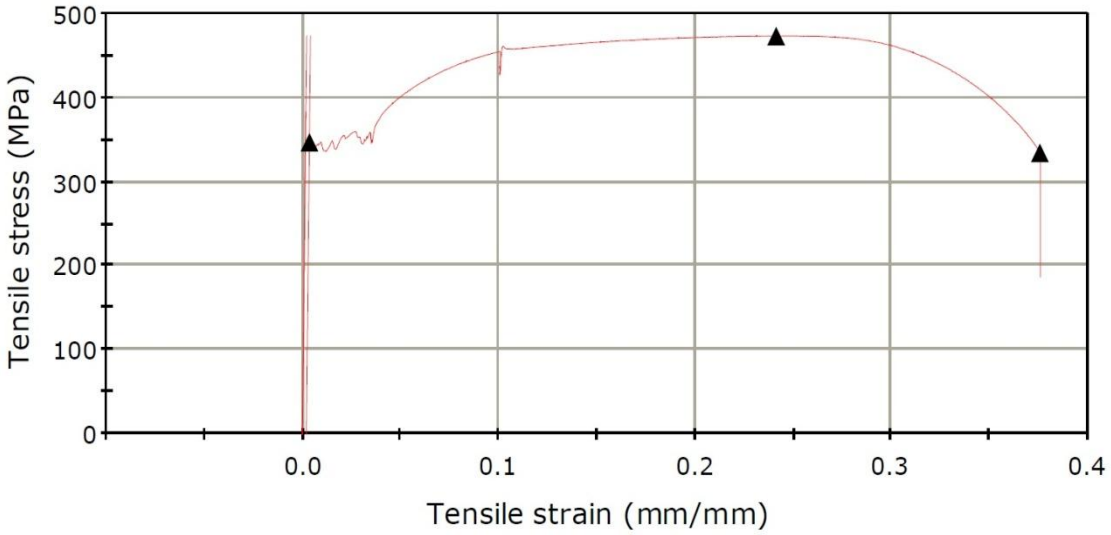

Fig 3.3(a): Tension Test of Mild Steel Specimen

Fig 3.3(b): Tension Test of Mild Steel Specimen

Fig 3.3(c): Tension Test of Mild Steel Specimen

Fig 3.3(d): Tension Test of Mild Steel Specimen

The test programme for model anchor tests has been shown in Tables 3.1 for unreinforced and reinforced clay using different embedment depth and position of geotextiles above the bottom of plate in embedded soil. For unreinforced case total six numbers of tests has been carried covering three different plate sizes with different embedment depth for each case. Three reinforced model test has been carried out only for 50 mm plate having a fixed width of geosynthetics and positioned at a distance of 0.25 times the depth of embedment from bottom of anchor plate. Different parameters involved in model test are shown in fig 3.4 and 3.5.

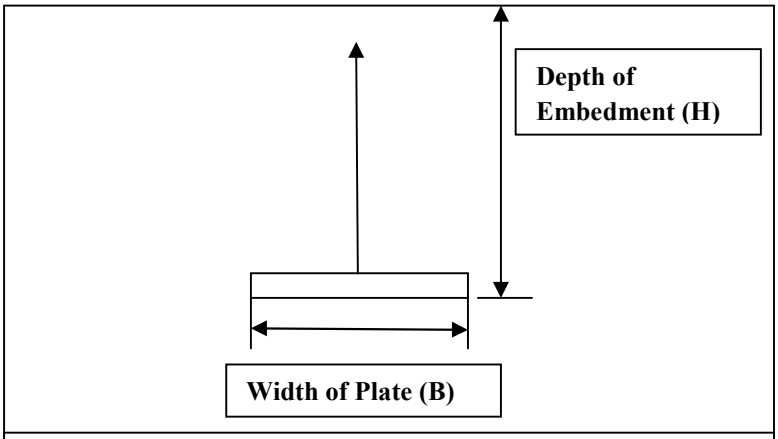

Fig 3.4: Schematic Representation of Model Anchor Test in Unreinforced Condition

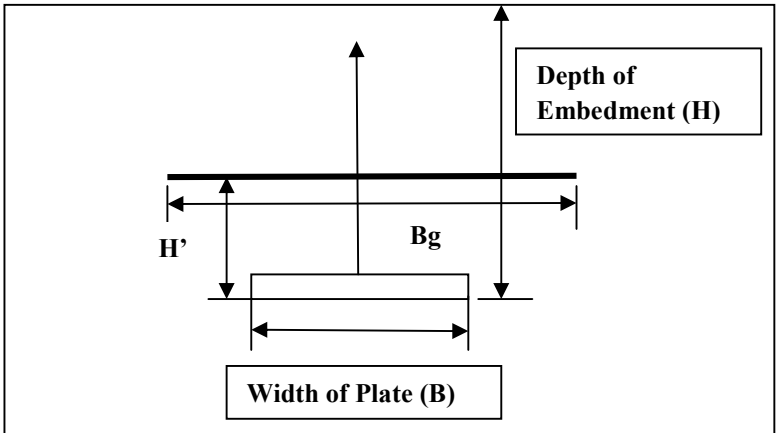

Fig 3.5: Schematic Representation of Model Anchor Test in Reinforced Condition

Table 3.1(a): Test Programme – Model Anchor Plate Test

TEST PROGRAMME- UNREINFORCED			
TYPE	**TEST NAME**	**PLATE SIZE**	**(H/B)**
UR	50_UR_(H/B=1)	50^{mm} X 50^{mm}	1
	50_UR_(H/B=2)		2
	50_UR_(H/B=3)		3
	75_UR_(H/B=1)	75^{mm} X 75^{mm}	1
	75_UR_(H/B=2)		2
	100_UR_(H/B=1) (*)	100^{mm} X 100^{mm}	1

(*)*(Note: Later it has been found from numerical studies that boundary effect influences the results for embedment ratio 2 and 3 in case 100 mm plate. Hence in case of 100 mm plate results are considered for embedment ratio equal to 1 only)*

Table 3.1(b): Test Programme – Model Anchor Plate Test

TEST PROGRAMME- REINFORCED					
TYPE	**TEST NAME**	**PLATE SIZE**	**(H/B)**	**(H'/H)**	**(Bg/B)**
RE	50_RE_(H/B=1)	50^{mm} X 50^{mm}	1	0.25	4
	50_RE_(H/B=2)		2		
	50_RE_(H/B=3)		3		

3.4 Model Test Set up

The model test set up comprises of different equipments assembled in order to achieve suitability in conducting experiment. A brief overview of the equipments used in model test has been furnished herein. Also a schematic representation of the test set up is shown in fig 3.6.

3.4.1 *Equipments*

The model set up consists of the following equipments described as follows

a) Foundation Tank
b) Loading Frame and Pulley Arrangement
c) Displacement Measurement
d) Anchor Plates and Dead Weight for Pullout Test

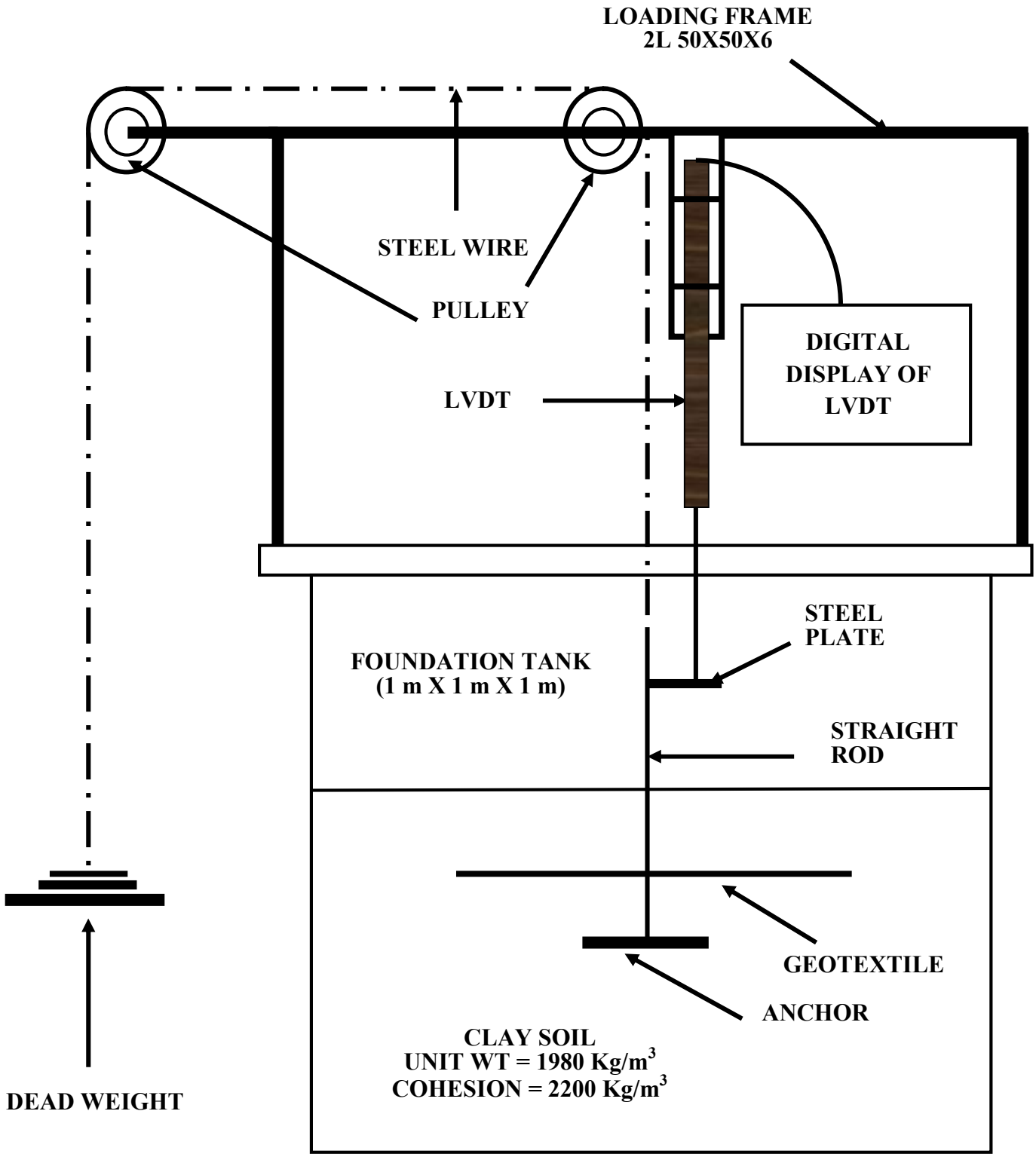

Fig 3.6: Test Set Up

a) Foundation Tank

In the present investigation foundation tank of plan dimension 1.0 m X 1.0 m and 1.0 m depth is used for carrying out pullout test. The dimension of tank is chosen in such a way that the effect of boundary on pullout capacity is negligible for the square anchor plates tested.

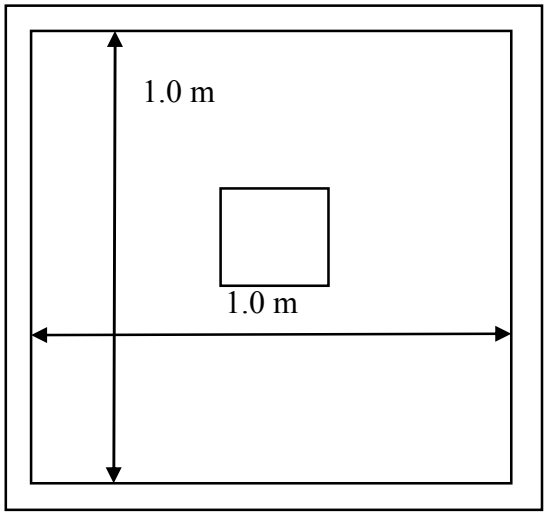

Fig 3.7: Plan View of Tank

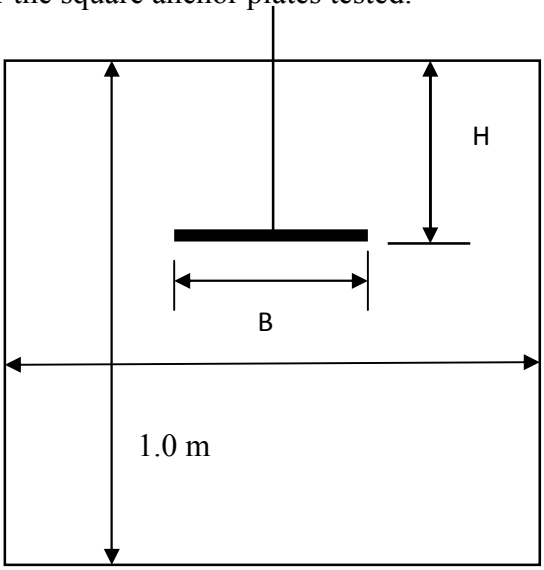

Fig 3.8: Elevation of Tank

A schematic view of the foundation tank is shown in fig 3.7 and 3.8. Results obtained from Numerical analysis also showed that by having a dimension of soil 1.0^{m} X 1.0^{m} X 1.0^{m}, the stress contour reaching to ground surface also finishes well before the soil boundary.

b) Loading Frame & Pulley Arrangement

To apply the monotonic pullout load a loading frame is constructed over the foundation tank forming two angles (2L50X50X6) placed back to back. The anchor plate is attached with a straight rod and pulled through a steel wire by turning over pulley arrangement as shown in fig 3.9.

c) Displacement Measurement

In the present investigation axial movement of anchor plate is measured by Linear Variable Differential Transformer (LVDT) by welding a horizontal flat plate on the straight rod and fixing the LVDT over that plate. Least count of LVDT is 0.01 mm. LVDT is supported with the help of an arrangement as shown fig 3.10 from the loading frame and fixed in its position with proper fastening

d) Anchor Plates and Dead Weight for Pullout Test

In the present investigation Square Anchor plates of mild steel is used. As shown in fig 3.11(b) for the ongoing investigation three different sizes of square anchor plates of width 50 mm, 75 mm and 100 mm with respective embedment ratio and with or without geotextile is used to estimate the Pullout capacity required up to a certain specified axial movement of anchor plates. For carrying out model test pullout load is applied through dead weights of different increment given as 180 gm, 360 gm, 575 gm, 1412 gm, 1960 gm, 2270 gm and 4500 gm as exhibited in fig 3.11(a). During pullout test anchor plate is attached with a 10 mm diameter shaft through a slotted hole at the middle of anchor plate, which in turn is tied with the steel wire used for pulling arrangement through pulley mechanism. During preparation of embedded soil after placement of anchor the loading arrangement supports a minimum load to keep the anchor-shaft assembly in proper alignment. This minimum load is taken as the zero load for model test results.

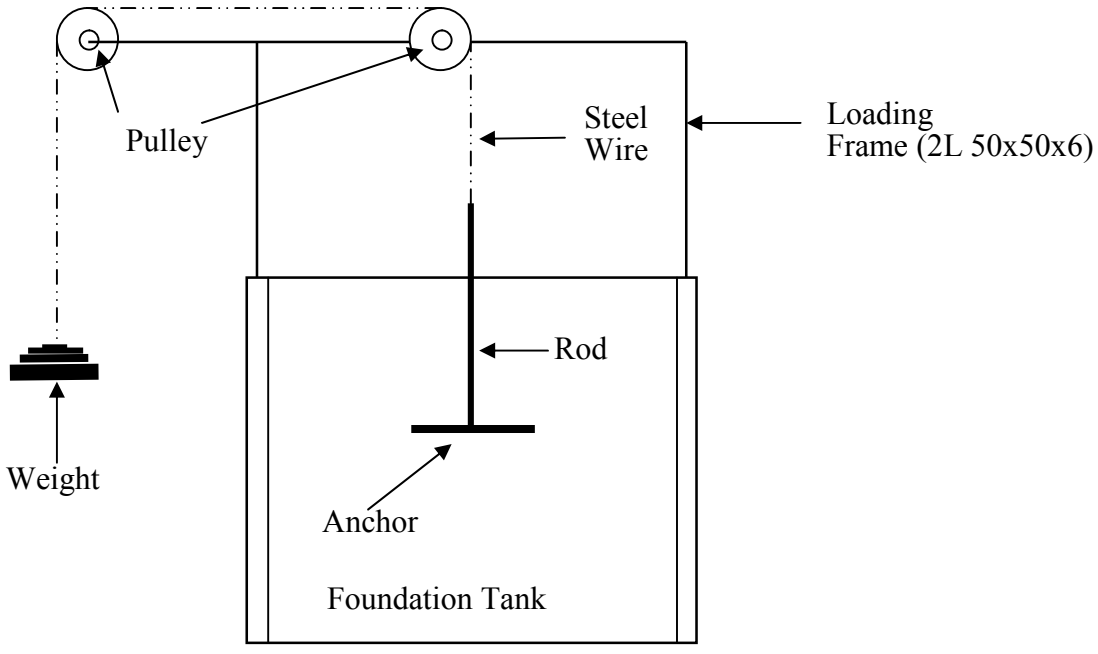

Fig 3.9: Loading Arrangement for Model Test

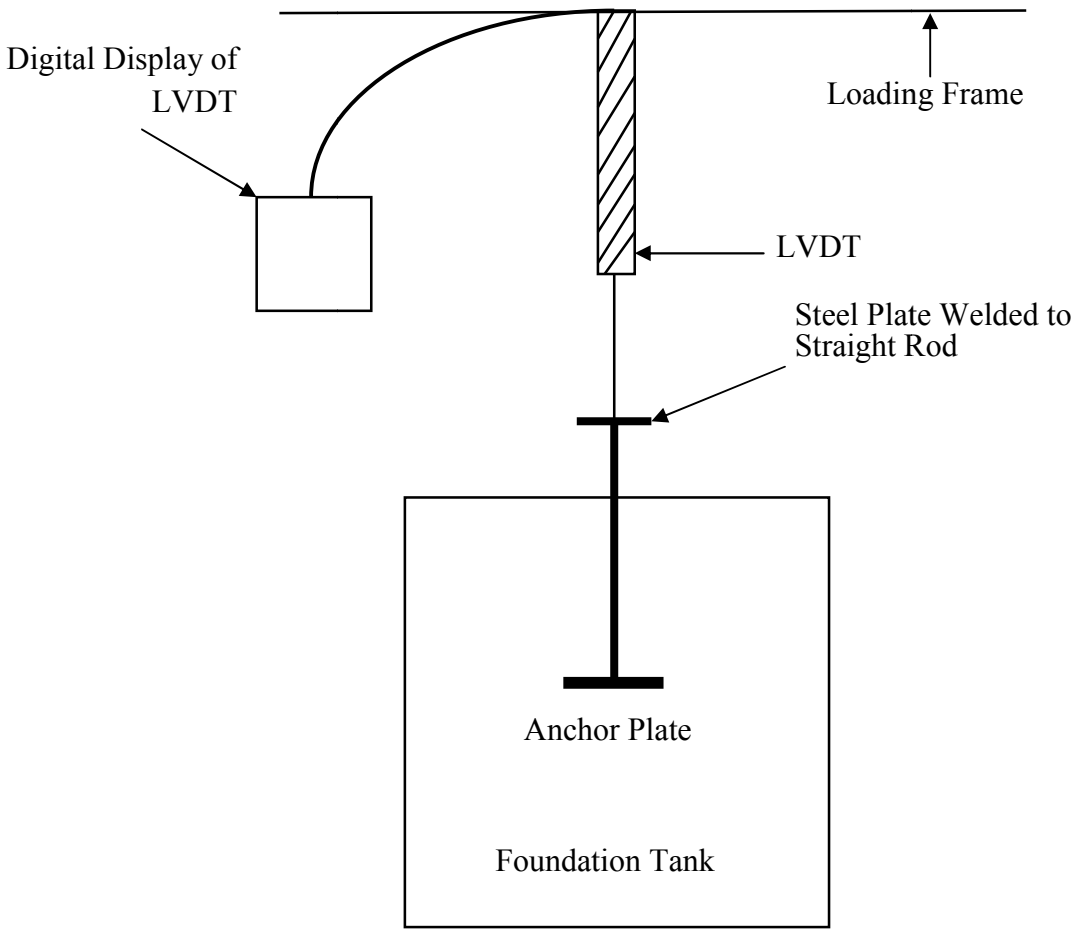

Fig 3.10: Displacement Measurement by LVDT

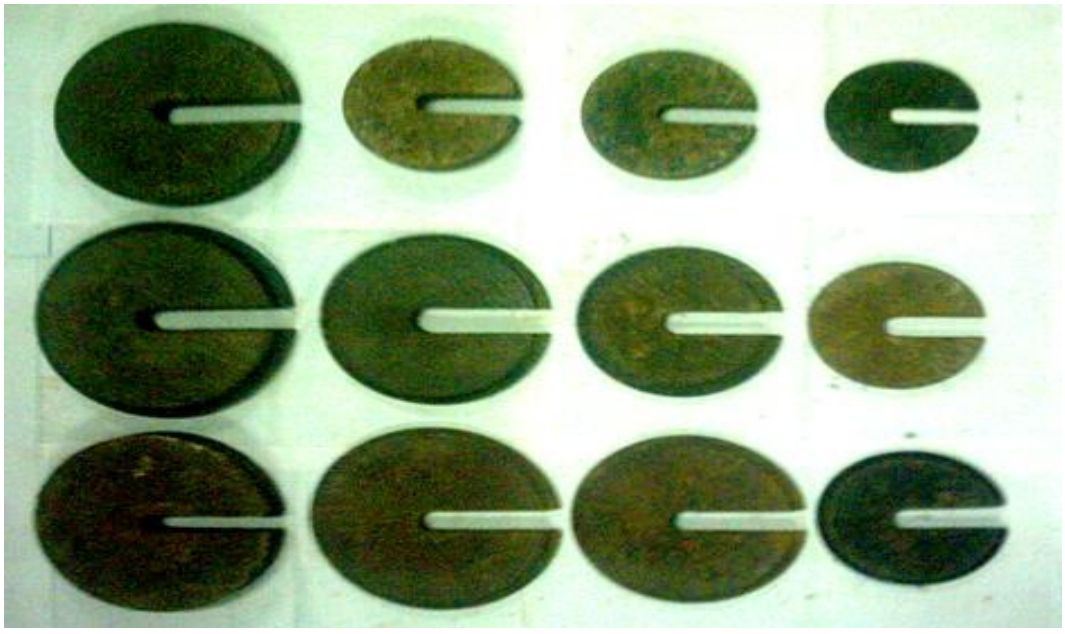

Fig 3.11(a): Dead Weight used for Pullout Test

Fig 3.11(b): 50 mm, 75 mm, 100 mm Square Anchor Plates used for Pullout Test

3.5 Experimental Procedure

3.5.1 Model Anchor Test

Pullout test for the three different size square anchor plates has been carried out under different embedment condition for unreinforced as well as for reinforced case. For all the model test foundation tank described earlier of size 1.0 ^{m} X 1.0 ^{m} X 1.0 ^{m} is used following the steps mentioned below. To carry out pullout test of anchor plates in cohesive soil, one of the critical point is compaction control and to achieve for homogeneity in the system.

a) ***Calibration Curve*:** For the present investigation an effort was made to calibrate between number of blows required to achieve a certain degree of compaction and the corresponding dry density and shear strength achieved. Calculation for number blows required to achieve standard proctor density is specified below. The need of calibration curve arrived due to the problem involved in achieving required density and strength in the foundation tank with the number blows counted from Standard Proctor procedure. The difference in the number blows required to achieve a certain degree of compaction is due to the change in the volume of soil involved in standard laboratory procedure of standard Proctor test with the volume of soil involved for model test.

As per the Indian standard equivalent of the Standard Proctor procedure for laboratory testing of compaction, called *Light Compaction* Test (*IS:2720, Part VII-1974*),

Volume of mould = 1000 cc

Weight of Hammer = 2.6 Kg

Height of Drop = 310 mm

Soil is compacted in three layers with each layer tamped for 25 times.

Total Compactive Effort required to compact 1000 cc of soil = 3X25X2.6X9.81X0.31 N-m

= 593.0145 N-m

In present investigation for 50 ^{mm} square anchor plate with embedment ratio one (H/B =1) the volume of soil required to be compacted = 0.05X1.0X1.0 = 0.05 m^3 = 50000 cc

Total Compactive Effort required = 593.0145X50 = 29650.725 N-m

Weight of Rammer used in model test = 4.5 Kg

Average Height of Drop = 250 mm

Total Number blows required for 0.05 m^3 of soil = 29650.725/ (4.5X9.81X0.25)

= 2686.67 ≈ 2687

Total Number of blows required as per Light Compaction per m^3 of soil = 2687/0.05 = 53740

As mentioned above, calibration curve for different embedment volume is established based on the number of blows and achieved strength and density and expressed in terms of Number blows of rammer required per 1 m^3 of soil as shown in fig 3.12(a) and fig 3.12(b).

Based on the calibration plot obtained in this study, the dry density and strength showed little increments with increase in compactive effort at a water content of OMC+4 %, which was 18% in this present study. To achieve the required amount of compaction control a particular range of number of blows per 1 m^3 of soil is specified which in this present study is 100,000 to 150,000. The obtained number of blows per m^3 of soil from calibration curve is approximately double the numbers required from interpolated results of light compaction. This can be accounted on the basis of quality control required during compaction. As stated earlier the volume of soil to be compacted differs from the standard light compaction considerably, thus the quality control needed during compaction to achieve a certain degree of strength for cohesive soil must be ascertained.

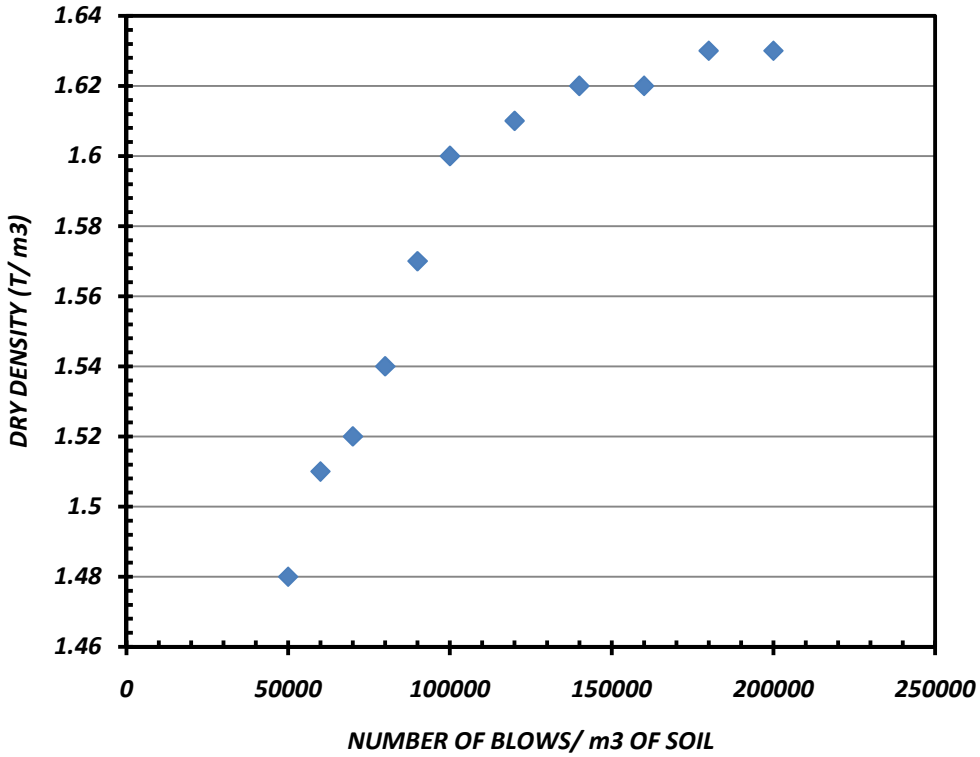

Fig 3.12(a): Calibration Plot of Dry Density and Number of Blows

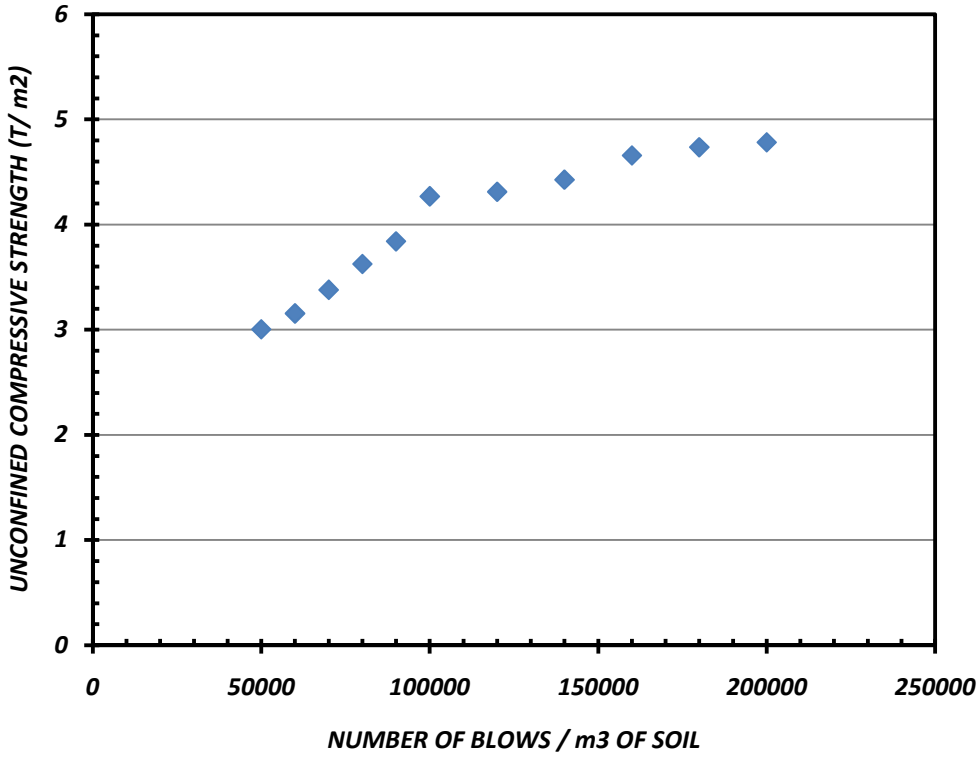

Fig 3.12(b): Calibration Plot of Unconfined Compressive Strength and Number of Blows

b) ***Preparation of Soil Bed:*** Before the placement of anchor a minimum soil bed thickness of 200 mm is provided as cushion for all the model tests. For the reinforced cases

the minimum thickness of soil bed is specified to 300 mm as the geosynthetic reinforcement tends to distribute the generated tensile stress to the soil below the anchor plate also. The same is specified on the basis of stress contour obtained from numerical analysis discussed in Chapter-4. The soil bed was also prepared to achieve the same density and strength that of the embedded soil to keep homogeneity of the entire soil assembly, and the top surface of soil bed is leveled properly for the placement of anchor.

c) ***Placement of Anchor & Preparation of Embedded Soil:*** After the preparation of soil bed anchor plate is placed horizontally at the middle of soil bed along with a 10 mm diameter shaft attached vertically to the anchor plate. This arrangement is tied through a steel wire to the counterweight by pulley arrangement as discussed earlier in this chapter. With sufficient precautions to keep the anchor – shaft assembly vertical, embedded soil is prepared depending on the number of blows referring to Table 3.2. The entire volume of soil is compacted in 2 to 3 layers depending on which approximate number of blows per layer is calculated. After preparing the embedded soil total number of blows for the entire volume of soil is noted.

d) ***Placement of Reinforcement:*** In the present study, reinforcement in the form of geotextile of width four times the width of plate is used, and placed at a distance of 0.25 times the depth of embedment from the bottom of anchor plate. A hole of 10 mm is made at the centre of the sheet to allow the shaft, connected to the anchor. After the placement of geotextile horizontally over the desired level the embedded soil left, are compacted in layers as discussed above.

e) ***Arrangement for Displacement Measurement*:** A horizontal flat plate is welded to the top of the vertical shaft attached with the anchor plate for the aid of displacement measurement. LVDT is placed vertically over this plate keeping same alignment with the shaft and attached firmly to the loading frame arrangement. After fixing, the LVDT is switched on and sufficient time is provided for the digital readings of the monitor to get adjusted to a value before the commencement of pullout test. The reading at the start of the pullout test on the monitor is taken as the zero value for displacement.

f) ***Pullout Test:*** Pullout test is carried out by different incremental loading through dead loads placed on the hanger attached to the steel wire and pulley arrangement. For each load increment the LVDT reading at the end of fluctuation is recorded and afterwards next load increment is applied. This load increment is continued until indicated by observed failure or the displacement exceeds 10% of plate dimension. The Load vs Displacement curves

obtained through the model tests are used to find out the ultimate pullout capacity by using double tangent method.

Table 3.2: Comparison of Number of Blows

TEST CONDITION			*NUMBER OF BLOWS*			
PLATE SIZE	*EMBEDMENT RATIO*	*VOLUME OF SOIL*	*LIGHT COMPACTION*	*CALIBRATION PLOT RANGE*		*Actual Value Adopted(*)*
				MINIMUM	*MAXIMUM*	
50 mm	1	0.05 m^3	2687	5000	7500	6300
	2	0.1 m^3	5374	10000	15000	10700
	3	0.15 m^3	8061	15000	22500	16700
75 mm	1	0.075 m^3	4031	7500	11250	8200
	2	0.15 m^3	8061	15000	22500	17300
	3	0.225 m^3	12092	22500	33750	-
100 mm	1	0.1 m^3	5374	10000	15000	13500
	2	0.2 m^3	10748	20000	30000	-
	3	0.3 m^3	16122	30000	45000	-

(*) To achieve the desired strength of soil

3.5.2 Model Anchor Test Results

In this section, the pullout test results with different sizes of model anchor plates used in the investigation have been presented for both reinforced and unreinforced soil. During pullout tests of anchor plates in both reinforced and unreinforced soil, the axial movement corresponding to incremental uplift load was recorded. For each tests, uplift load and axial movement values has been shown for different sizes of plates in figs 3.12(a) to 3.12(i) for both reinforced and unreinforced soil for different embedment ratio H/B. The width of geosynthetics has been kept to four times the width of plate at a distance of 0.25 times the embedment depth from bottom of plate. The ultimate capacity in each case was obtained by conventional double tangent method as shown in these figures. For all the tests conducted, the ultimate uplift capacities as well as ultimate displacements obtained were read out from the graphs and presented in Table 3.3 for different sizes of anchors used in the investigation.

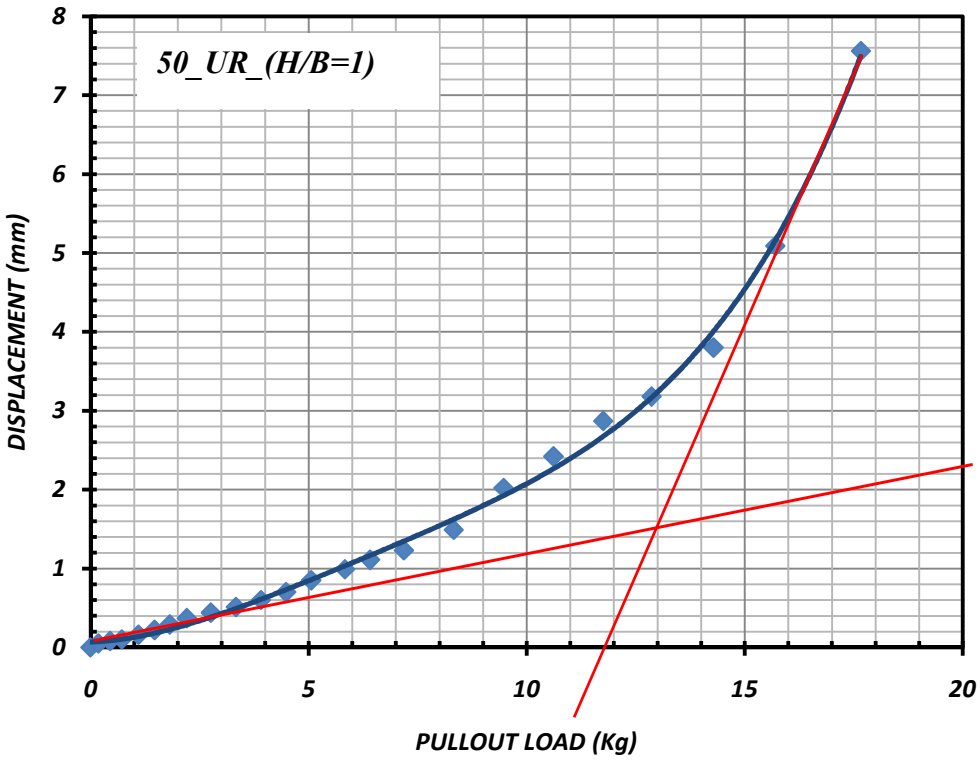

Fig 3.13(a): Typical Load vs Axial Movement for 50 ^{mm} Square Plate with (H/B =1) (Unreinforced)

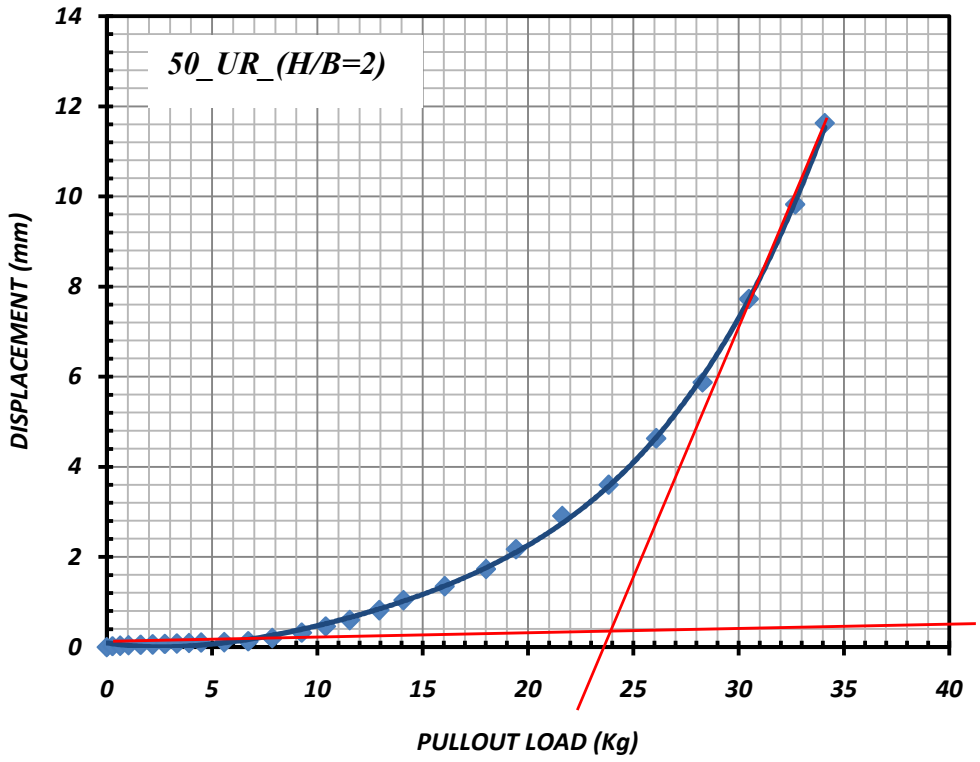

Fig 3.13(b): Typical Load vs Axial Movement for 50 ^{mm} Square Plate with (H/B =2) (Unreinforced)

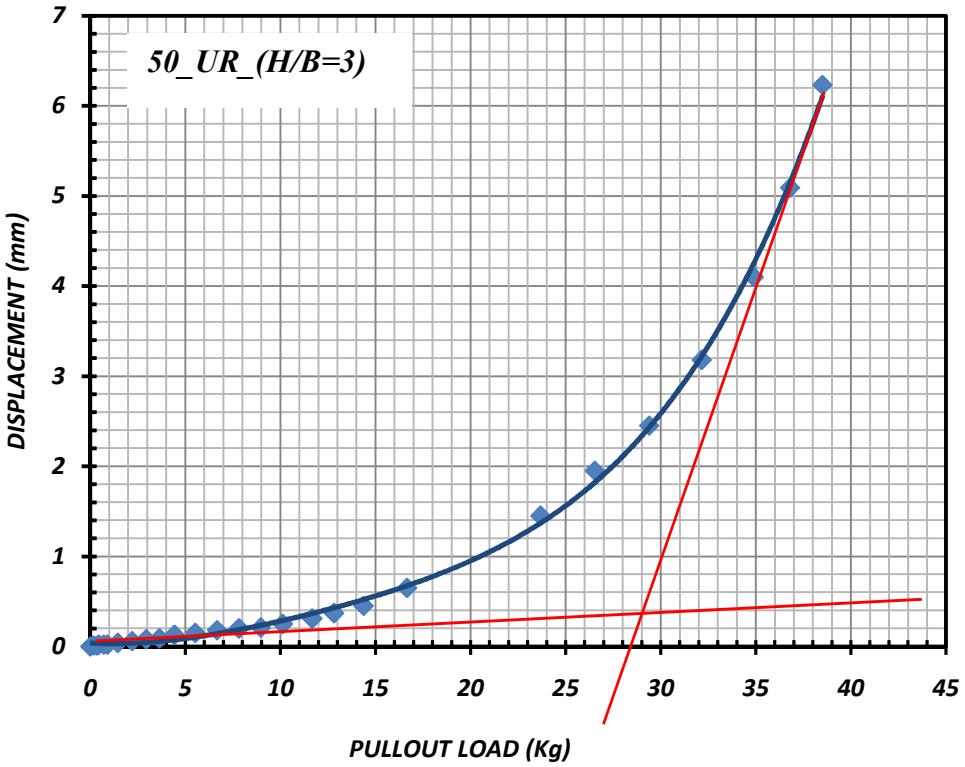

Fig 3.13(c): Typical Load vs Axial Movement for 50 mm Square Plate with (H/B =3) (Unreinforced)

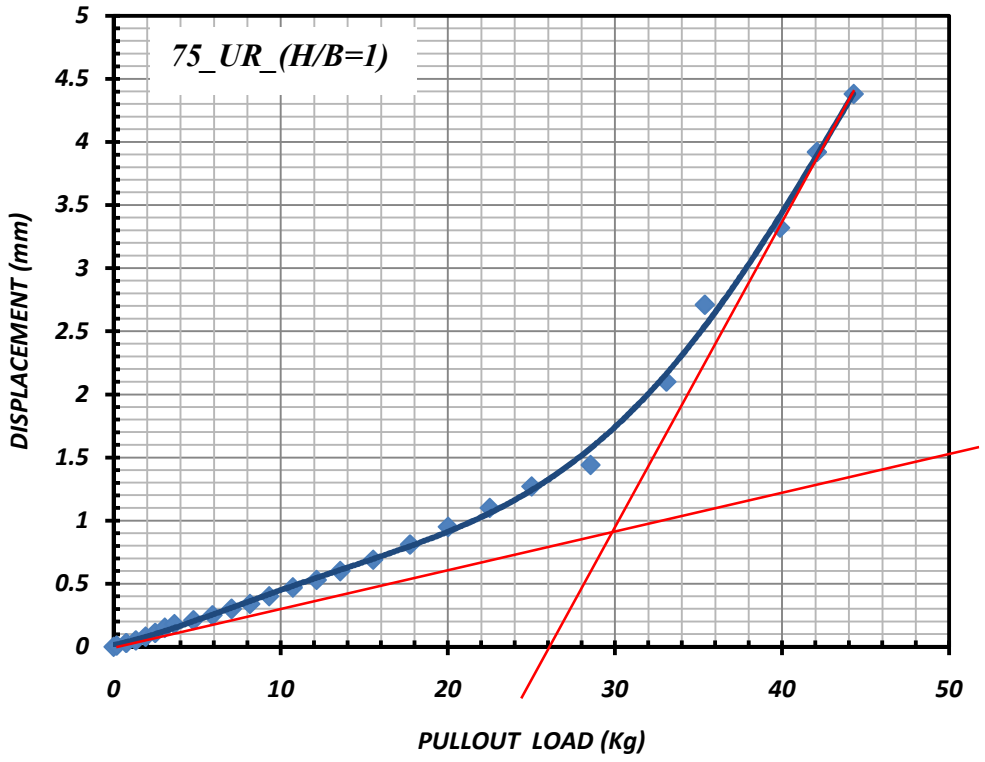

Fig 3.13(d): Typical Load vs Axial Movement for 75 mm Square Plate with (H/B =1) (Unreinforced)

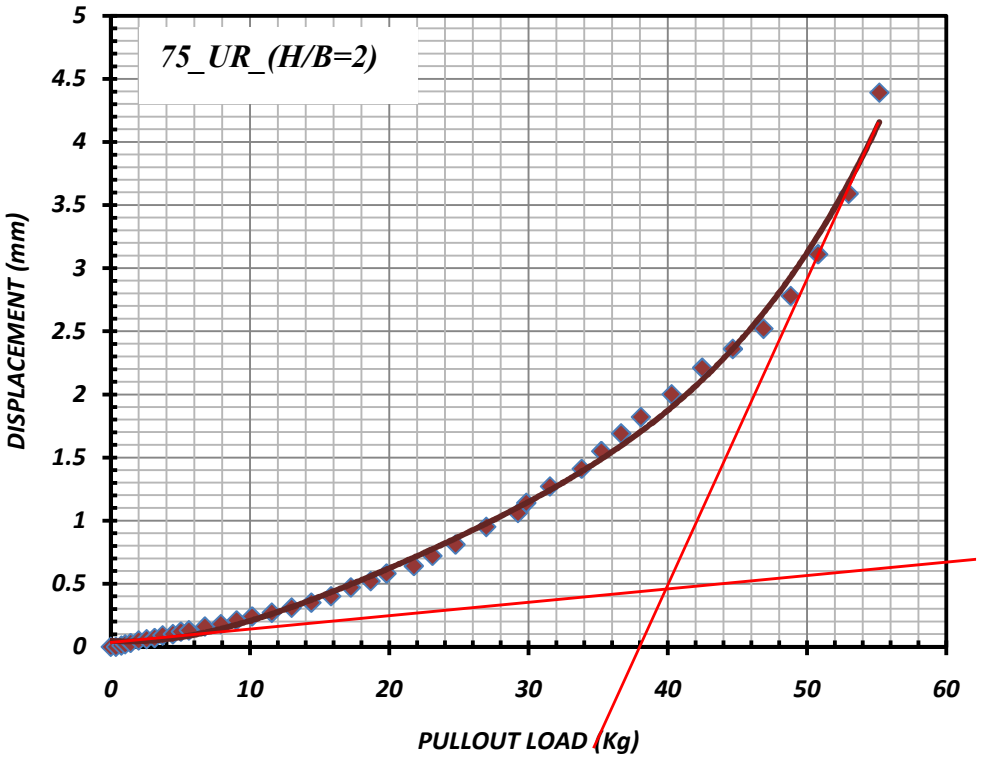

Fig 3.13(e): Typical Load vs Axial Movement for 75 mm Square Plate with (H/B =2) (Unreinforced)

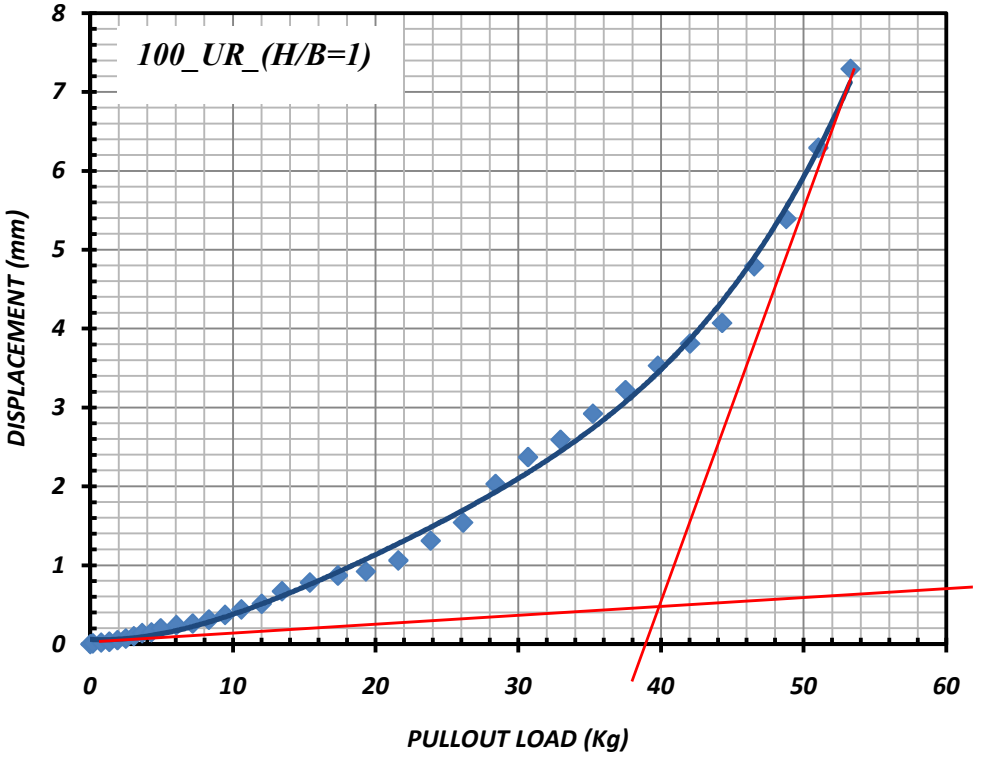

Fig 3.13(f): Typical Load vs Axial Movement for 100 mm Square Plate with (H/B =1) (Unreinforced)

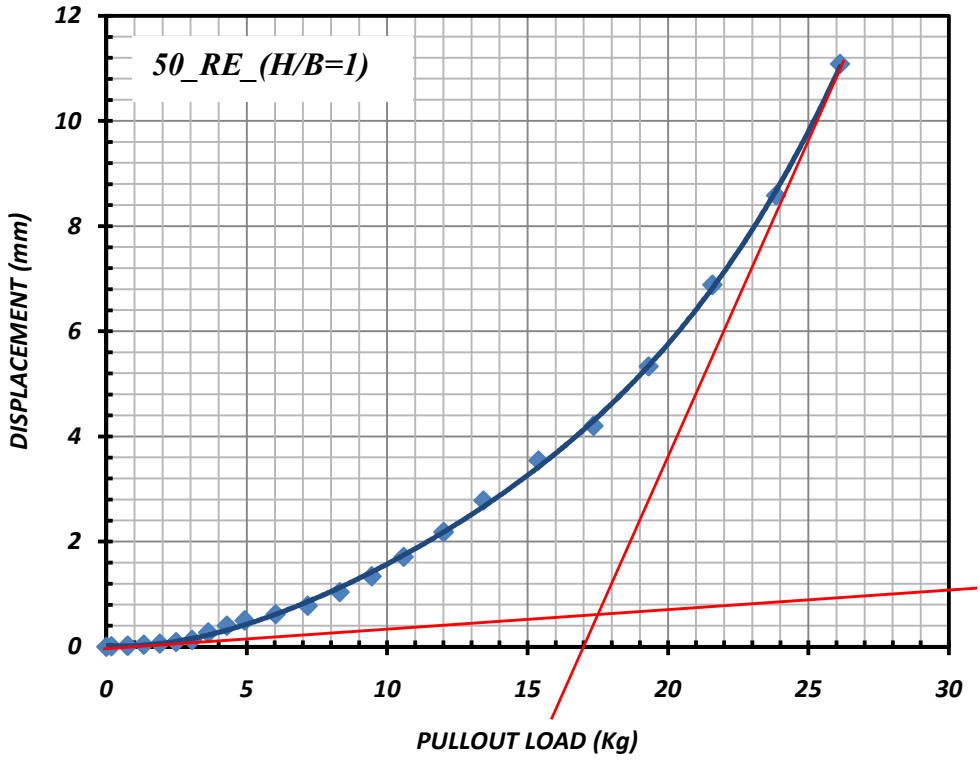

Fig 3.13(g): Typical Load vs Axial Movement for 50 ^{mm} Square Plate with (H/B =1) (Reinforced)

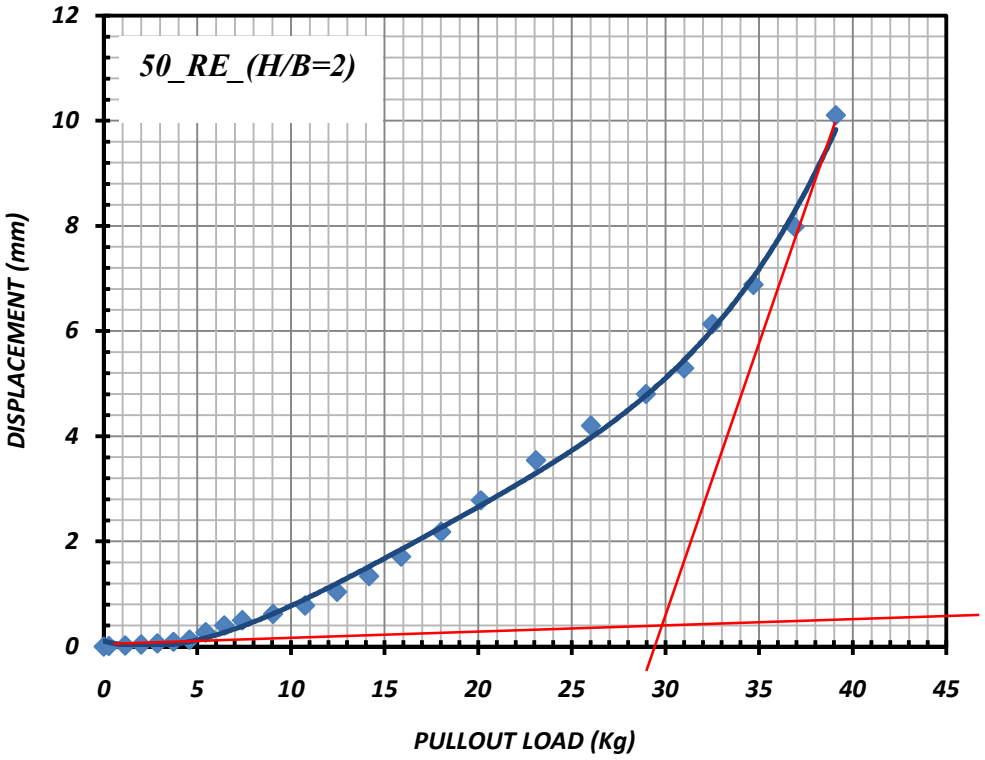

Fig 3.13(h): Typical Load vs Axial Movement for 50 ^{mm} Square Plate with (H/B =2) (Reinforced)

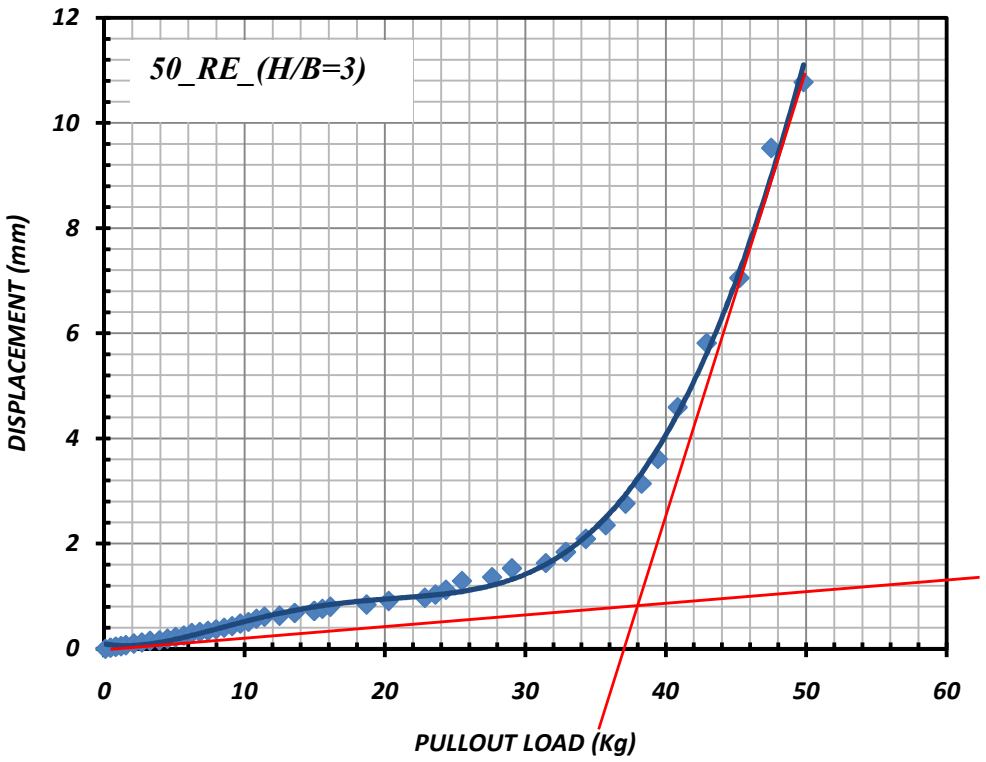

Fig 3.13(i): Typical Load vs Axial Movement for 50 [mm] Square Plate with (H/B =3) (Reinforced)

Table 3.3: Model Test Results – Unreinforced & Reinforced

TYPE	*TEST NAME*	*PULLOUT LOAD (F) (KG)*	*DISP (mm)*	*WEIGHT OF SOIL(W)*	*BREAKOUT FACTOR (F-W)/(A*Cu)*	*EMBEDMENT RATIO (H/B)*
UR	50_UR_(H/B =1)	13	3.6	0.225	2.56	1
	50_UR_(H/B =2)	24	3.6	0.45	4.71	2
	50_UR_(H/B =3)	29	2	0.675	5.67	3
UR	75_UR_(H/B =1)	30	1.5	0.76	2.6	1
	75_UR_(H/B =2)	40	2.5	1.52	3.42	2
	100_UR_(H/B =1)	40	3.4	1.8	1.91	1
RE	50_RE_(H/B =1)	17.5	5.2	0.225	3.46	1
	50_RE_(H/B =2)	30	5.2	0.45	5.91	2
	50_RE_(H/B =3)	38	2.8	0.675	7.47	3

Chapter 4

NUMERICAL STUDY

4.1 General

Several numerical techniques have been developed to analyze the behavior of plate anchors in reinforced and unreinforced soils with different loading conditions. The numerical modeling of plate anchors is associated with relevant input data like different sizes of anchor plates, depth of embedment and position of reinforcement.

Finite element analysis software ABAQUS v6.14 is used for the numerical modelling of both reinforced and unreinforced analysis. The verification study of computed results has been done with the results obtained from the experimental studies of model test. It builds the confidence for the use of numerical modelling techniques with the complex problems which are difficult to model in the test field.

The general layout of the problem is shown in Fig. 4.1, where the horizontal rough anchor plate placed at a depth of 'H' from the ground surface with plate width of 'B'. The undrained cohesion of soil is 'C_u' and the density is 'ϒ'. The soil is reinforced with single layer of geotextile at 0.25 times of depth of embedment measured from the bottom of plate. The corresponding Load-Displacement behavior has been calculated for the square plates of sizes 50 mm, 75 mm and 100 mm. The Embedment Ratio used in the analysis are varied form 1 to 3, having the width of geotextile limited to four times the width of plate. Factors considered in the analysis are embedment ratio, size of the plate, width of reinforcement.

4.2 Finite Element Modeling

The finite element software ABAQUS-v6.14 has been used to create the model graphically, run the analysis, and then view the results. The software ABAQUS can handle a wide array of problems ranging from simple linear problems to more complicated nonlinear analyses. It contains nine modules that divide the modeling tasks into functional units. These modules are: Part, Property, Assembly, Step, Interaction, Load, Mesh, Job, and Visualization. Schematic representation of the present problem is shown in Fig.4.1.

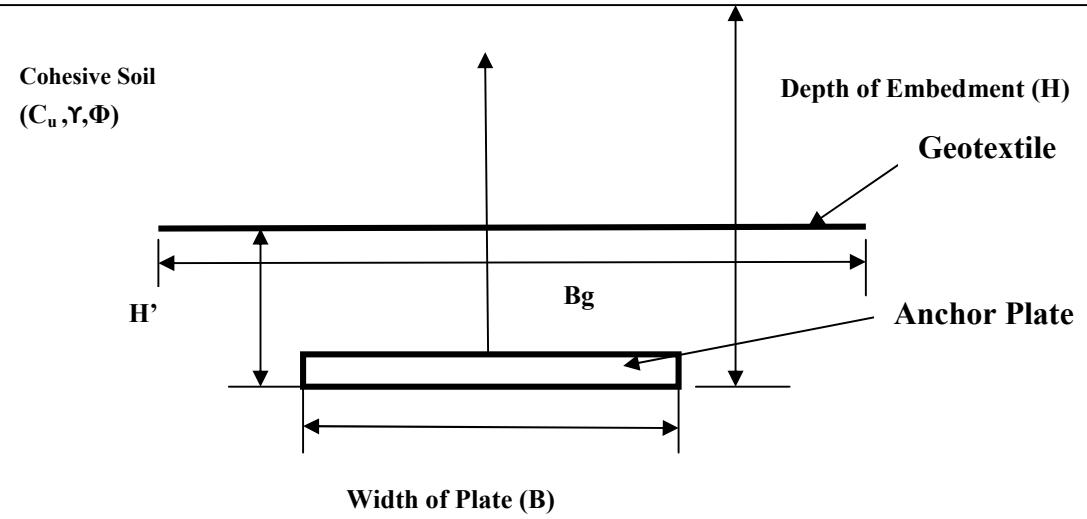

Fig 4.1: Schematic Representation of Model Anchor Test in Reinforced Condition

The model consists of three parts; the soil, the anchor and the reinforcement. The soil has been modelled using Mohr-Coulomb model available in the software.The anchor and Geotextile have been modelled as linear-elastic materials.

Total three square anchor plates of size 50mm, 75 mm and 100mm have been considered for analysis. The width of reinforcement has been kept four times the width of anchor plate in the model. The position of reinforcement is 0.25 times the embedment depth which is proved to be generating more load carrying capacity of anchor as described in literature. Single layer of geotextile reinforcement used for the analysis. The size of soil medium defined is 1m x 1m which is enough to minimize the influence of boundary constraints on the behavior of anchor plates. Clay soil has been used for the study on plate anchors; with square shape anchor plates in reinforced and unreinforced soils. Various laboratory tests have been conducted to define the properties of soil as given in Table 4.1. Determination of material properties for anchor plate defined in Table 4.1 have been conducted through tension test of a mild steel specimen in UTM (Ref: 3.4.1c), page 33) and for the geotextile those values have been taken from Tension test specified in chapter 3(Ref: 3.4.1b), page 32).

Table 4.1: Properties of Materials considered in Numerical Modelling

Properties of Material			
SOIL		**Anchor Plate**	
Property	Value	Property	Value
Density (ϒ) (Kg/m^3)	1980	Density (ϒ) (Kg/m^3)	7850
Cohesion(Cu) (Kg/m^2)	2200	Poisson's Ratio (μ)	0.29
Angle of Internal Friction, Φ, Deg	5	Young's Modulus (Es) (Mpa)	2 X 10^5
Tensile Cut-off Stress (Kg/m^2)	5000	**Geotextile**	
Liquid Limit (WL)(%)	42	Density (ϒ) (Kg/m^3)	0.146
Plastic Limit (Wp)(%)	24	Poisson's Ratio (μ)	0.42
Plasticity Index(Ip)	18	Young's Modulus (Es) (Gpa)	0.42
Poisson's Ratio (μ)	0.33	Tensile Strength (KN/m)	27.6
Young's Modulus (Es) (Mpa)	110	Thickness (mm)	4.6

The Part module is used to create individual parts and to sketch the geometry of that part. The part can be deformable, discrete rigid, or analytical rigid. Also, the available shape features are solids, wires, cuts, and blends. For the present study a solid homogeneous part has been considered for soil body and for anchor plate as well as geotextile, 2D wire elements has been considered. The Property module is used to define the properties of each part, including the material and geometry. An elastic, isotropic material has been chosen, where Young's Modulus and Poisson's ratio are defined for anchor material, whereas for soil along with this plasticity has been defined using Mohr-Coulomb plasticity model. The geosynthetic has been modeled as elastic element with No Compression and Isotropic hardening. The Assembly module creates an assembly of the parts in the global coordinate system. The Step module allows the user to create analysis steps and output requests. The first analysis step is Initial, which is the default that is already there. For the model, a Load step was added. There are many types of loads that can be added: static, dynamic, heat transfer, soils, and geostatic. A static, general load was chosen, and the NLGEOM command was turned on. This option includes nonlinear effects of large displacements. The Interaction module is used to specify mechanical and thermal interactions between regions. This module allowed for defining Soil Structure Interaction properties at the interface of soil and anchor plate as well as for the soil geosynthetics interface. Loads, boundary conditions, and fields are created in the Load module. These are step dependent, meaning that the analysis step in which they are performed must be specified. The Step was created to calculate the pullout load required for a prescribed displacement of anchor plate for monotonic loading, defined as RAMP. The Mesh

module allows the user to create the mesh and choose the number and type of elements to be used in the analysis. The mesh control and element type used for the model can be obtained from Table 4.2. For the current study soil was modeled with CPE4R element type of quadrilateral shape and for anchor as well as for geotextile B21 element type of line shape is considered. The model for Reinforced case contains the maximum number of element and nodes which are 637 and 690 respectively in the current study. Once the previously discussed modules are complete, the Job module is used to create the input file and submit the job for analysis. Then the Visualization module is used to view and interpret the results obtained

Table 4.2: Mesh Statistics considered in Numerical Modelling

INSTANCE NAME	ELEMENT TYPE	ELEMENTS	NODES	ELEMENT SHAPE	GEOMETRIC ORDER
SOIL	CPE4R	625	676	QUADRILATERAL	LINEAR
ANCHOR	B21	2	3	LINEAR	LINEAR
GEOTEXTILE	B21	10	11	LINEAR	LINEAR

4.3 Salient Aspects of Numerical Modeling:

The following salient aspects have been considered in Numerical Analyses:

1) Numerical analysis is carried out based on 2D plain strain condition
2) Geotextile is modeled as linear elastic material
3) Soil is modeled with Mohr-Coulomb plasticity model with specific Tension Cut-off value, which proved to be a very important parameter for calculation of Pullout capacity. Although the effect of this parameter was found to be pronounced for larger plate sizes and higher embedment depth.
4) Interaction at the soil-anchor interface is formulated considering soil as slave surface and anchor as master surface with Node to Surface discretization due to the rigidity of anchor material than the deformable soil, with small sliding behavior accounting for the cohesive property used in the interaction property. The tangential and Normal behavior at the soil-anchor interface was specified as Penalty (Standard) provided with coefficient of friction obtained from Direct Shear Test. Separation of anchor plate from initial slave surface was allowed with non-linear stiffness effects in normal behavior.

5) The Soil-Geotextile interface is formulated considering soil as slave surface and geotextile as master surface with Surface to Surface discretization due to the flexibility of geotextile with respect to deformable soil body. Small sliding behavior accounting for the cohesive property and tangential as well as normal behavior, similar to that specified in soil-anchor interaction, was specified with no separation allowed for the geotextile from initial slave surface.

4.4 Finite Element Formulation

For the present investigation soil has been modeled with 2D isoparametric quadrilateral element of linear geometric order and for anchor and geotextile 2D isoparametric linear element of linear geometric order was considered. Finite element formulation for the above mentioned elements have been presented herein. Isoparametric finite elements are based on the parametric definition of both coordinate and displacement functions. The same shape functions are used for specification of the element shape and for interpolation of the displacement field.

The 2D generalized displacement vector {u} at a point within an element is related to nodal displacement vector {q} by shape function matrix [N] as,

$$\{u\} = \begin{pmatrix} u \\ v \end{pmatrix} = [N]\ \{q\} \qquad \text{…….(4.1)}$$

where {u} = displacement vector at the point within an element,

$$\{q\}^T = \{u_1, v_1, u_2, v_2 \text{ ……., } u_8, v_8\} \qquad \text{…….(4.2)}$$

$$\text{and } [N] = \begin{bmatrix} N1 & 0 & N2 & 0 & \cdots \\ 0 & N1 & 0 & N2 & \cdots \end{bmatrix} \qquad \text{……..(4.3)}$$

The strain vector, {ε} is expressed in terms of the nodal displacements as given below :

$$\{\varepsilon\} = \begin{Bmatrix} \varepsilon_x \\ \varepsilon_y \\ \gamma_{xy} \end{Bmatrix} = \begin{Bmatrix} \dfrac{\partial u}{\partial x} \\ \dfrac{\partial v}{\partial y} \\ \dfrac{\partial u}{\partial y} + \dfrac{\partial v}{\partial x} \end{Bmatrix} = [B]\ \{q\} \qquad \text{…….(4.4)}$$

where {ε} = strain vector

[B] = strain displacement transformation matrix consisting of derivatives of shape function

i.e. [B] = [$[B_1]$ $[B_2]$ ……..$[B_i]$

$$\text{and } [B_i]=\begin{bmatrix} \frac{\partial N_i}{\partial x} & 0 \\ 0 & \frac{\partial N_i}{\partial y} \\ \frac{\partial N_i}{\partial y} & \frac{\partial N_i}{\partial x} \end{bmatrix} \qquad \text{……(4.5)}$$

The stress-strain relationship for elastic material is expressed as,

$$\{\sigma\} = [D_e]\ \{\varepsilon\}$$

$$\{\sigma\} = \begin{Bmatrix} \sigma_x \\ \sigma_y \\ \sigma_z \\ \tau_{xy} \\ \tau_{yx} \\ \tau_{zx} \end{Bmatrix} = \frac{E\,(1-\upsilon)}{(1+\upsilon)\,(1-2\upsilon)} \begin{bmatrix} 1 & \frac{\upsilon}{1-\upsilon} & \frac{\upsilon}{1-\upsilon} & 0 & 0 & 0 \\ & 1 & \frac{1}{1-\upsilon} & 0 & 0 & 0 \\ & & 1 & 0 & 0 & 0 \\ & & & \frac{1-2\upsilon}{2(1-\upsilon)} & 0 & 0 \\ & & & & \frac{1-2\upsilon}{2(1-\upsilon)} & 0 \\ & & & & & \frac{1-2\upsilon}{2(1-\upsilon)} \end{bmatrix} \qquad \text{….(4.6)}$$

and $[D_e]$ = elasticity matrix

where E = modulus of elasticity, υ being the Poisson's ratio

The shape functions used for describing the geometry of the element and displacement variation are expressed in terms of local co-ordinates (s, t) and it is required to determine the derivatives of the functions with respect to global coordinates (x, y).

From chain rule of differentiation the relationship between two co-ordinate systems is given below :

$$\begin{Bmatrix} \frac{\partial N_i}{\partial x} \\ \frac{\partial N_i}{\partial y} \end{Bmatrix} = J^{-1} \begin{Bmatrix} \frac{\partial N_i}{\partial s} \\ \frac{\partial N_i}{\partial t} \end{Bmatrix} \qquad \text{……..(4.7)}$$

where [J] = Jacobian Matrix = $\begin{bmatrix} \frac{\partial x}{\partial s} & \frac{\partial y}{\partial s} \\ \frac{\partial x}{\partial t} & \frac{\partial y}{\partial t} \end{bmatrix}$ ……..(4.8)

and $[J]^{-1}$ is the inverse of Jacobian Matrix

The determinant of the Jacobian matrix [J] is used for the transformation of integrals from the global coordinate system to the local coordinate system:

$dV = dx\ dy = |J|\, ds\ dt$

The variational function for the displacement method is given by the potential energy Π_p of the system and it can be expressed as:

$$\Pi_p = \int_v dv\ (u, v, w)\ dv - \int_v (\bar{x}\, u + \bar{y}\, v + \bar{z}\, w)\ dv \qquad \text{…….(4.9)}$$

Where, dv (u, v, w) = strain energy per unit volume

$\bar{x}$, $\bar{y}$, $\bar{z}$ = components of body forces

v = volume of element

For a linearly elastic isotropic material behaviour,

$$dv = \tfrac{1}{2} \{\varepsilon\}^T \{\sigma\}\ dv \qquad \text{…..(4.10)}$$

$$\therefore \Pi_p = \int_v \tfrac{1}{2} \{\varepsilon\}^T [D_e] \{\varepsilon\}\ dv - \int_v \{u\}^T \{F\}\ dv \qquad \text{…..(4.11)}$$

$$= \int_v \tfrac{1}{2} \{q\}^T [B]^T [D_e] [B] \{q\}\ dv - \int_v \{q\}^T [N]^T \{F\}\ dv \qquad \text{…..(4.12)}$$

where, $\{F\} = \{\ \bar{x}, \bar{y}, \bar{z}\ \}^T$

Now for static equilibrium of a system, condition of minimum potential energy is to apply for

which $\dfrac{\partial(\Pi_p)}{\partial\{q\}} = 0$ …..(4.13)

Now $\frac{\partial(\Pi_p)}{\partial\{q\}} = \int_v [B]^T [D_e] [B] \{q\} dv - \int_v [N]^T \{F\} dv = 0$ …..(4.14)

Or, $\int_v [B]^T [D_e] [B] \{q\} dv = \int_v [N]^T \{F\} dv$ …..(4.15)

The above equation may be represented by

$[K] \{q\} = \{Q\}$

Where, $[K] = \int_v [B]^T [D_e] [B] dv =$ stiffness matrix ….(4.16)

And, $\{Q\} = \int_v [N]^T \{F\} dv$ = Equivalent nodal vector ……(4.17)

In global relationship the stiffness matrix [K] for the entire system is given by

$[K] \{\delta\} = \{F_s\}$ ……(4.18)

Where, [K] = global stiffness matrix

$\{\delta\}$ = global nodal displacement

$\{F_s\}$ = global nodal force vector

The global stiffness matrix has been obtained by adding appropriately for the individual contributions from element which are common to a node.

2D-Linear Element:

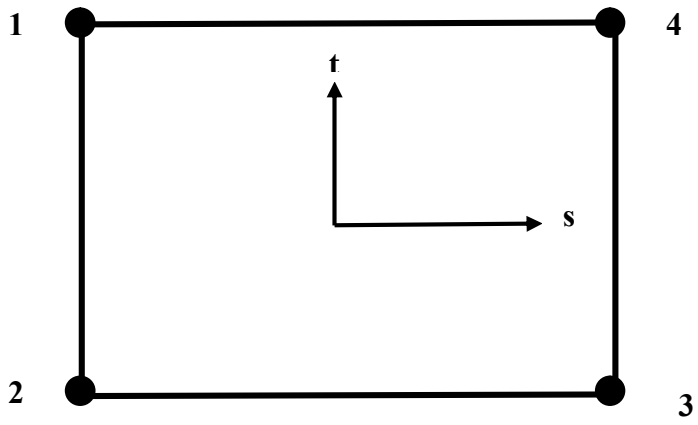

Fig 4.2: 2D Isoparametric Linear element in vertical plane with Local Co-ordinates

The shape functions of 4 nodded isoparametric Line element in local co-ordinates (s,t) as shown in fig 4.2 are taken as

$$N_i = \{(1+ s_0)(1+ t_0)\}/4 \qquad \ldots\ldots 5.5\ (a)$$

Where, $s_0 = s.s_i$ and $t_0 = t.t_i$

The nodal displacements are

$$u = \sum_{i=1}^{4} N_i\ u_i \qquad \ldots\ldots 5.6\ (a)$$

$$v = \sum_{i=1}^{4} N_i\ v_i \qquad \ldots\ldots 5.6\ (b)$$

2D-Quadratic Element:

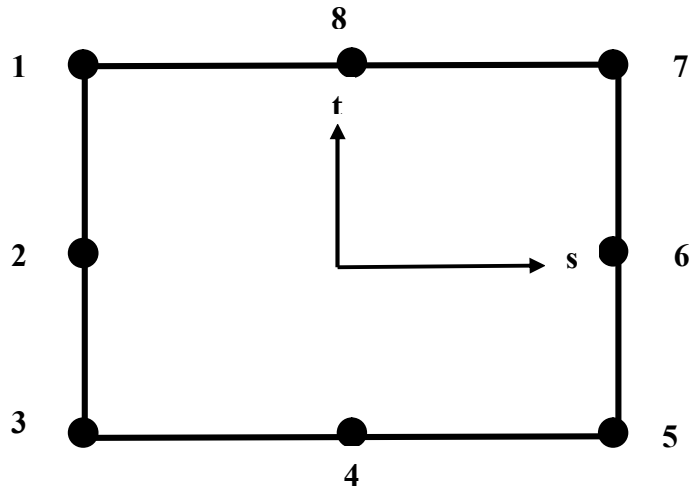

Fig 4.3: 2D Isoparametric Quadratic element in vertical plane with Local Co-ordinates

The shape functions of 8 nodded isoparametric Quadratic element in local co-ordinates (s,t) as shown in fig 4.3 are taken as

$$N_i = \{(1+ s_0)\ (1+ t_0)\}/4 - \{(1- s^2)(1+ t_0)\}/4 \qquad \ldots\ldots 5.5\ (a)$$

For i = 1, 3, 5, 7

$$N_i = \{(1- s^2)(1+ t_0)\}/2 \quad \text{……5.5 (a)}$$

For i = 2, 6

$$N_i = \{(1- t^2)(1+ s_0)\}/2 \quad \text{……5.5 (a)}$$

For i = 4, 8

Where, $s_0 = s.s_i$ and $t_0 = t.t_i$

The nodal displacements are

$$u = \sum_{i=1}^{8} N_i\, u_i \quad \text{……5.6 (a)}$$

$$v = \sum_{i=1}^{8} N_i\, v_i \quad \text{……5.6 (b)}$$

4.5 Boundary Conditions

Boundary conditions were created in the step specified for analyses. Mechanical, displacement/rotation boundary conditions were chosen, defining hinge and roller condition as shown in fig 4.4.

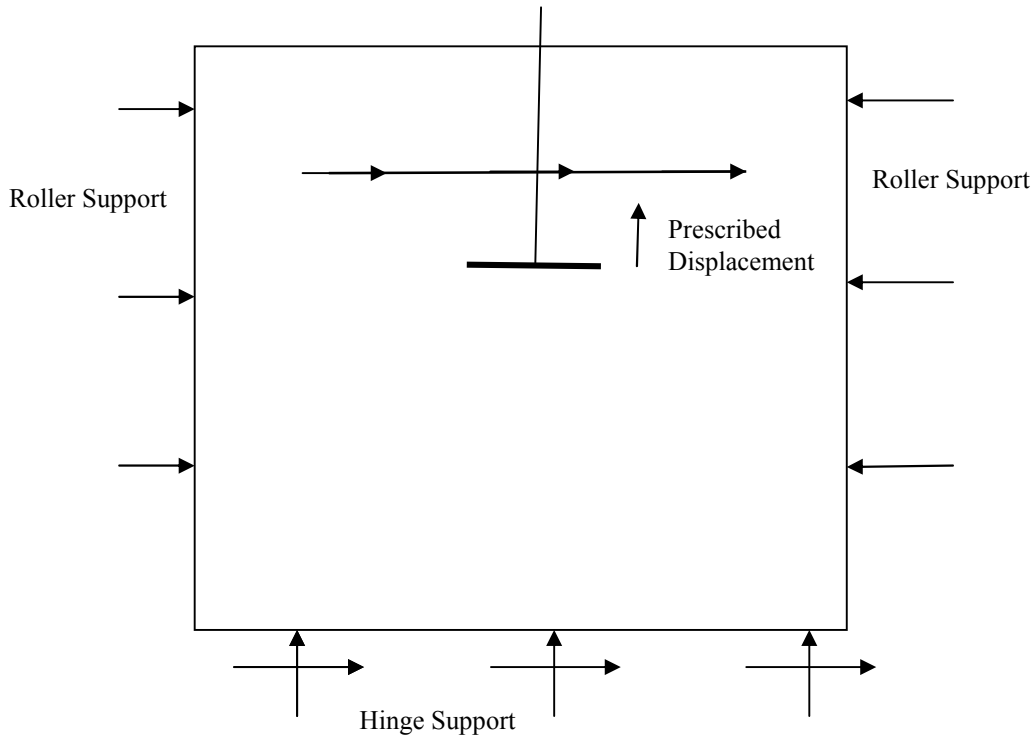

Fig 4.4: Schematic Representation of Boundary Condition specified in Abaqus

4.6 Solution Procedure

For the present numerical study analyses have been carried out under monotonic loading by providing a definite displacement in vertical direction at the anchor plates. Direct method of equation solver with unsymmetrical matrix storage is specified in analysis step. Full newton method of solution technique with linear extrapolation is considered for the present study. Mohr Coulomb failure model has been adopted for inclusion of non linearity of soil, which has been considered as an isotropic strain hardening material.

4.7 List of Numerical Cases

The cases for numerical study have been shown in Tables 4.3(a) and 4.3(b) for unreinforced and reinforced clay using different embedment depth and position of geotextiles above the top of plate in embedded soil. Total eighteen numbers of analyses including both unreinforced and reinforced cases have been carried out covering three different plate sizes with three different embedment depth for each plate size and having a fixed width of geosynthetics four times the width of plate positioned at a distance of 0.25 times the depth of embedment from bottom of anchor plate (Ref: based on the study by **Bhattacharya et al. (2008)**, Chapter 2, page 18)

Table 4.3 (a) : Test Programme for Numerical Study (Unreinforced)

NUMERICAL CASES- UNREINFORCED			
TYPE	**TEST NAME**	**PLATE SIZE**	**(H/B)**
UR	50_UR_(H/B=1)	50 X 50	1
	50_UR_(H/B=2)		2
	50_UR_(H/B=3)		3
UR	75_UR_(H/B=1)	75 X 75	1
	75_UR_(H/B=2)		2
	75_UR_(H/B=3)		3
UR	100_UR_(H/B=1)	100 X 100	1
	100_UR_(H/B=2)		2
	100_UR_(H/B=3)		3

Table 4.3 (b) : Test Programme for Numerical Study (Reinforced)

NUMERICAL CASES- REINFORCED					
TYPE	**TEST NAME**	**PLATE SIZE**	**(H/B)**	**(H'/H)**	**(Bg/B)**
RE	50_RE_(H/B=1)	50 X 50	1	0.25	4
	50_RE_(H/B=2)		2		
	50_RE_(H/B=3)		3		
RE	75_RE_(H/B=1)	75 X 75	1	0.25	4
	75_RE_(H/B=2)		2		
	75_RE_(H/B=3)		3		
RE	100_RE_(H/B=1)	100 X 100	1	0.25	4
	100_RE_(H/B=2)		2		
	100_RE_(H/B=3)		3		

4.8 Results of Numerical Analyses

Finite element analysis software ABAQUS v6.14 is used for the numerical modeling of both reinforced and unreinforced analysis. Results obtained from Numerical analysis for different plate sizes and respective embedment ratio both in unreinforced as well for reinforced case show excellent qualitative but good quantitative agreement with the results obtained from model test. For the present numerical study analyses have been carried out on 2D plain strain condition with geotextile and anchor being modeled as linear elastic material. Soil is modeled with 2D isoparametric quadrilateral element and 2D isoparametric linear element is considered for anchor and geotextile. Non-linearity for soil is modeled with mohr-coulomb plasticity and the interaction between soil and anchor is formulated with Node to Surface discretization and the same is formulated with Surface to Surface discretization for soil-geotextile interface.

Results of the numerical analysis carried out for the present investigation has been tabulated in Table 4.4. For each of the cases tabulated below the plot of load vs Axial movement is exhibited below in fig 4.5(a) to 4.5(r) and the respective stress contour obtained from numerical analyses are shown in fig 4.6(a) to 4.6(r).

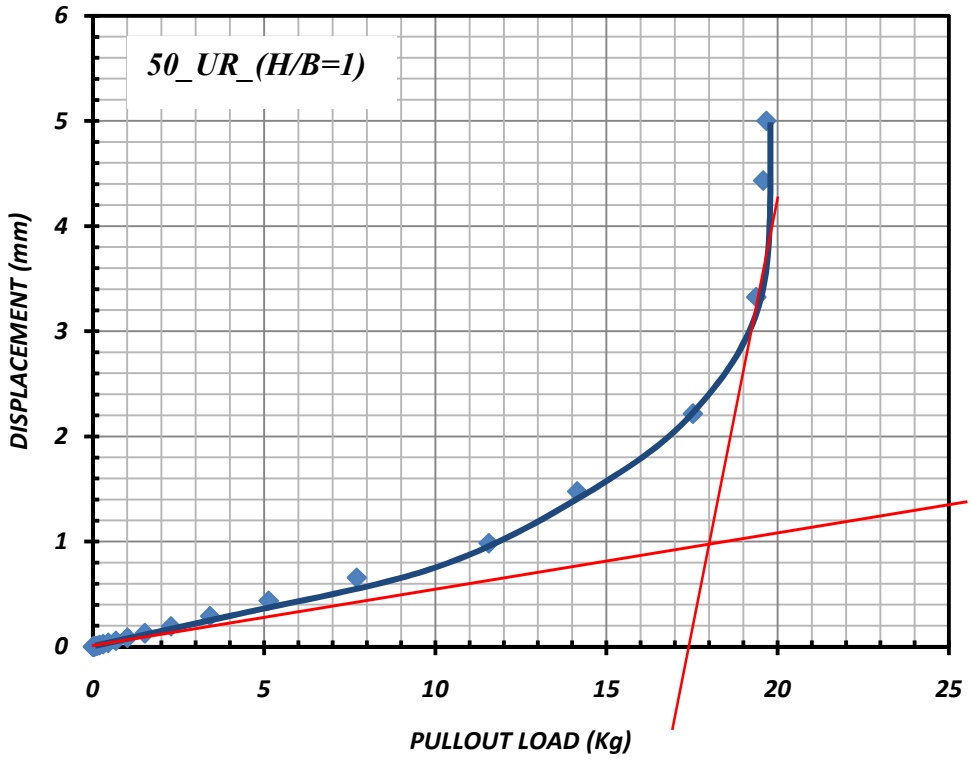

Fig 4.5(a): Typical Load vs Axial Movement for 50 mm Square Plate with (H/B =1) (Unreinforced)

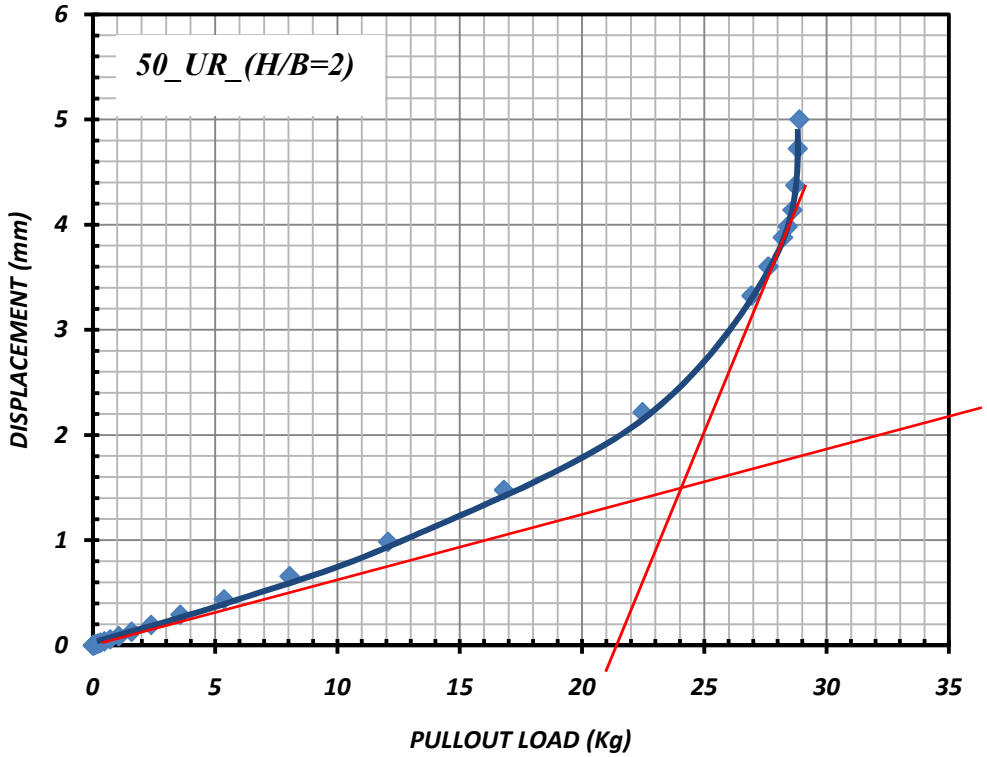

Fig 4.5(b): Typical Load vs Axial Movement for 50 mm Square Plate with (H/B =2) (Unreinforced)

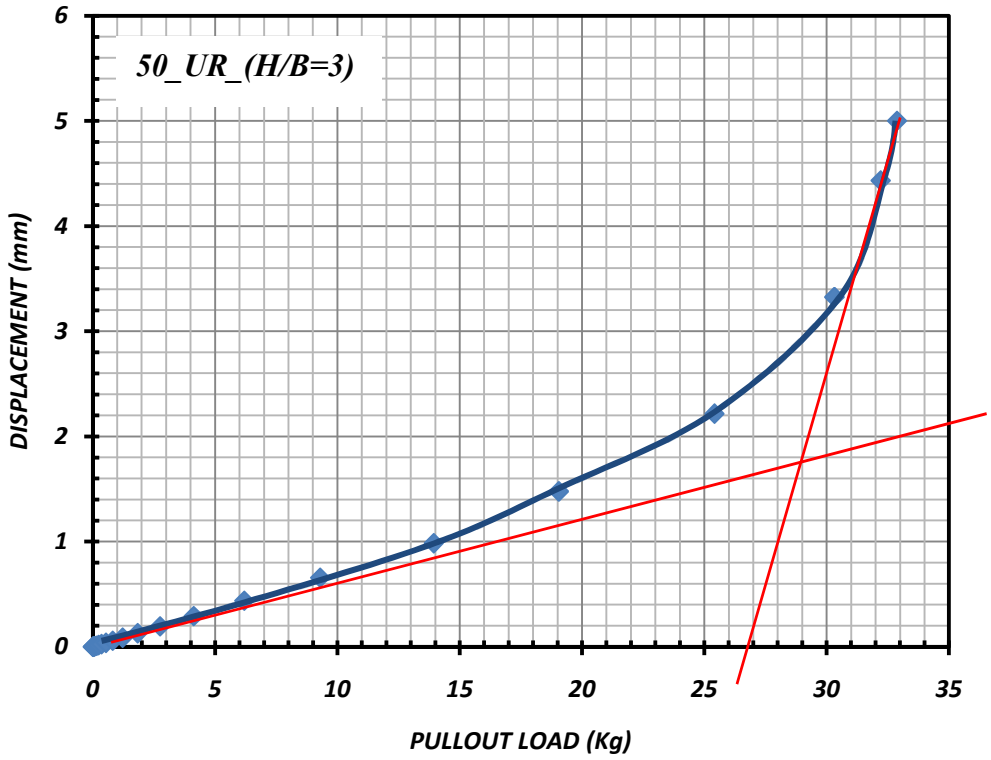

Fig 4.5(c): Typical Load vs Axial Movement for 50 mm Square Plate with (H/B =3) (Unreinforced)

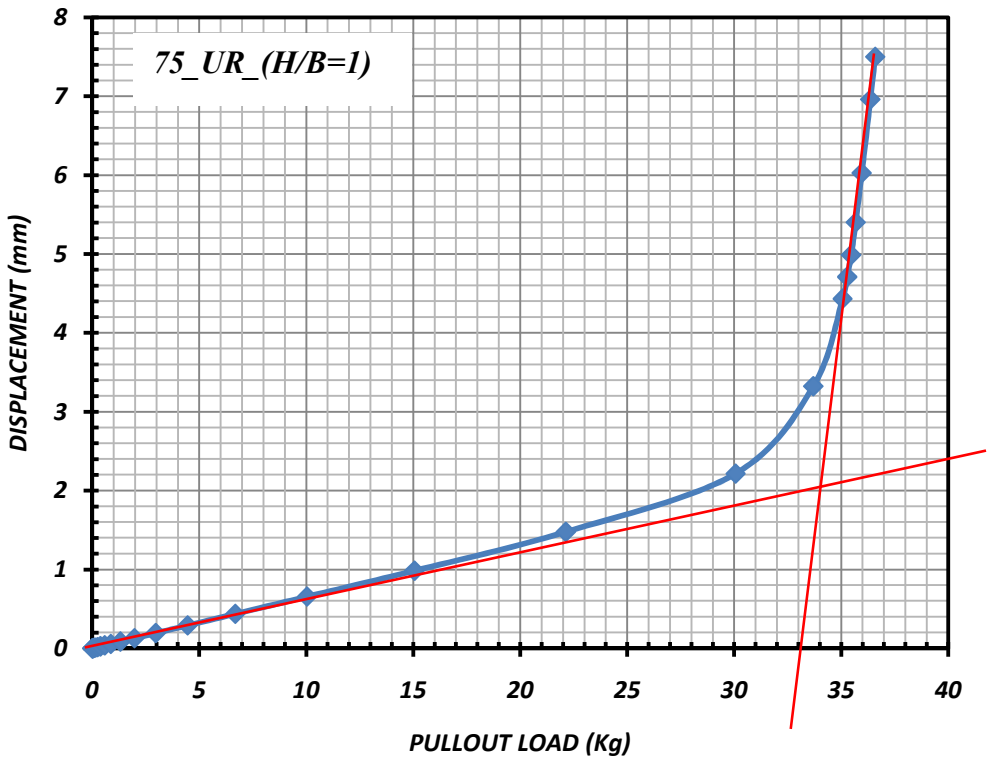

Fig 4.5(d): Typical Load vs Axial Movement for 75 mm Square Plate with (H/B =1) (Unreinforced)

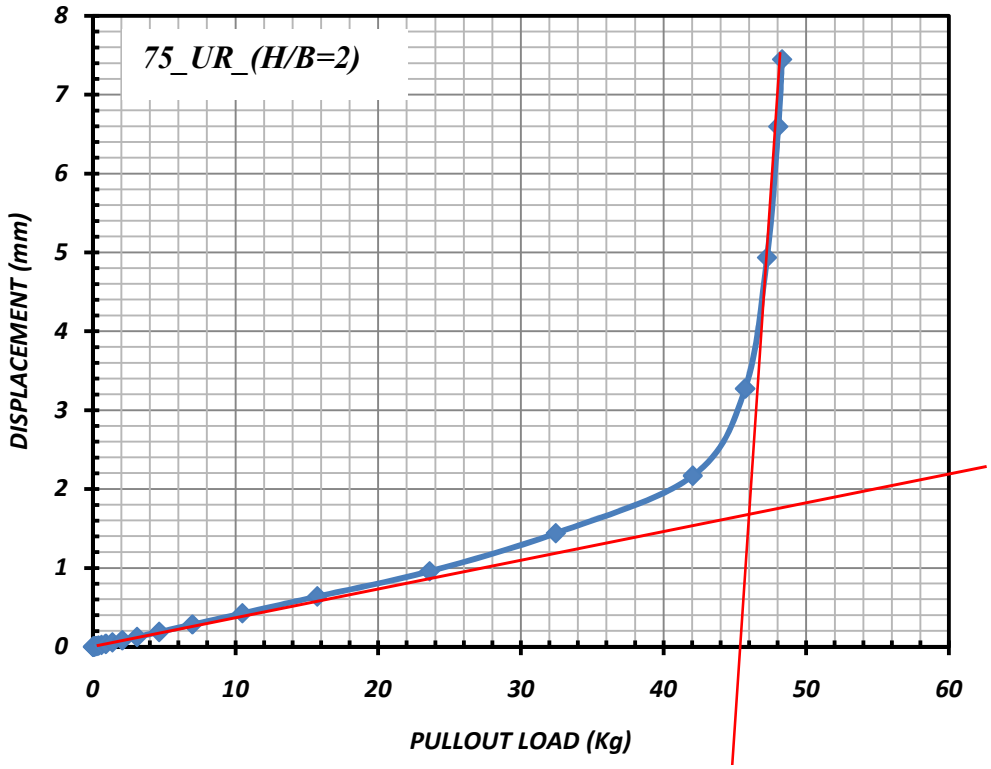

Fig 4.5(e): Typical Load vs Axial Movement for 75 ^{mm} Square Plate with (H/B =2) (Unreinforced)

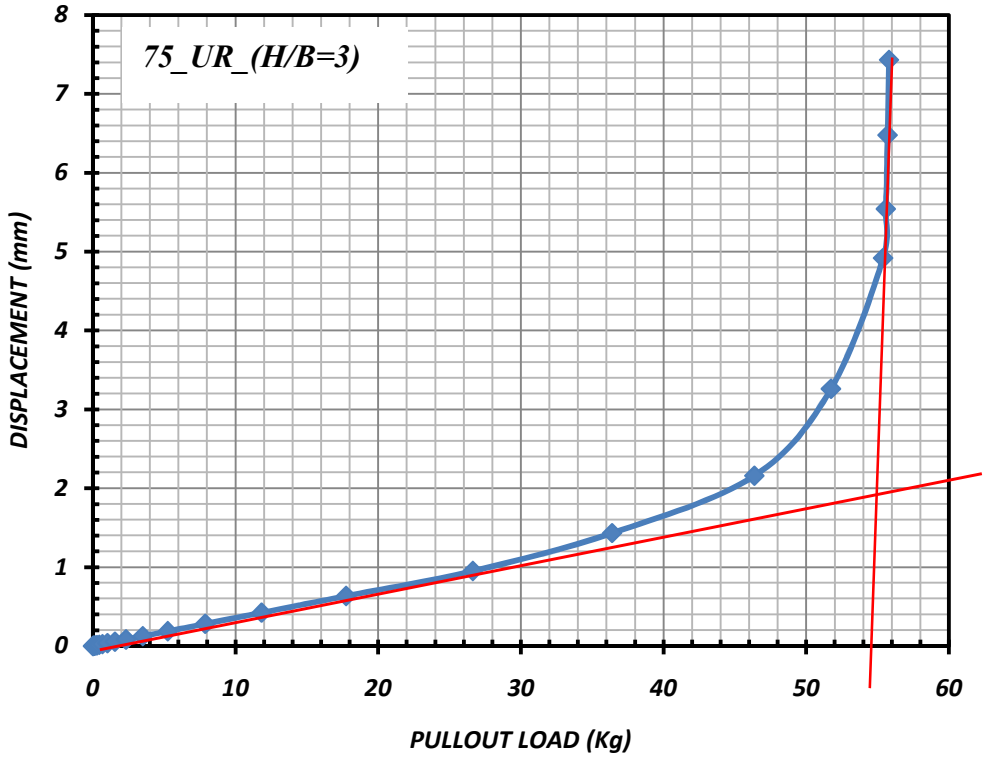

Fig 4.5(f): Typical Load vs Axial Movement for 75 ^{mm} Square Plate with (H/B =3) (Unreinforced)

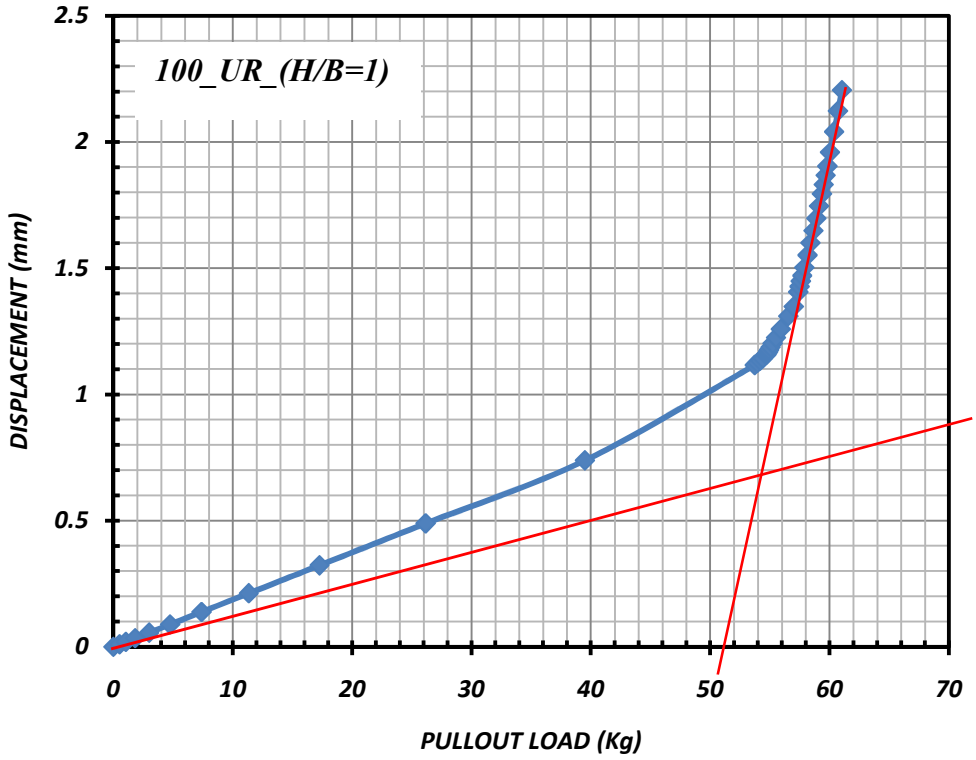

Fig 4.5(g): Typical Load vs Axial Movement for 100 ^{mm} Square Plate with (H/B =1) (Unreinforced)

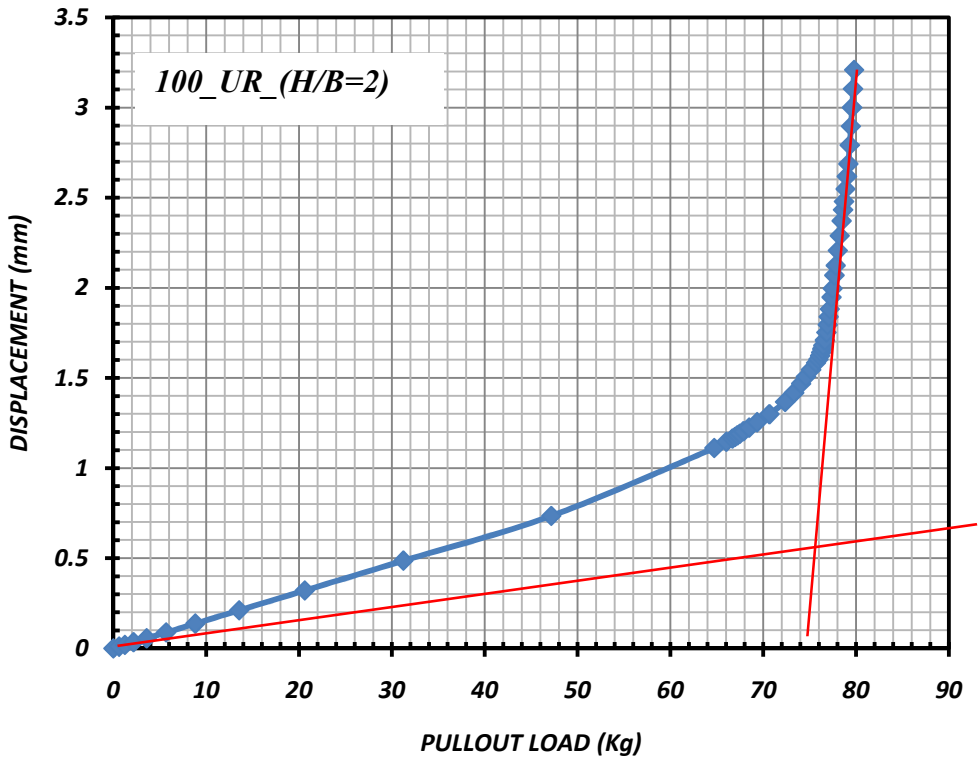

Fig 4.5(h): Typical Load vs Axial Movement for 100 ^{mm} Square Plate with (H/B =2) (Unreinforced)

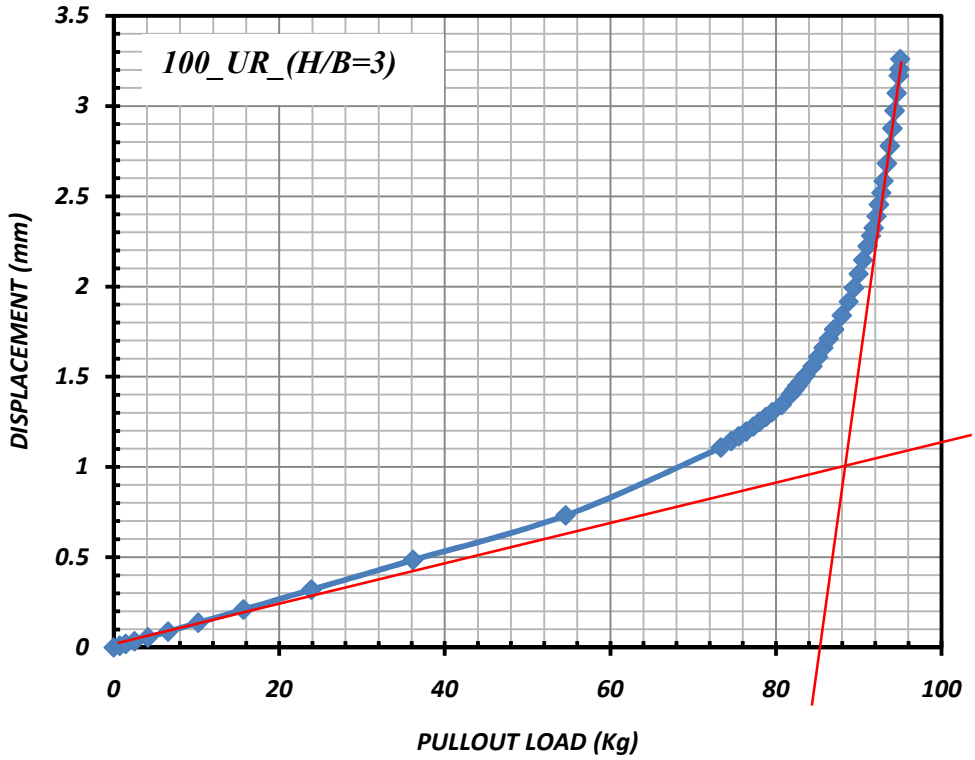

Fig 4.5(i): Typical Load vs Axial Movement for 100 mm Square Plate with (H/B =3) (Unreinforced)

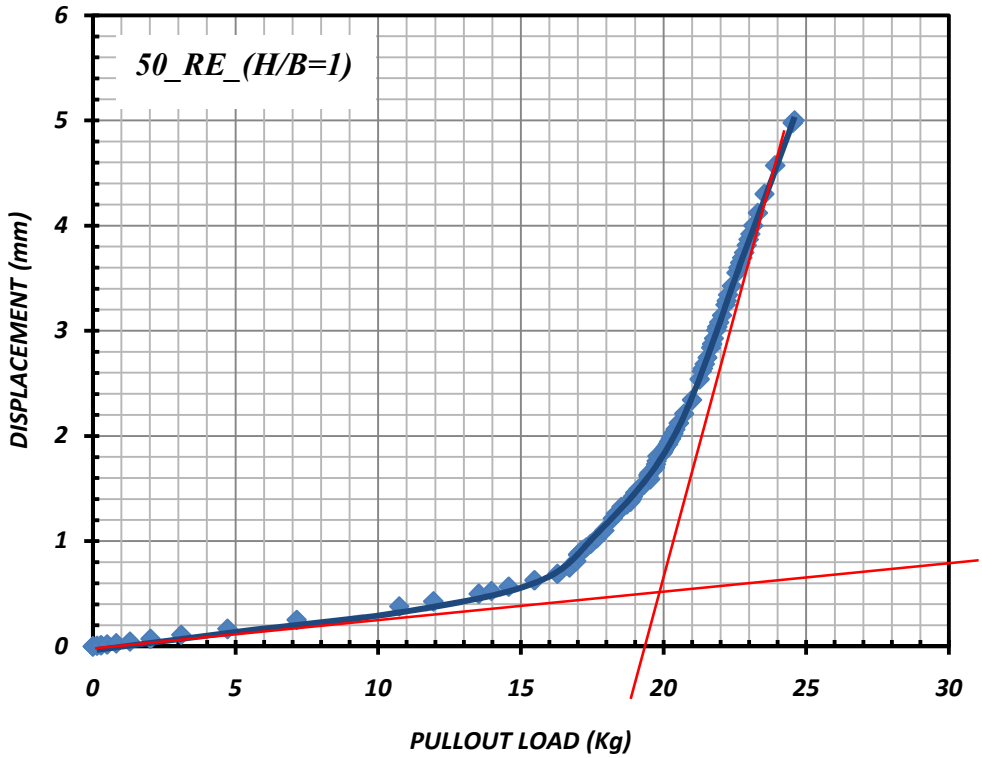

Fig 4.5(j): Typical Load vs Axial Movement for 50 mm Square Plate with (H/B =1) (Reinforced)

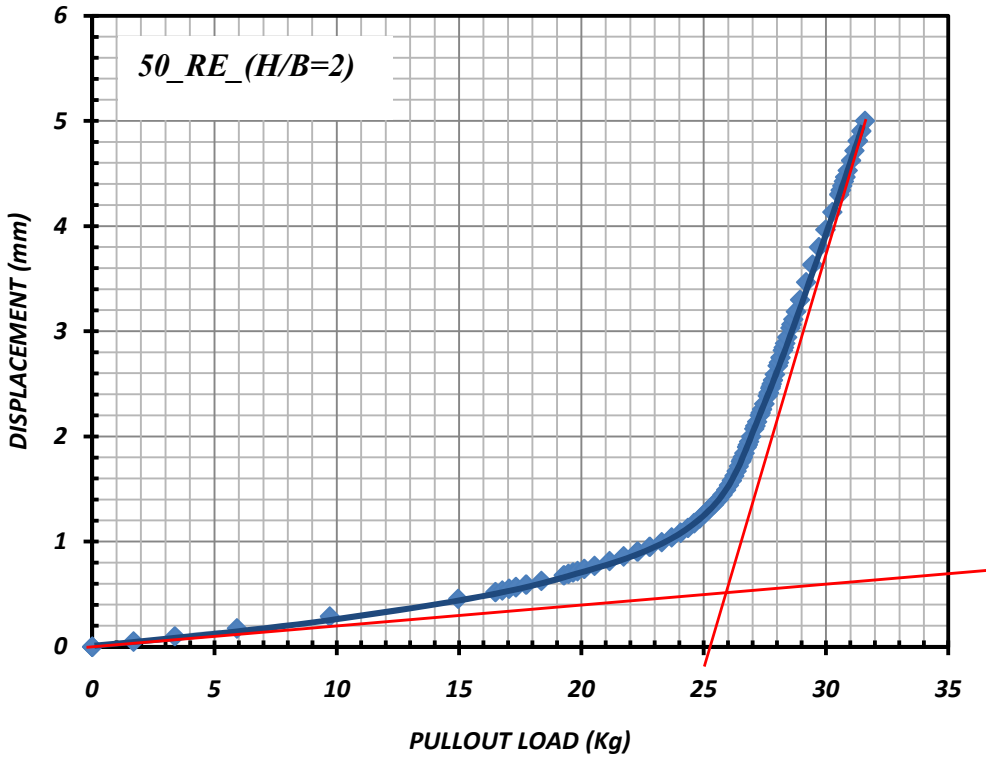

Fig 4.5(k): Typical Load vs Axial Movement for 50 ^{mm} Square Plate with (H/B =2) (Reinforced)

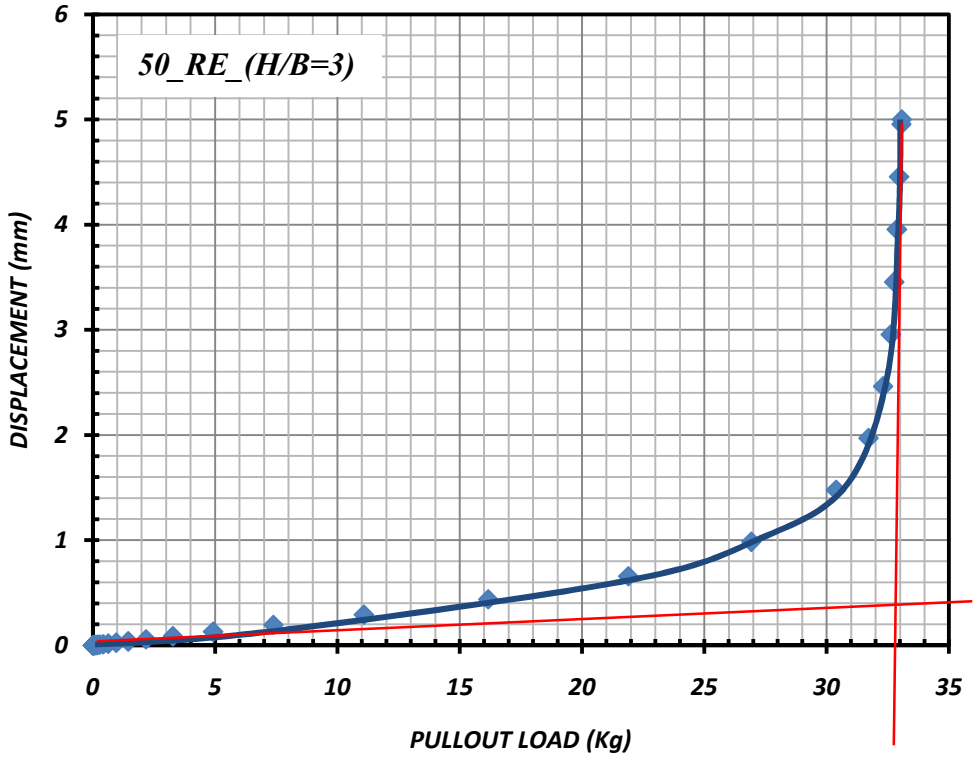

Fig 4.5(l): Typical Load vs Axial Movement for 50 ^{mm} Square Plate with (H/B =3) (Reinforced)

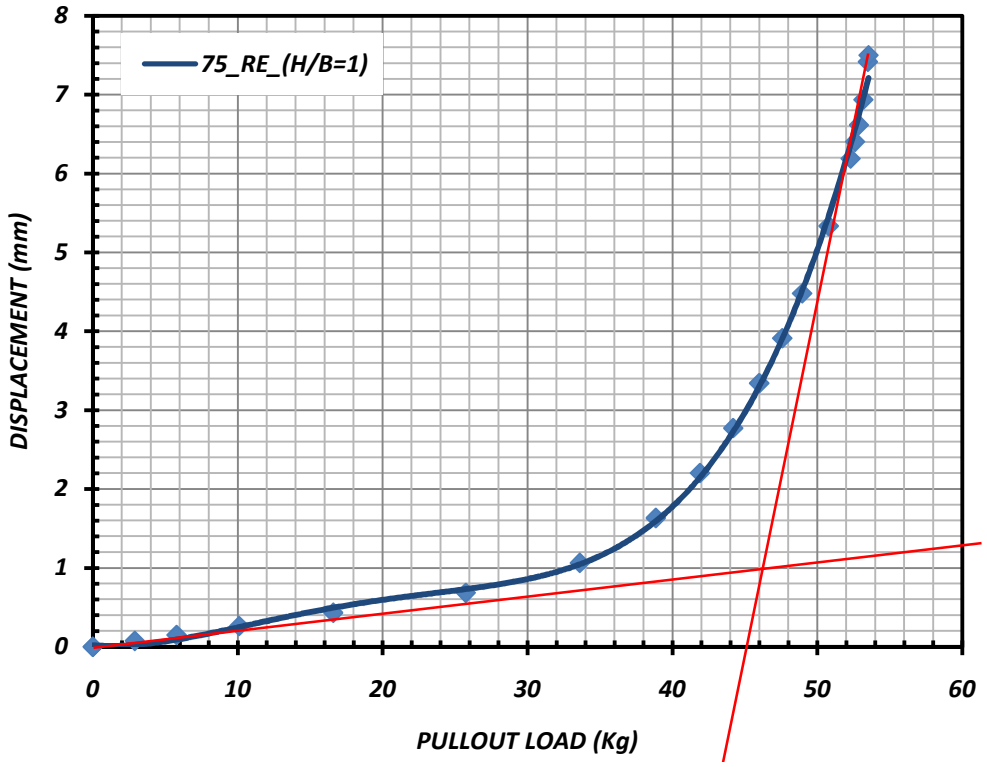

Fig 4.5(m): Typical Load vs Axial Movement for 75 ^{mm} Square Plate with (H/B =1) (Reinforced)

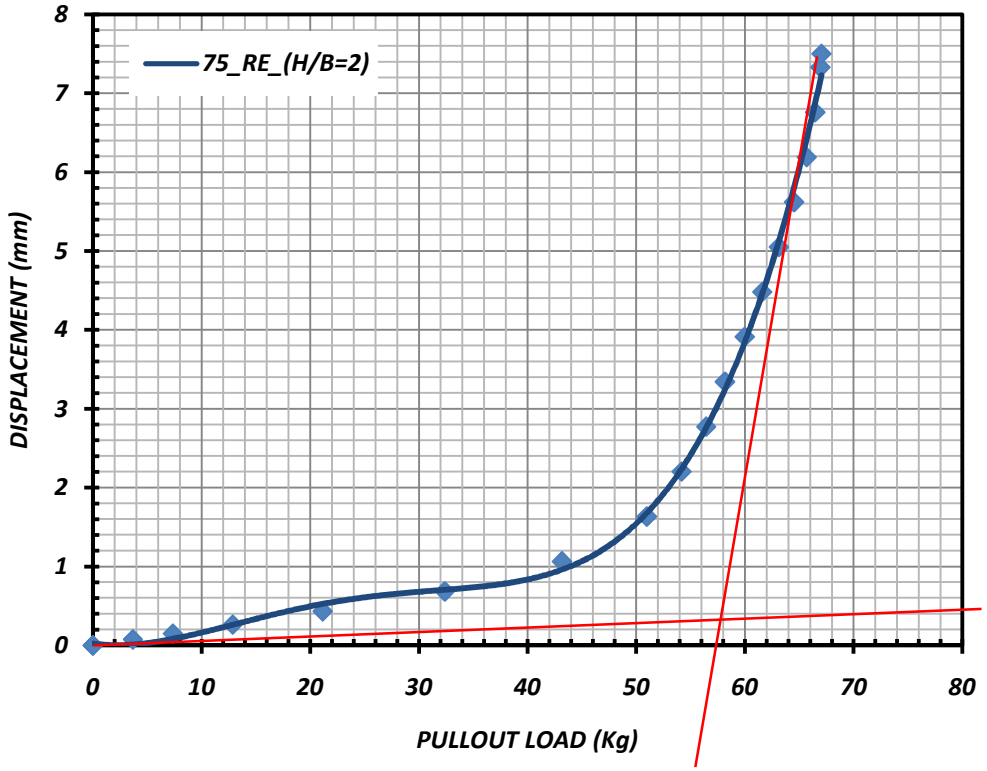

Fig 4.5(n): Typical Load vs Axial Movement for 75 ^{mm} Square Plate with (H/B =2) (Reinforced)

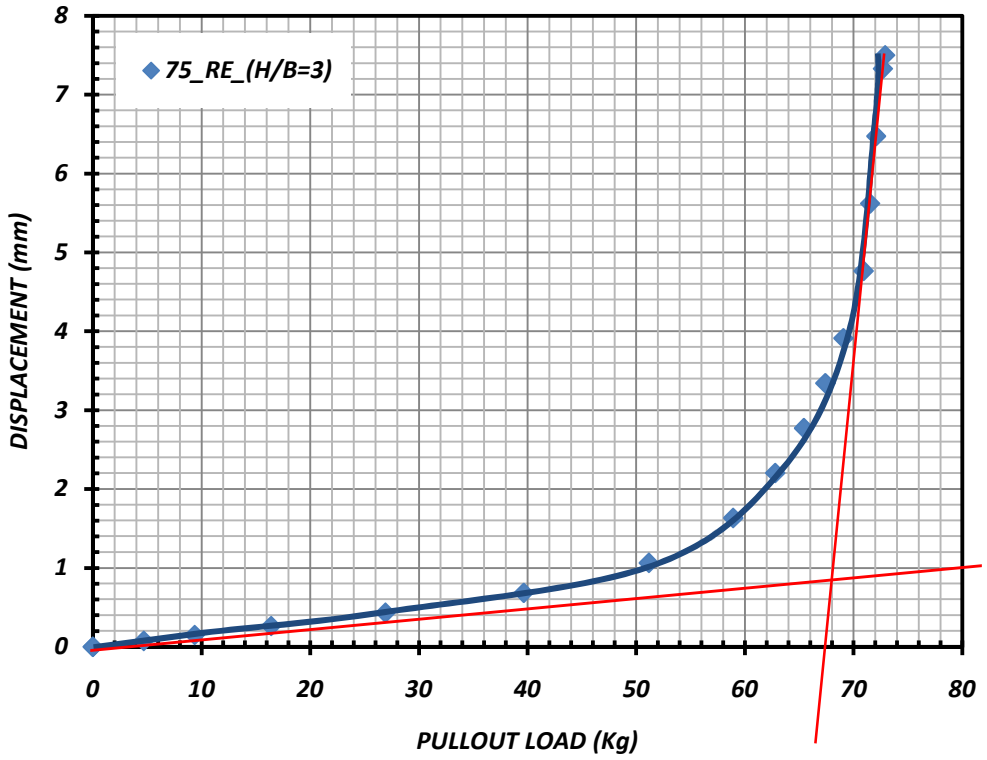

Fig 4.5(o): Typical Load vs Axial Movement for 75 ^{mm} Square Plate with (H/B =3) (Reinforced)

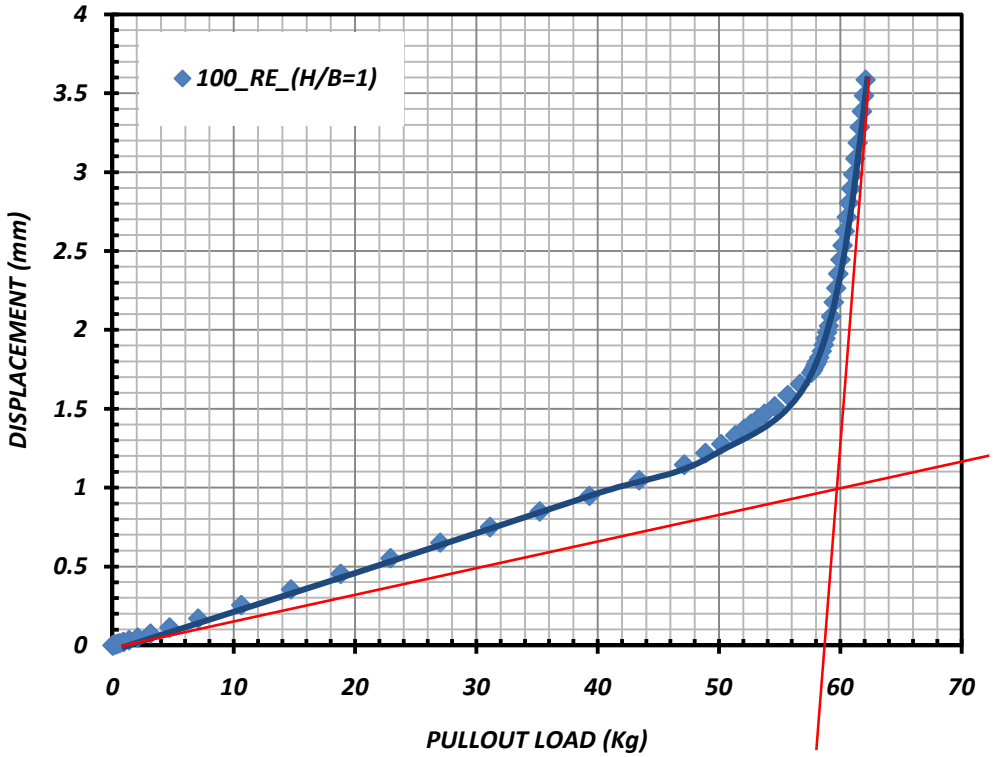

Fig 4.5(p): Typical Load vs Axial Movement for 100 ^{mm} Square Plate with (H/B =1) (Reinforced)

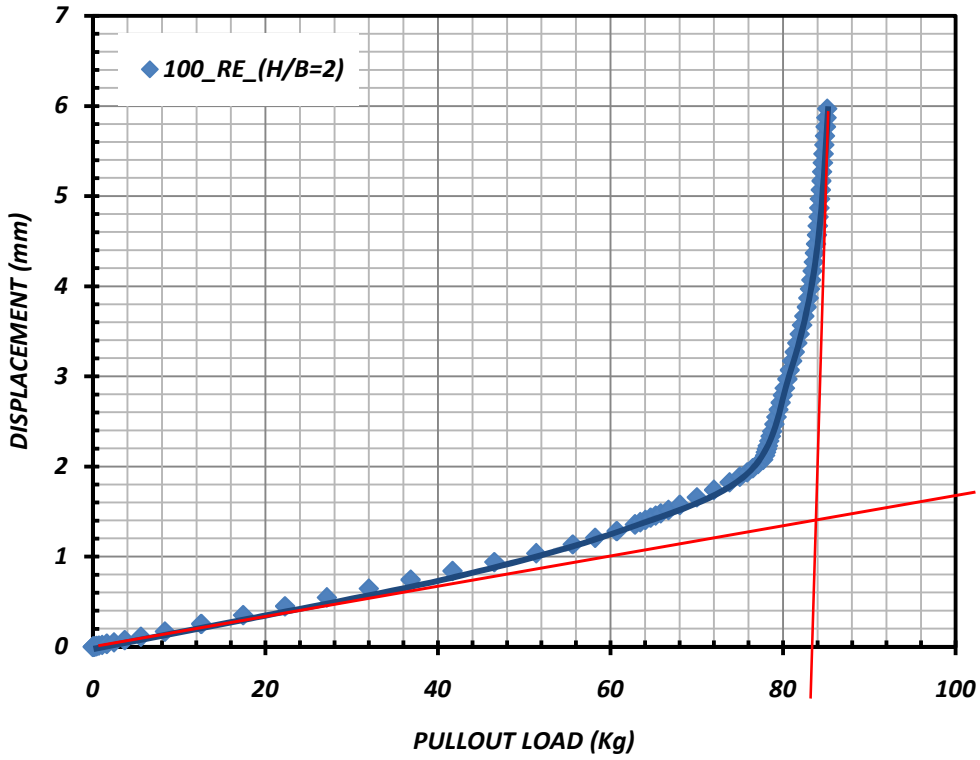

Fig 4.5(q): Typical Load vs Axial Movement for 100 mm Square Plate with (H/B =2) (Reinforced)

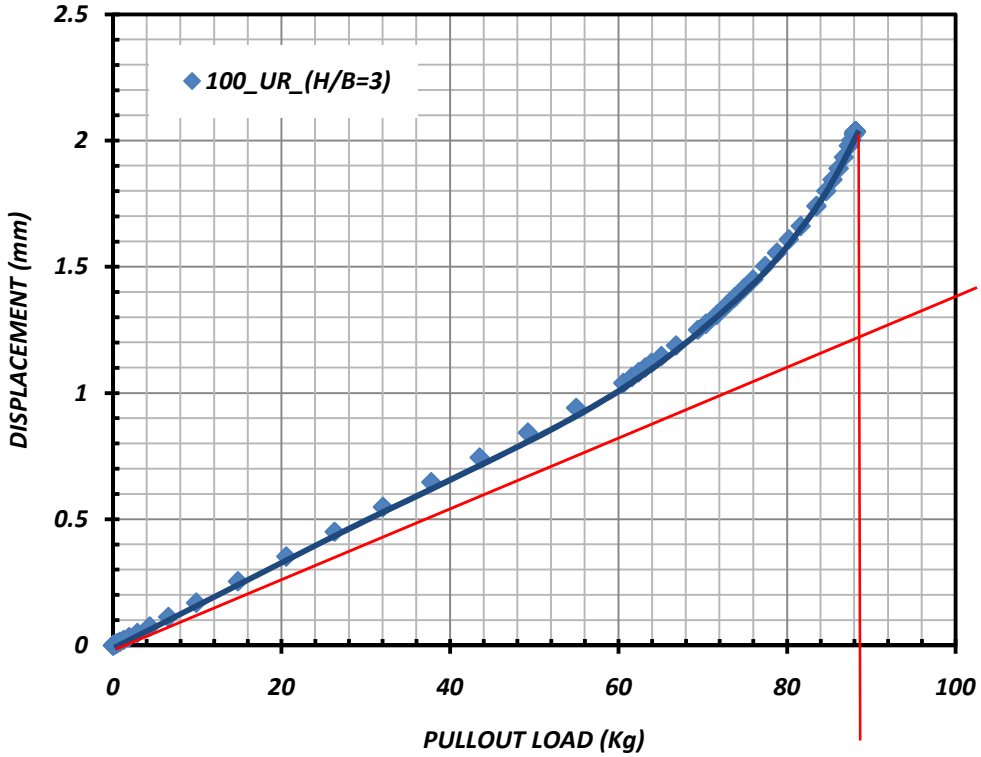

Fig 4.5(r): Typical Load vs Axial Movement for 100 mm Square Plate with (H/B =3) (Reinforced)

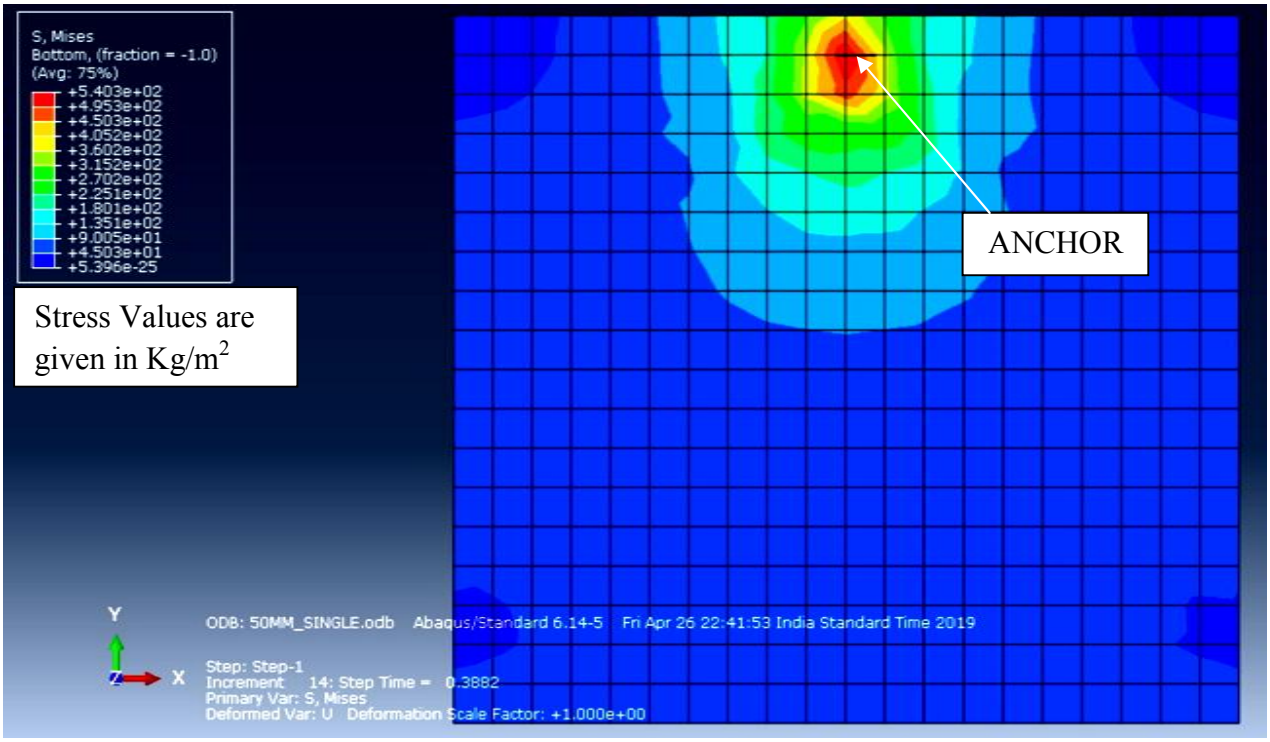

Fig 4.6(a): Stress Contour for 50 mm Square Anchor Plate with (H/B=1) (Unreinforced)

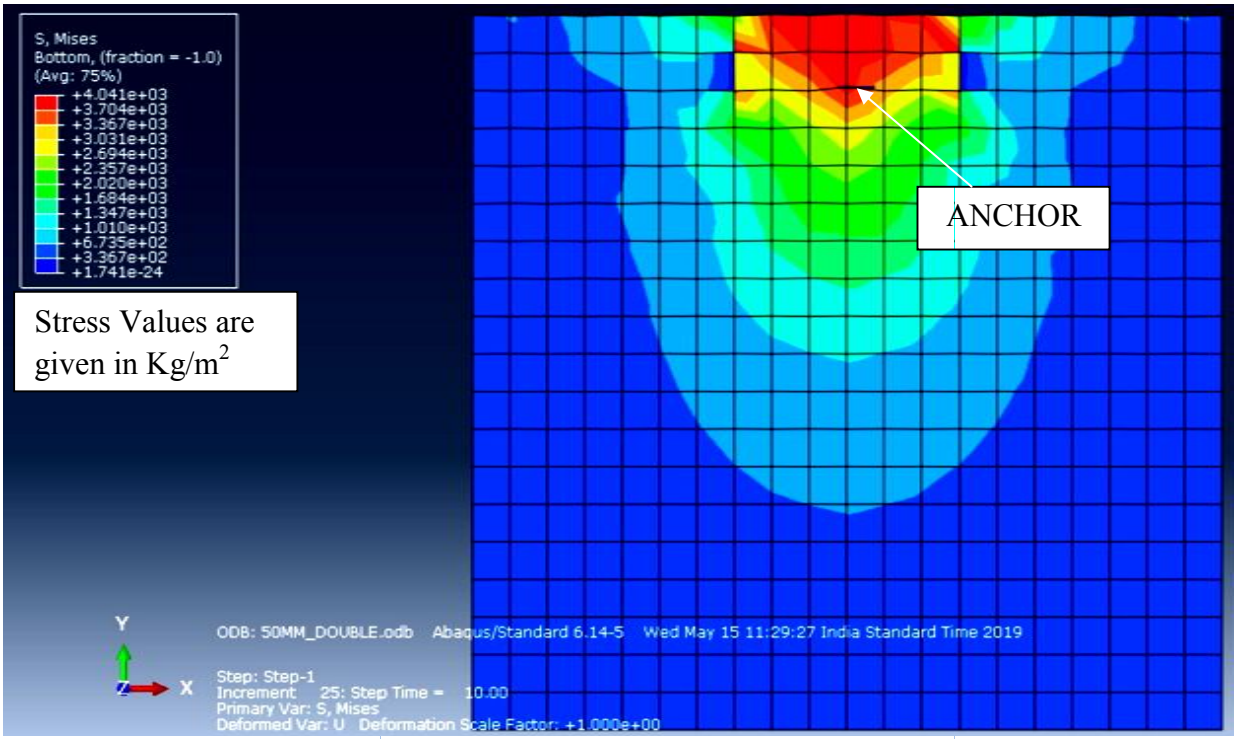

Fig 4.6(b): Stress Contour for 50 mm Square Anchor Plate with (H/B=2) (Unreinforced)

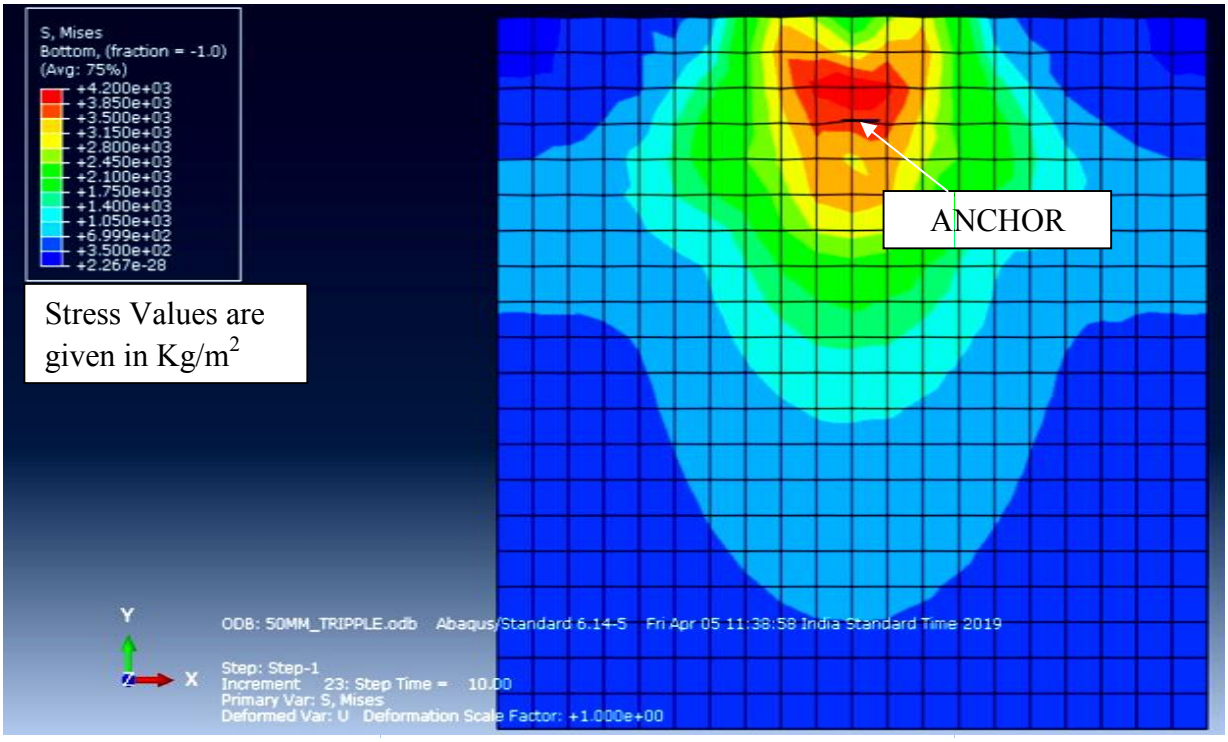

Fig 4.6(c): Stress Contour for 50 ^{mm} Square Anchor Plate with (H/B=3) (Unreinforced)

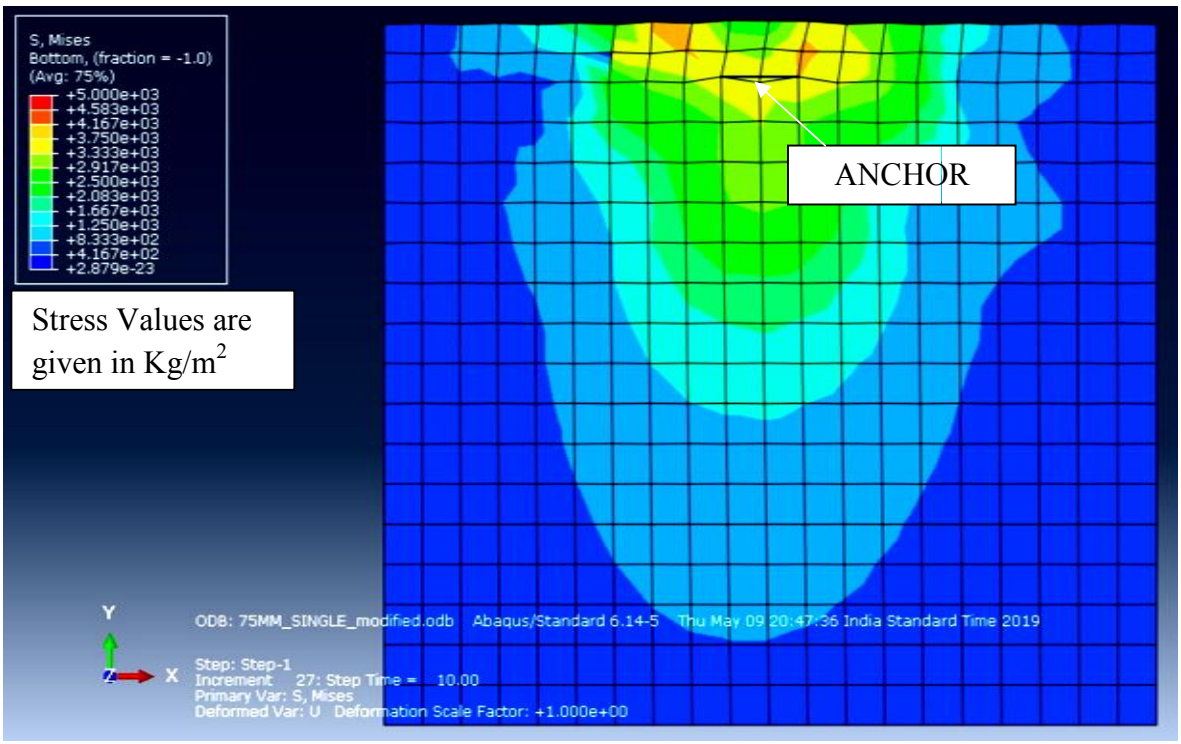

Fig 4.6(d): Stress Contour for 75 ^{mm} Square Anchor Plate with (H/B=1) (Unreinforced)

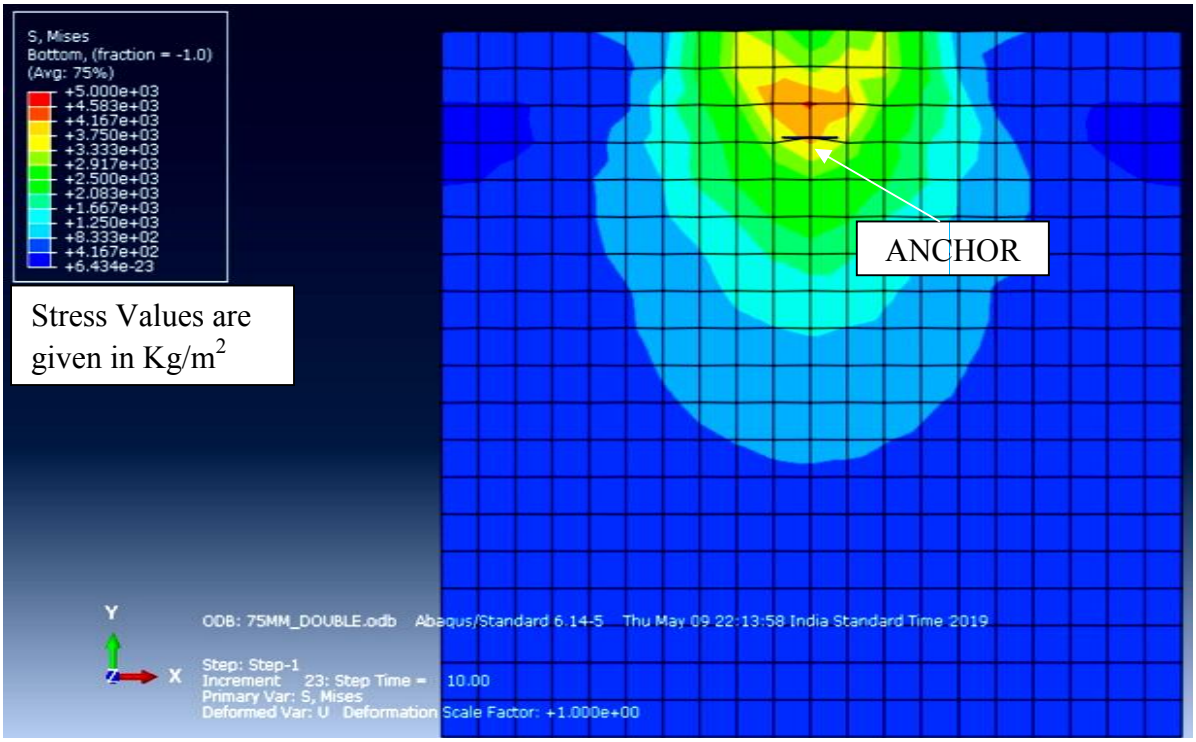

Fig 4.6(e): Stress Contour for 75 mm Square Anchor Plate with (H/B=2) (Unreinforced)

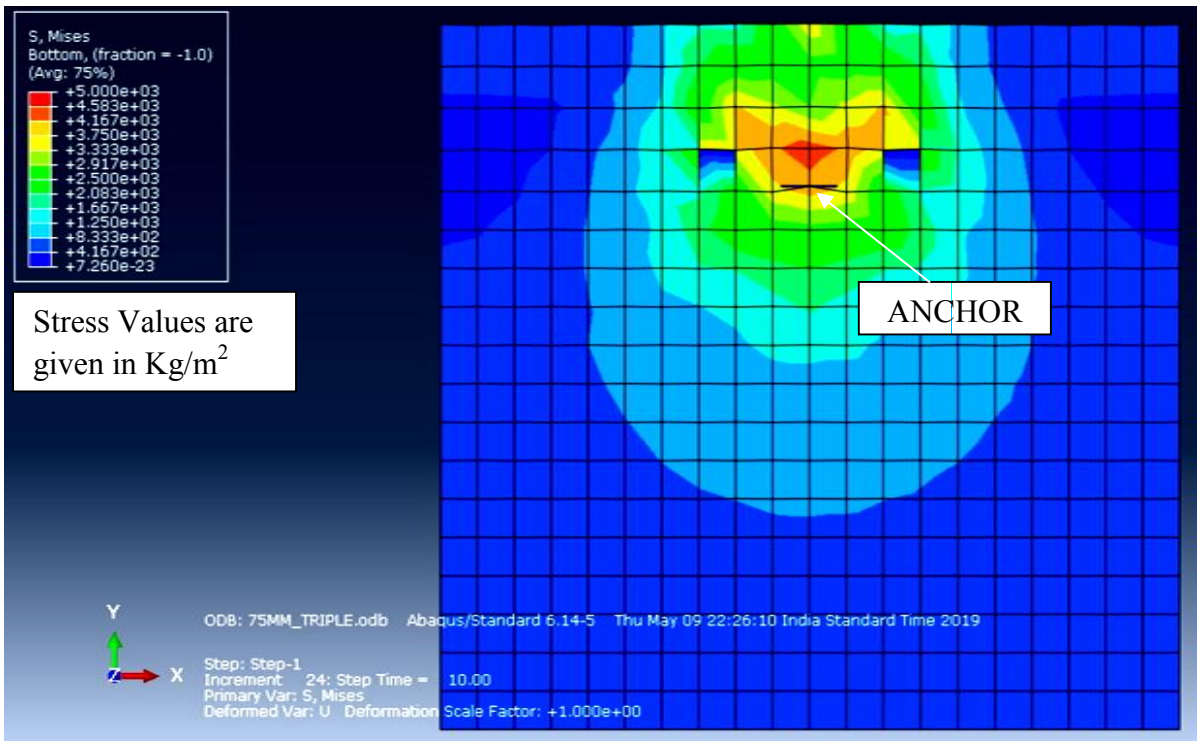

Fig 4.6(f): Stress Contour for 75 mm Square Anchor Plate with (H/B=3) (Unreinforced)

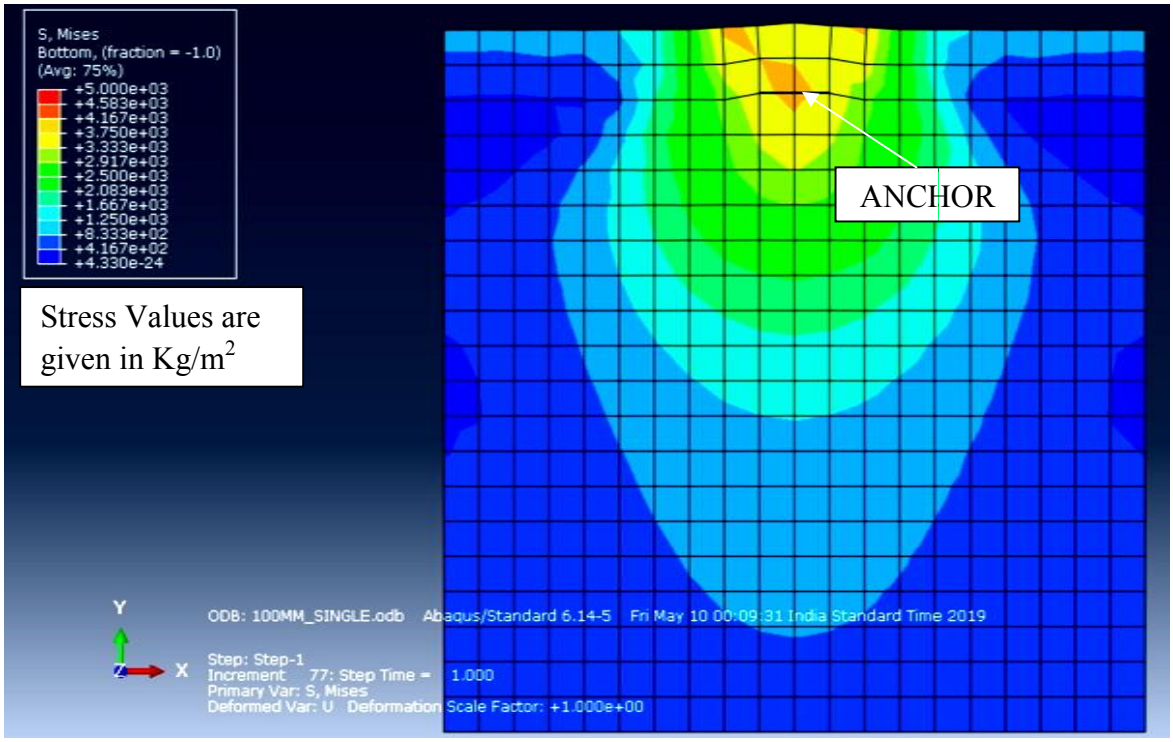

Fig 4.6(g): Stress Contour for 100 mm Square Anchor Plate with (H/B=1) (Unreinforced)

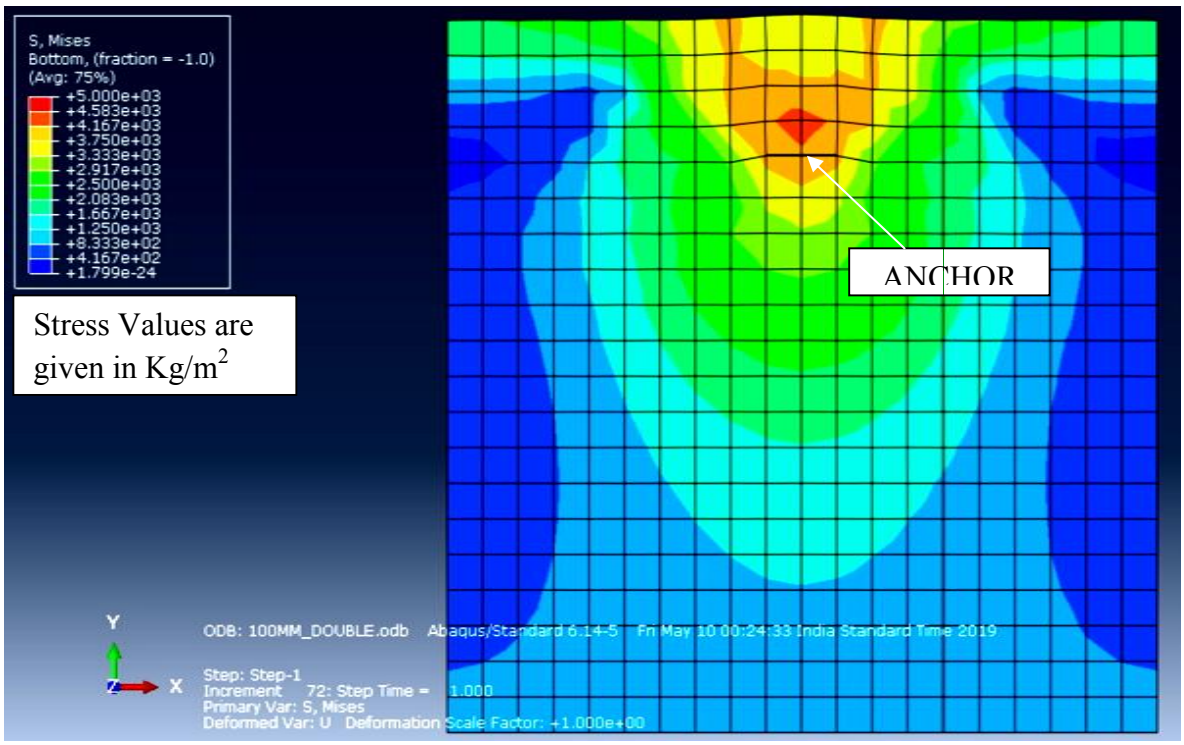

Fig 4.6(h): Stress Contour for 100 mm Square Anchor Plate with (H/B=2) (Unreinforced)

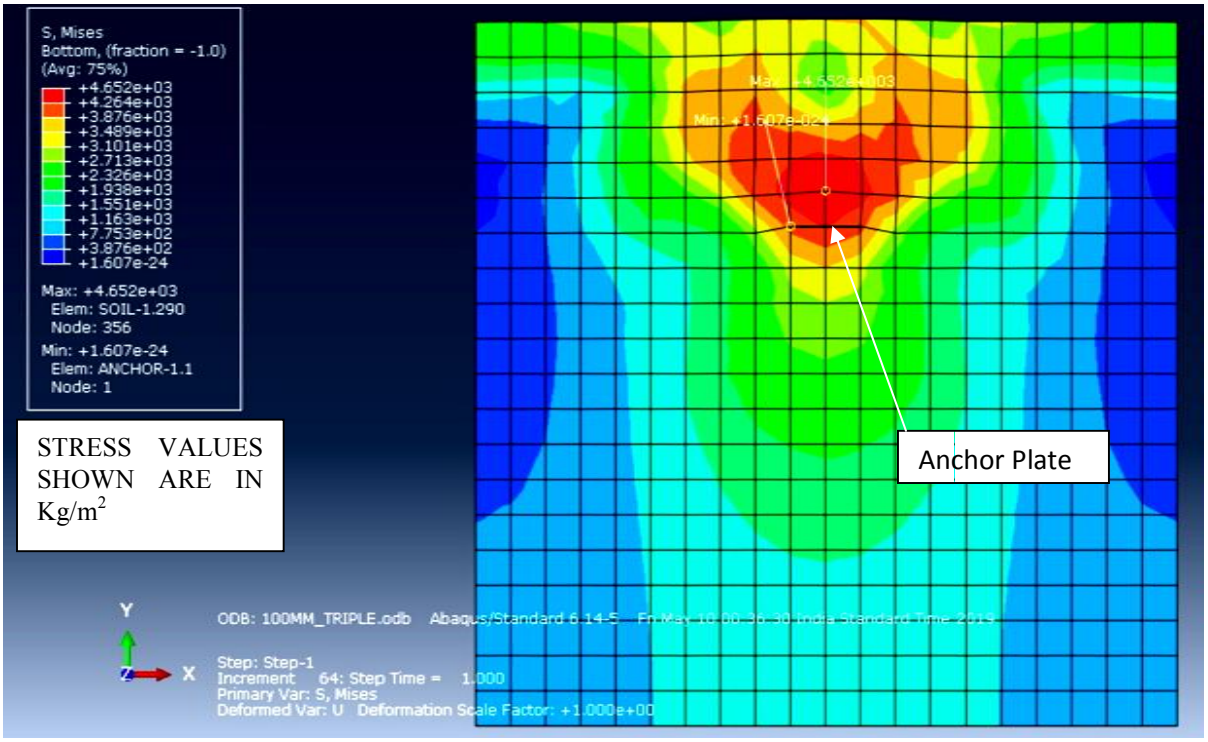

Fig 4.6(i): Stress Contour for 100 mm Square Anchor Plate with (H/B=3) (Unreinforced)

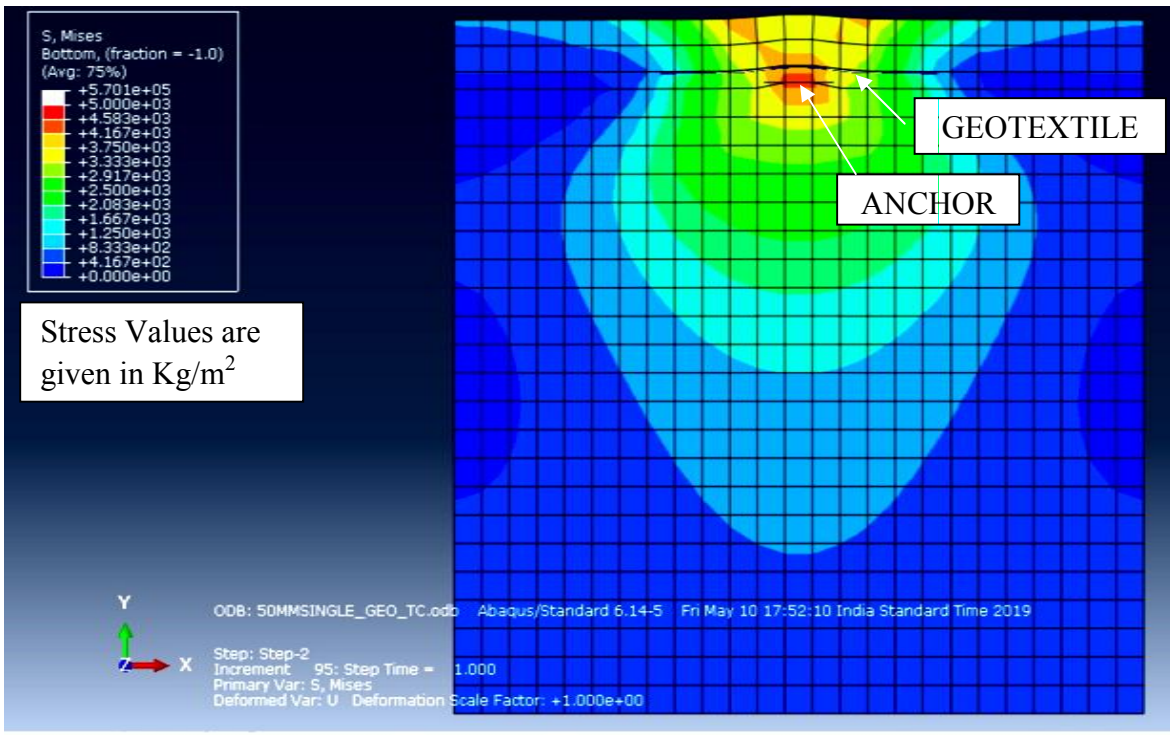

Fig 4.6(j): Stress Contour for 50 mm Square Anchor Plate with (H/B=1)(Reinforced)

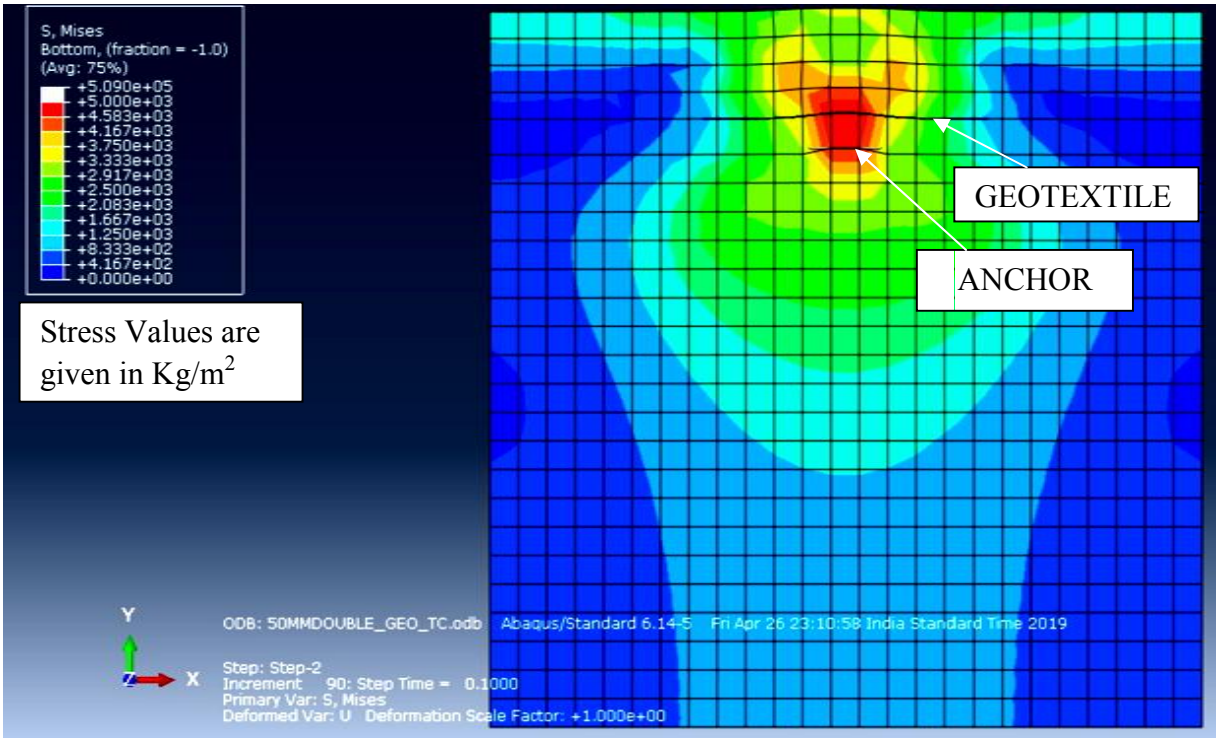

Fig 4.6(k): Stress Contour for 50 mm Square Anchor Plate with (H/B=2)(Reinforced)

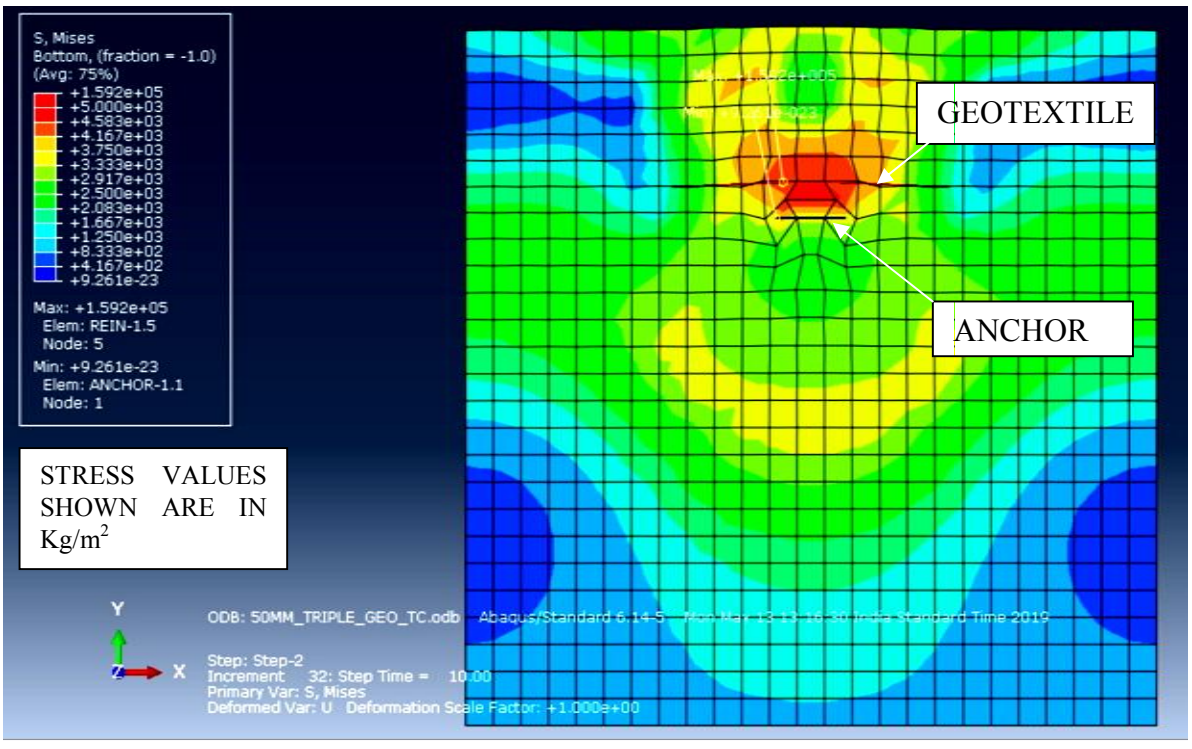

Fig 4.6(l): Stress Contour for 50 mm Square Anchor Plate with (H/B=3)(Reinforced)

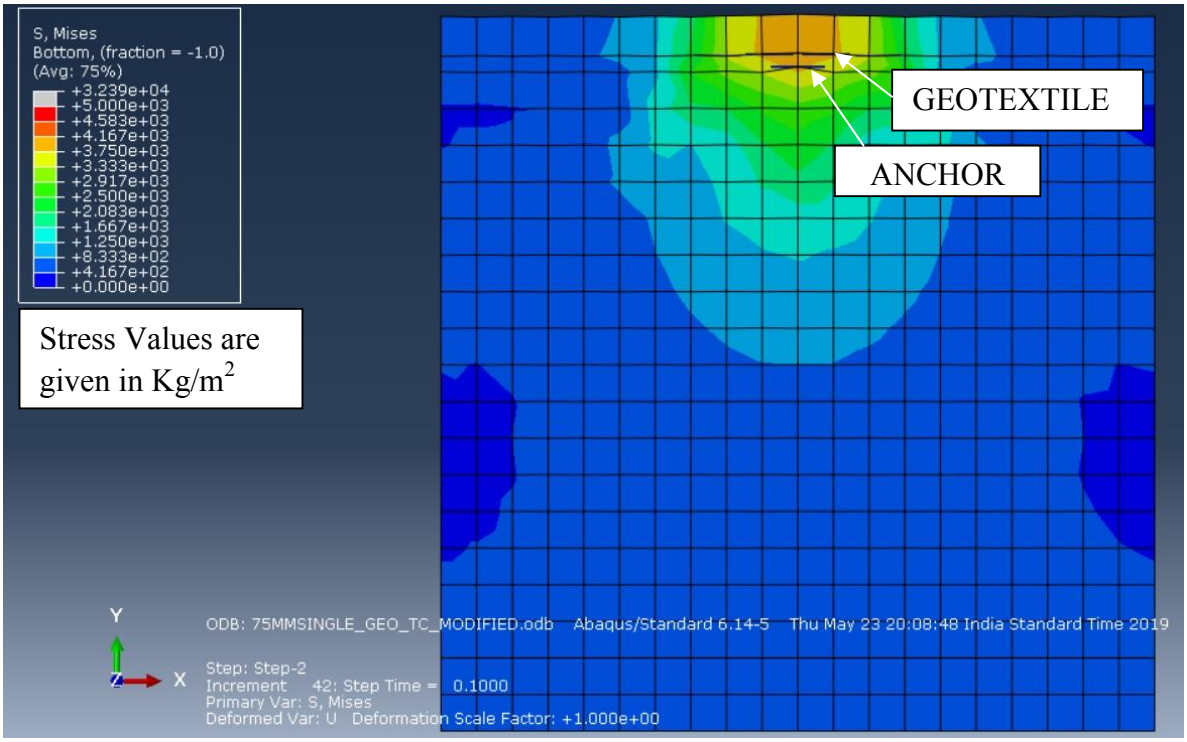

Fig 4.6(m): Stress Contour for 75 mm Square Anchor Plate with (H/B=1)(Reinforced)

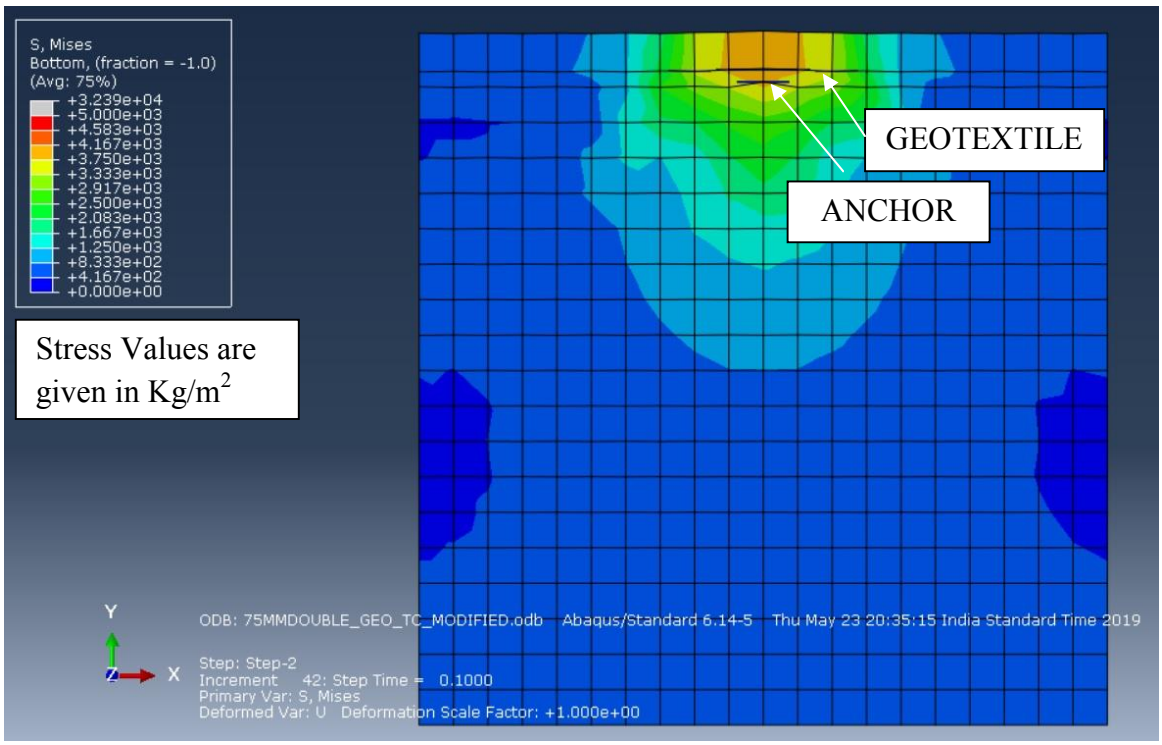

Fig 4.6(n): Stress Contour for 75 mm Square Anchor Plate with (H/B=2)(Reinforced)

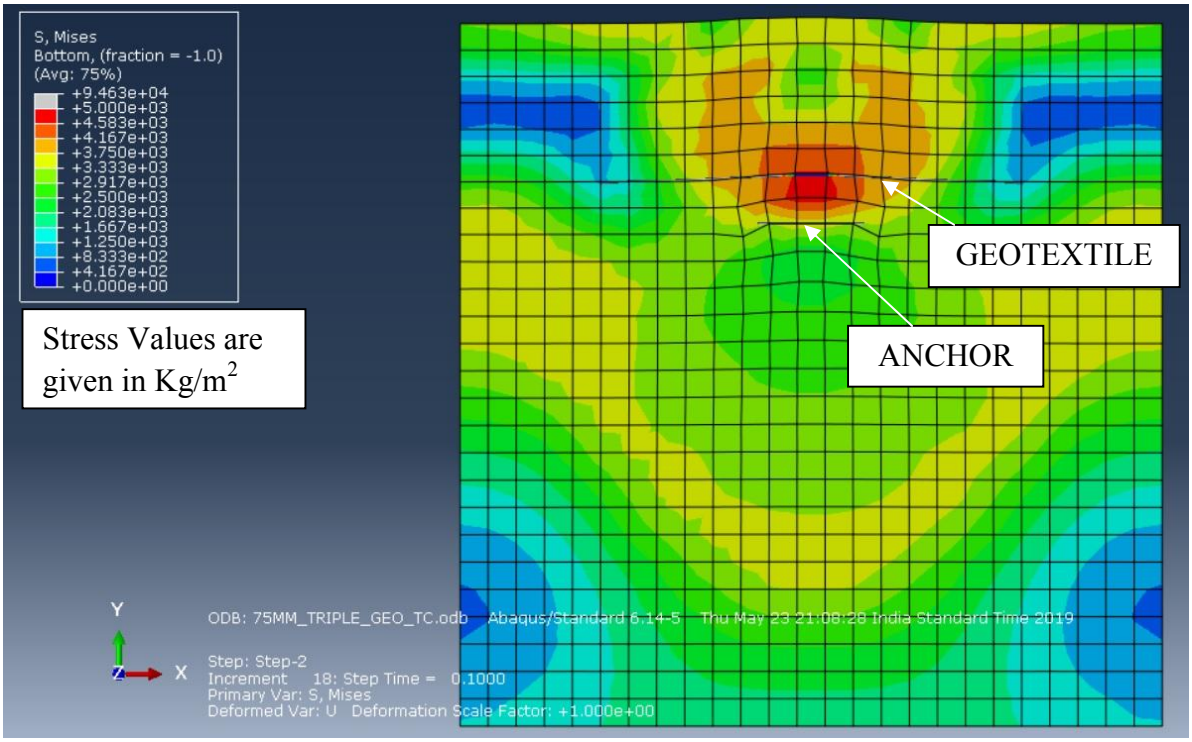

Fig 4.6(o): Stress Contour for 75 ^{mm} Square Anchor Plate with (H/B=3)(Reinforced)

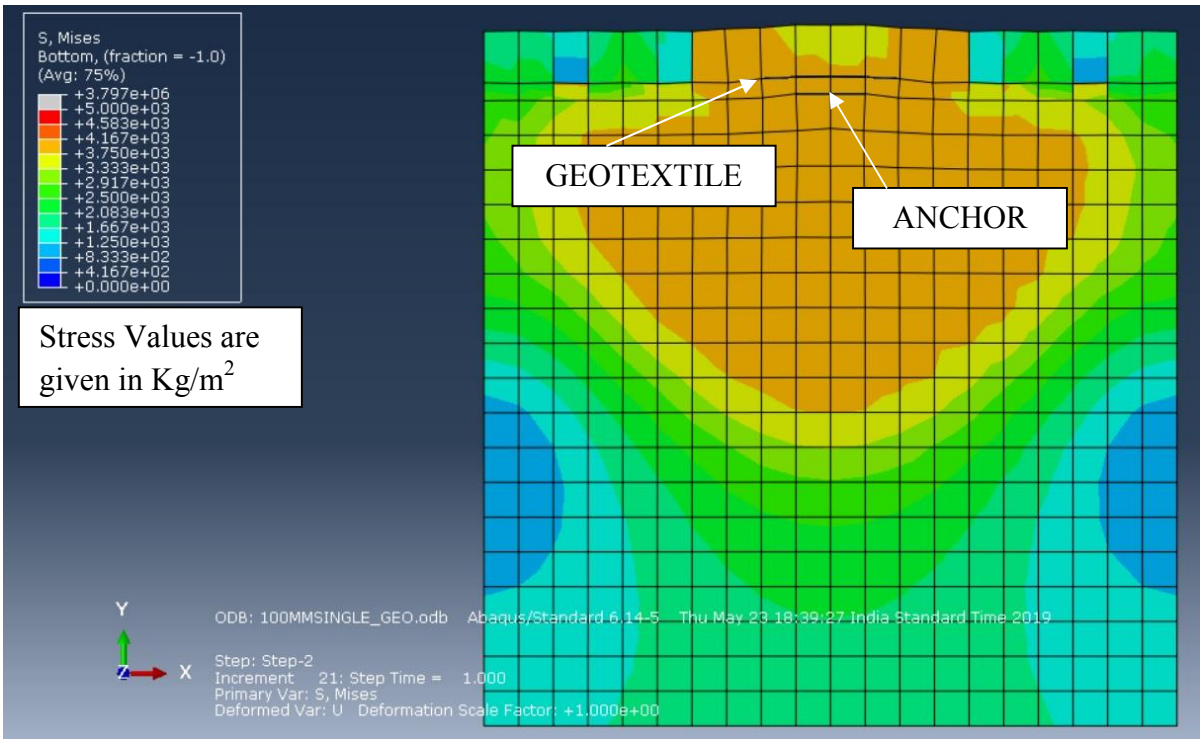

Fig 4.6(p): Stress Contour for 100 ^{mm} Square Anchor Plate with (H/B=1)(Reinforced)

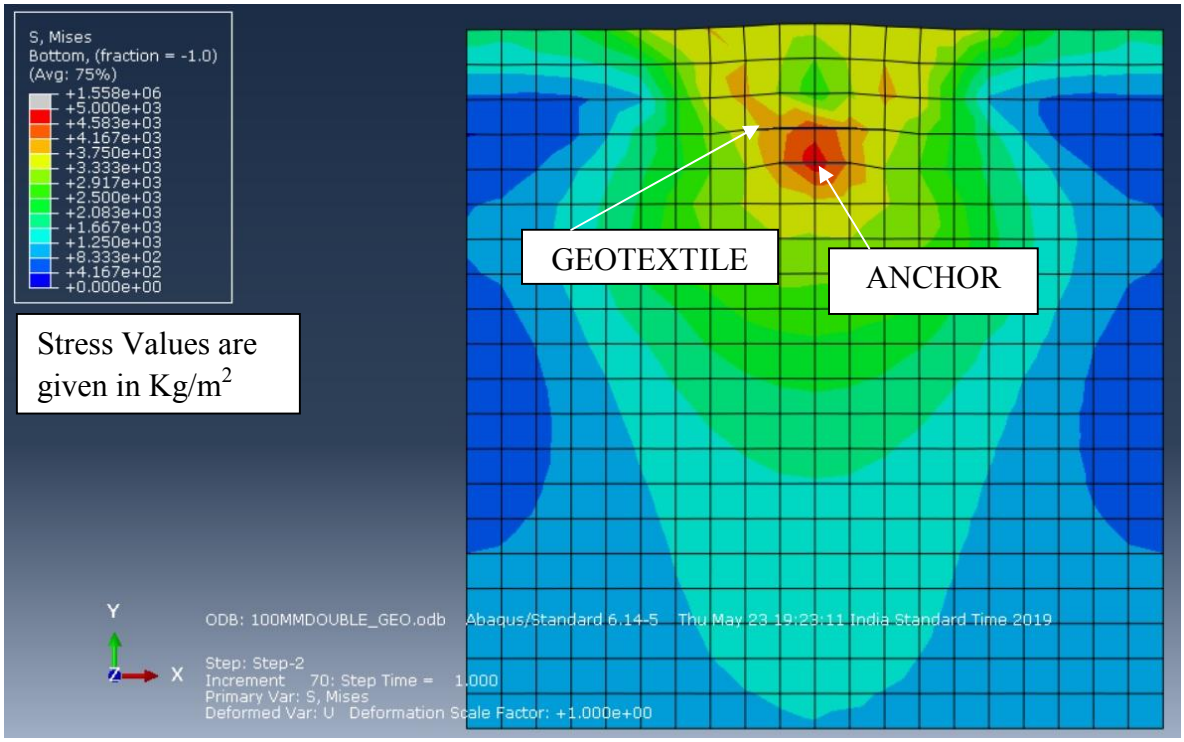

Fig 4.6(q): Stress Contour for 100 mm Square Anchor Plate with (H/B=2)(Reinforced)

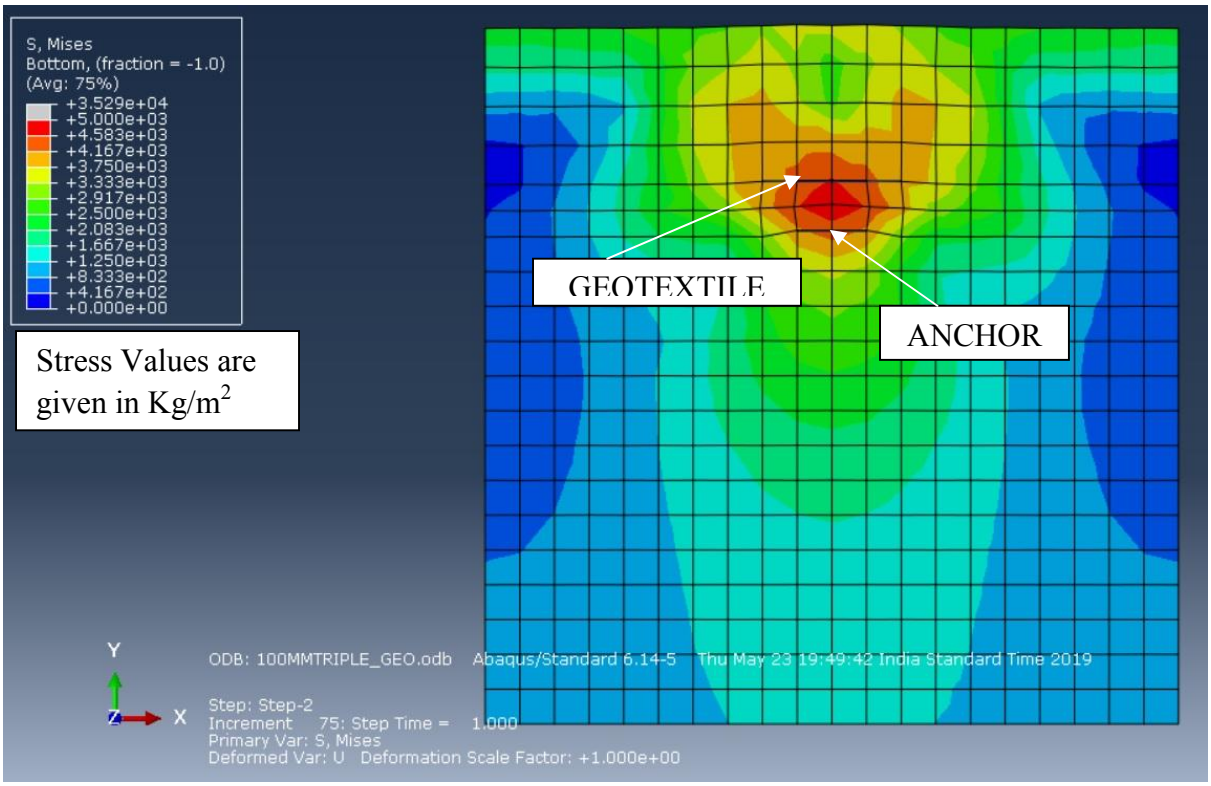

Fig 4.6(r): Stress Contour for 100 mm Square Anchor Plate with (H/B=3)(Reinforced)

Table 4.4: Numerical Analysis Results- Unreinforced & Reinforced

TYPE	TEST NAME	PULLOUT LOAD (KG)	DISP (mm)	WEIGHT OF SOIL(W)	BREAKOUT FACTOR (F-W)/(A*Cu)	EMBEDMENT RATIO
UNREINFOCED	50_UR_(H/B =1)	18	3	0.225	3.56	1
	50_UR_(H/B =2)	24	3	0.450	4.71	2
	50_UR_(H/B =3)	29	3	0.675	5.67	3
	75_UR_(H/B =1)	34	3.4	0.759	2.95	1
	75_UR_(H/B =2)	46	3.2	1.519	3.95	2
	75_UR_(H/B =3)	55	4.8	2.278	4.69	3
	100_UR_(H/B =1)	54	1.1	0.055	2.70	1
	100_UR_(H/B =2)	76	1.5	0.110	3.79	2
	100_UR_(H/B =3)	88	1.7	0.165	4.39	3
REINFORCED	50_RE_(H/B =1)	20	1.8	0.225	3.96	1
	50_RE_(H/B =2)	26	1.4	0.450	5.11	2
	50_RE_(H/B =3)	33	3	0.675	6.47	3
	75_RE_(H/B =1)	46	3.4	0.759	4.02	1
	75_RE_(H/B =2)	58	3	1.519	5.02	2
	75_RE_(H/B =3)	68	3.2	2.278	5.84	3
	100_UR_(H/B =1)	60	2	1.800	2.91	1
	100_UR_(H/B =2)	84	6	3.600	4.02	2
	100_UR_(H/B =3)	88	2	5.400	4.13	3

Chapter 5

DISCUSSION ON RESULTS

5.1 General

Preceding chapters, Chapter 3 and Chapter 4 describe the details of the experimental and numerical model of the plate anchor embedded in geotextile reinforced clay under different conditions. The responses of different sizes of anchors placed with different embedment ratios for unreinforced and reinforced conditions have been discussed in this chapter. For the reinforced conditions, the geosynthetic, having a width of four times the width of plate, is placed at a distance of 0.25 times the depth of embedment from the bottom of anchor plate and effect of inclusion of reinforcement on the load-displacement is obtained. There are several parameters considered in the analysis like embedment ratio of plate, position of reinforcement and size of plate. Response of plate anchors has been studied by monotonic loading up to a specified displacement, which is considered as 10% of the plate dimension.

5.2 Discussion on Results

Based on the results obtained from the experimental and numerical modeling, an attempt has been made to study the following aspects of behavior of the anchor plates under monotonic loading embedded in soft clay material with geosynthetic reinforcement.

a) The load-displacement behavior of the anchor plates in unreinforced and reinforced soil.
b) The influence of embedment ratio on the pull-out load in both the cases of unreinforced and reinforced conditions.
c) Effect of variation of plate size on pullout capacity of anchor in unreinforced and reinforced condition
d) Effect of reinforcement on the pull-out load.
e) Breakout factor in the form of Non-dimensional form of Pullout load

f) Stress Contours obtained from Numerical Analysis

5.2.1 Load - Displacement Behavior

The verification study of computed results has been done with the results obtained from the experimental studies of model test. Comparative analysis of the data obtained from experiment and numerical analysis shows excellent qualitative agreement and good quantitative agreement for all the cases, although for higher plate sizes the computed displacement corresponding to pullout load, goes on the higher side for experimental values, i.e in case of model test the displacement required to achieve the pullout load is more than the same required in numerical analysis. Similar difference in displacement was observed in the study of pullout capacity of circular plate anchors in sand by **Makarchian et al. (2012)**. The differences obtained in the computed results of pullout loads from both sets of investigation are exhibited in Table 5.1. Following observations have been made based on the comparative analyses carried out between load vs displacement plot obtained from both set of investigations (Ref: Chapter 3-Fig 3.12(a) to 3.12(i) and Chapter 4-Fig 4.5(a) to 4.5(l))

1) The data points obtained from all the model tests followed a polynomial trend, but the same is not true for numerical investigation. For the numerical case best fit curve through obtained data points are constructed for calculation of pullout load
2) In unreinforced case the value of pullout capacities obtained from numerical investigations overestimates that of model tests with maximum deviation of 28% for 50 mm plate with H/B =1.
3) For reinforced condition results obtained from numerical investigations underestimates the pullout capacity owing to the fact that material non-linearity for geotextile material was not considered in numerical modeling. For 50 mm plate with embedment ratio 1 the respective numerical results overestimates pullout capacity by 15% but for embedment ratio 2 and 3, numerical analysis underestimates pullout capacity by 13%.
4) The initial slope of load vs displacement plot decreases with the introduction of reinforcement for a certain plate size and embedment ratio, and the same holds true with increase in plate size and embedment ratio as can be observed from fig 5.1(a) and fig 5.1(b).
5) For higher plate sizes, load vs displacement plot obtained from numerical analyses showed steep rise at the end depicting plastic failure of the soil mass.

Table 5.1: Comparison of Pullout Load in Experiment and Numerical Analysis

TYPE	*PLATE SIZE (B)*	*EMBEDMENT RATIO (H/B)*	*PULLOUT LOAD(Kg)*		
			EXPERIMENT	*NUMERICAL*	*DEVIATION (%)*
UR	50 X 50	1	14	18	-28.57
		2	24	24	0.00
		3	29	29	0.00
UR	75 X 75	1	30	34	-13.33
		2	40	46	-15.00
	100 X 100	1	40	54	-35.00
RE	50 X 50	1	17.5	20	-15.29
		2	30	26	13.33
		3	38	33	13.16

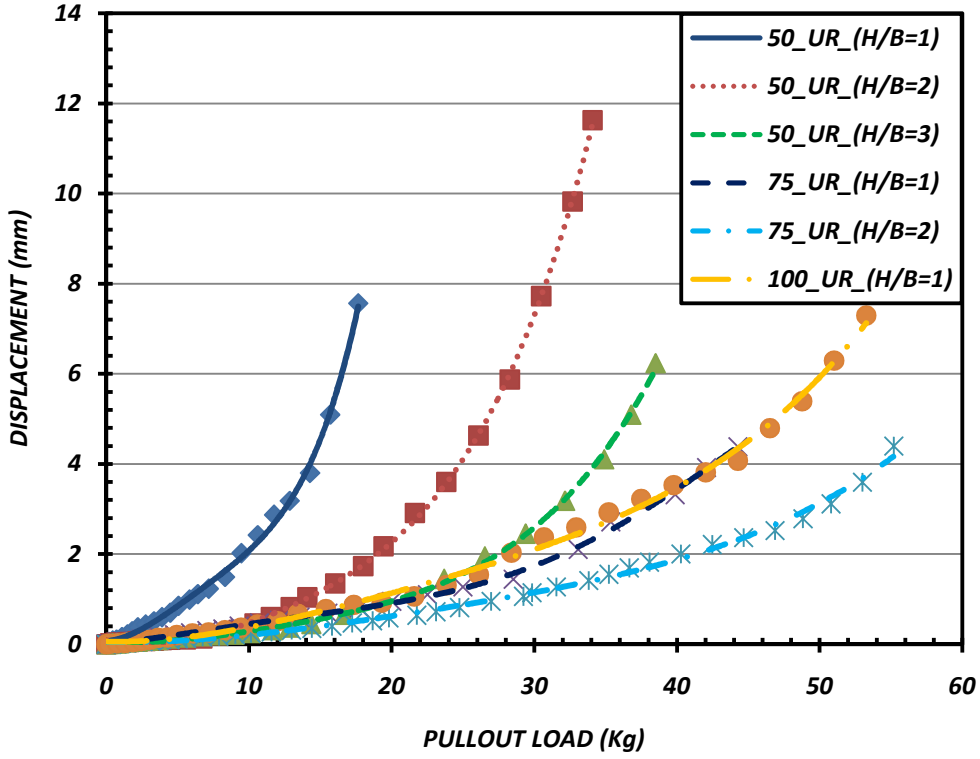

Fig 5.1(a): Comparative Study of Load vs Displacement plot from Model Tests (Unreinforced)

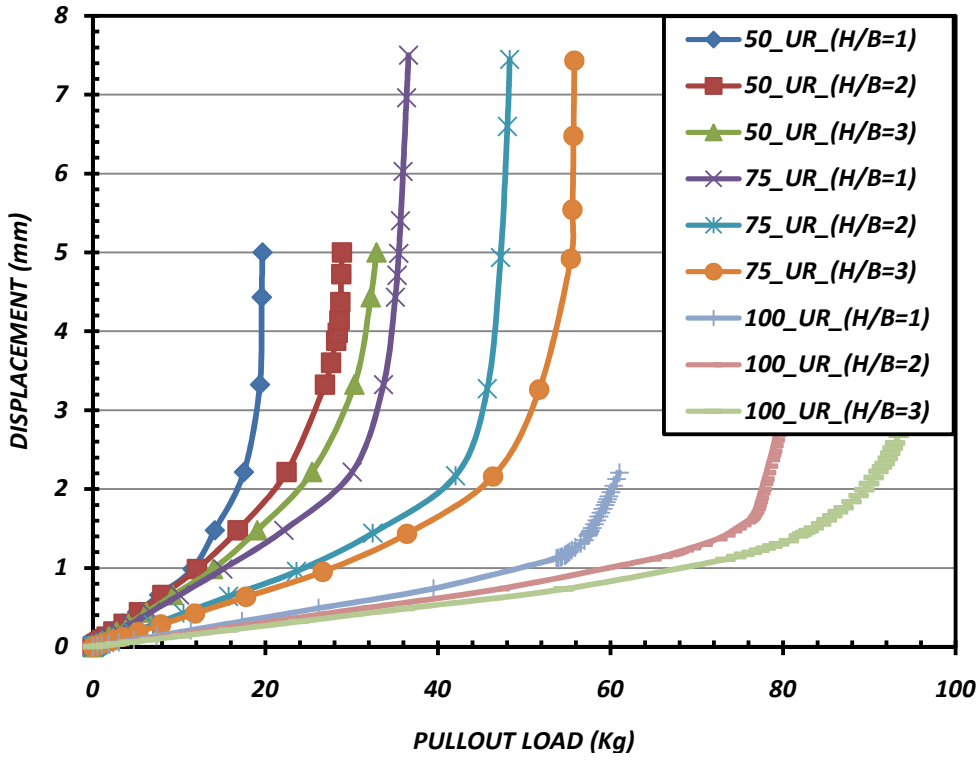

Fig 5.1(b): Comparative Study of Load vs Displacement plot from Numerical Analyses (Unreinfroced)

5.2.2 Effect of Embedment Ratio

The increase in pull out capacity due to increase in embedment ratio is matching well with the study by **Bhattachrjee et al. (2008)**. Even for the different sizes of plate anchor it holds good. In the unreinforced and reinforced conditions also the increase embedment ratio increases the pull out capacity.

Following observations are made from the results obtained for pullout capacity from numerical and experimental investigations

1) With increase in embedment ratio for any particular plate size, pullout capacity increases both in unreinforced and reinforced condition as shown in fig 5.2. This increase in capacity is accounted on the basis of larger volume of soil resisting the upward axial movement of anchor leading to increased value of ultimate pullout load.
2) Comparing results obtained from numerical analysis for 50^{mm} X 50^{mm} plate in unreinforced condition the increase in pullout capacity for H/B =2 is about 33% than that is obtained by H/B =1 and this increment is 61% for H/B =3 than H/B=1. Similar observations for 75 mm plate shows that the increase in pullout capacities for increase in embedment ratio from H/B =1 to H/B =2 and 3 are 47% and 66%

respectively. Thus for a given plate size pullout capacity increases with increase in embedment ratio as exhibited in Table 5.2.

This occurs due to the fact that with increase in plate size for a particular embedment ratio, both the weight of overburden as well as the friction surface area of the soil resisting the axial movement increases. This combined effect of increase in overburden and friction area accounts for the increase in increments of pullout capacity for higher embedment ratios and with increase in plate sizes.

Table 5.2: Comparison of Variation of Pullout Capacity with Embedment Ratio for different Plate Sizes (Numerical)

TYPE	PLATE SIZE	PULLOUT CAPACITY FOR DIFFERENT (H/B) in (Kg)			COMPARITIVE INCREMENT OF PULLOUT CAPACITY (%)	
		(i) (H/B=1)	(ii) (H/B=2)	(iii) (H/B=3)	[(ii)-(i)] /(i)	[(iii)-(i)] /(i)
UR	50 X 50	18	24	29	33.33	61.11
	75 X 75	42	62	70	47.62	66.67
	100 X 100	50	80	85	60.00	70.00
RE	50 X 50	20	26	33	30.00	65.00
	75 X 75	46	58	68	26	47.82
	100 X 100	60	84	88	40	46.67

5.2.3 Effect of Plate Size

Three square horizontal anchor plates of size 50 mm, 75 mm and 100 mm considered in the analysis. It is observed from fig 5.2 that as the plate size increases the pull out capacity also increases. The patterns are same for both unreinforced and reinforced soil. Comparative study of pullout capacity for same embedment depth and varying plate sizes yielded the following

1) Effect of plate size on pullout capacity can be observed by comparing pullout load for 50 mm square anchor plate with H/B = 3 and 75 mm square anchor plate with H/B = 2. This comparison shows that the pullout capacity obtained with 75 mm plate is about 213% of the pullout capacity obtained for 50 mm plate. This increase in pullout capacity for higher plate sizes having same depth of embedment may be accounted on the basis of increase in frictional surface area of soil.
2) . Effect of plate size on pullout capacity shows similar trend between numerical study and model test results. For similar depth of embedment with increase in plate size pullout capacity increased for experimental and numerical investigations.

Thus for a certain embedment depth with increase in plate size pullout capacity is observed to increases. This occurs due to the fact that with increase in plate size the volume of soil resisting axial movement of anchor also increases leading to higher pullout capacity.

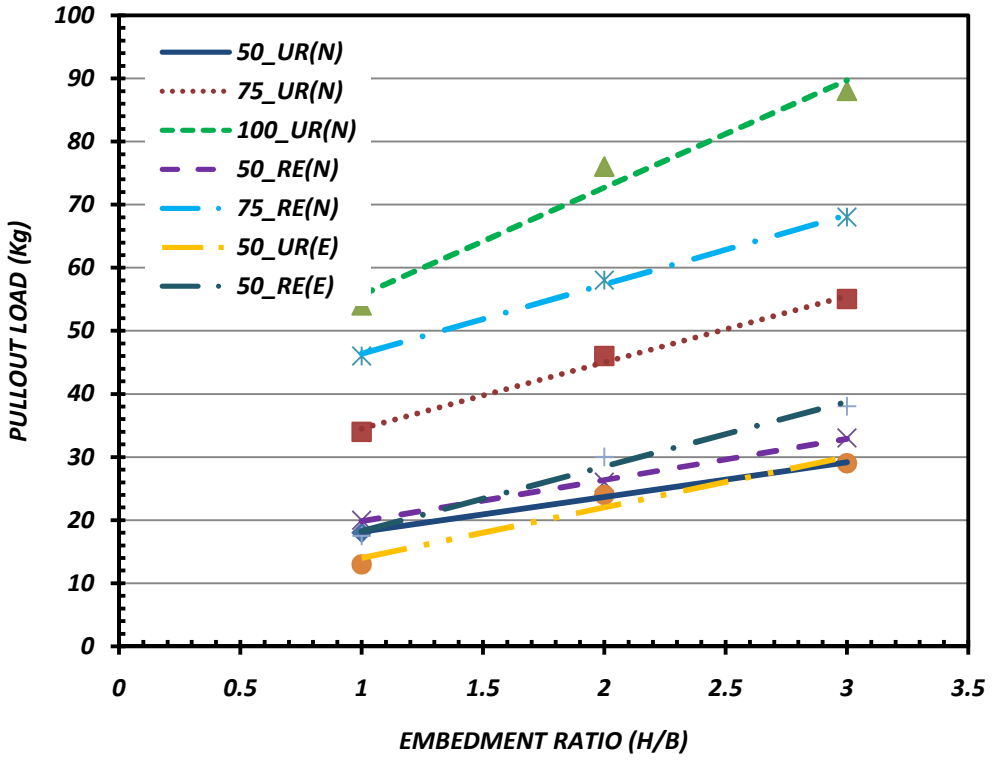

Fig 5.2: Comparative Study of Pullout Capacity with Embedment Ratio (E)-EXPERIMENT; (N)-NUMERICAL

5.2.4 Effect of Reinforcement

For the present investigation reinforcement in the form of geotextile of width four times the width of plate is used and placed at a position in a fixed ratio of 0.25 with embedment depth form the bottom of plate. The extent and position of geotextile is chosen based on the study conducted by **Bhattachrya et al. (2008)**, where they concluded that the above mentioned ratios would yield maximum increase in pullout capacity as discussed in Chapter 2 (Ref: page 18). Effect of reinforcement on pullout capacity is observed as follows:

1) The pull-out load is higher in reinforced soil compared to the unreinforced soil for all depths of embedment for a given position of reinforcement. It can be explained as the anchor is pulled out from the reinforced soil the additional frictional forces developed between the soil and geosynthetic reinforcement results in increase in pull-out capacity.

2) As discussed earlier that numerical analyses underestimates the pullout capacity owing to the fact that material non-linearity has not been considered for geotextile, the improvement ratio, defined as the ratio of pullout capacity in reinforced case to that of unreinforced case has been found to be on the higher side for experimental results.
3) It can be observed that model tests show 25 % increment of capacity in reinforced case for 50 mm plate with single embedment ratio (H/B=1), whereas the same has been reported to be 11 % from numerical investigation as furnished in Table 5.3 and 5.5.
4) For 75 mm plate, numerical analyses show 35% increase for H/B=1, and 26% and 23% for H/B =2 and 3 respectively.
5) The increment of pullout capacity obtained due to inclusion of geotextile increased with increase in plate size. As for the present investigation geotextile has been introduced with a fixed ratio with the width of plate and embedment depth; thus with increase in plate size the extent of geotextile increases. This leads to mobilization of shear strength along a greater zone around the anchor plate.

Table 5.3: Improvement in Pullout Capacity with Reinforcement (Numerical)

TEST NAME	PULLOUT (UR)(Kg)	PULLOUT (RE)(Kg)	IMPROVEMENT RATIO (P_{RE}/P_{UR})
50X50_RE_(H/B =1)	18	20	1.11
50X50_RE_(H/B =2)	24	26	1.08
50X50_RE_(H/B =3)	29	33	1.14
75X75_RE_(H/B =1)	34	46	1.35
75X75_RE_(H/B =2)	46	58	1.26
75X75_RE_(H/B =3)	55	68	1.23

Table 5.4: Improvement in Pullout Capacity with Reinforcement for 50 mm Plate (Experiment)

TEST NAME	PULLOUT (UR)(Kg)	PULLOUT (RE)(Kg)	IMPROVEMENT RATIO (P_{RE}/P_{UR})
50X50_(H/B =1)	14	17.5	1.25
50X50_(H/B =2)	22	30	1.36
50X50_(H/B =3)	29	38	1.31

5.2.5 Break Out Factor

The ultimate anchor pullout capacity for square plate anchors in clay is usually expressed as a function of the undrained shear strength as given by Das and Puri (1989) in the following form. $Q_u = A_p C_u F_c + W\text{Cos}\beta$ …… (5.1)

Where, F_c is the Breakout Factor, Q_u is the ultimate pullout load, A_p is area of anchor plate, W is the soil weight immediately above anchor plate and β is the inclination of anchor plate with the horizontal as described in fig. 2.2. Considering the above formulation the breakout factors for model anchors of different sizes embedded at different depths have been obtained from the obtained pullout loads for both reinforced and un-reinforced soil and the same has been tabulated in Table 5.5. Comparative analyses have been carried out with the results obtained from experimental and numerical investigation and the following points have been observed:

1) The trend of breakout factor obtained from experimental and numerical investigation follows good qualitative and quantitative agreement.
2) Breakout Factor has been observed to increase with embedment ratio for any particular plate size because for higher embedment ratios soil area resisting pullout increases leading to the increase in breakout factor. For 50 mm plate size the increase in breakout factor has been observed to be 70% when embedment ratio changed from 1 to 2, and the same was 105% for H/B =3.Similar observations for 75 mm plate has shown 33% and 59% increase in breakout factor for change of embedment ratio from 1 to 2 and 3 respectively.
3) It can also be observed from fig 5.3(a) and 5.3(b), for equal embedment ratio with increase in plate size breakout factor decreases. With increase in plate size the pullout capacity increases but this increase is less in proportion to the increase in area of plate. Thus with increase in plate size the increment in shear mobilization area is less than the increase of plate area, leading to decrease of breakout factor for higher plate sizes. For 150 mm depth of embedment with increase in plate size from 50 mm to 75 mm, breakout factor decreased by 40%.
4) Inclusion of geotextile as a reinforcing material increases the breakout factor by enhancing the pullout capacity. This increment is accounted on the basis of increase in volume of soil involved in resisting the axial movement due to the inclusion of

geotextile as seen in stress contour (Ref: Fig 3.6(j) to 3.6(l)). For 50 mm plate breakout factor has been found to increase in reinforced case than unreinforced case on an average by 25% for all embedment ratios.

5) After comparing breakout factor obtained from experimental and numerical investigations, maximum deviation has been obtained to be 29% for 50 mm plate with embedment ratio equal to 1 as shown in Table 5.5.

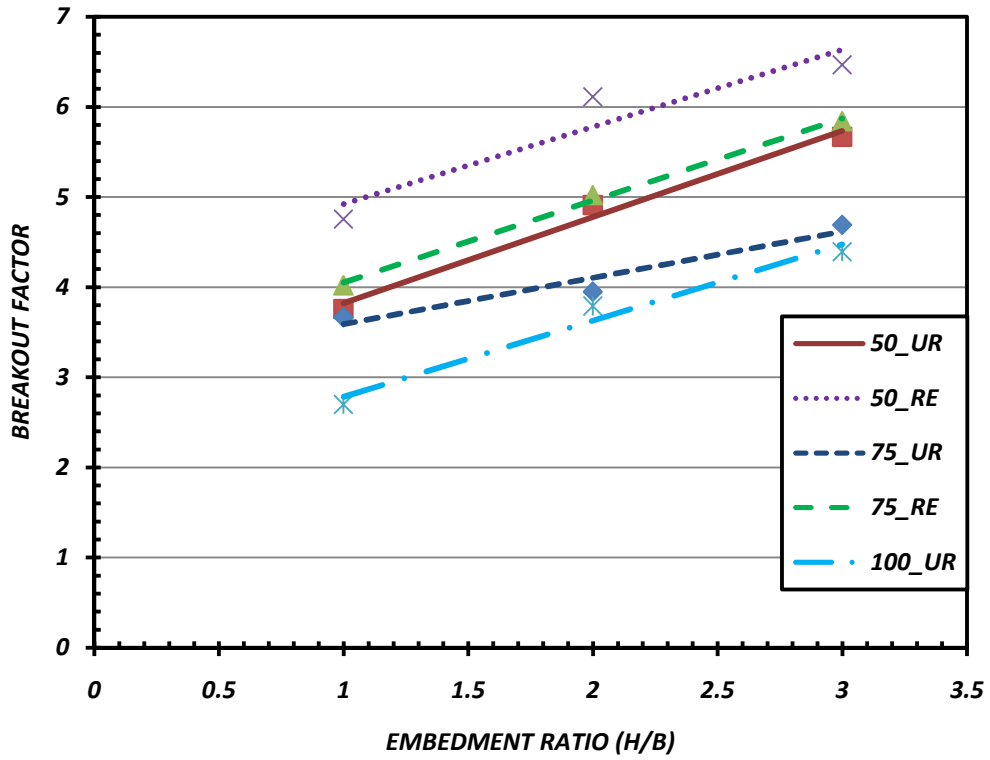

Fig 5.3(a): Breakout Factor vs Embedment Ratio (Numerical)

Table 5.5: Variation of Breakout Factor

TYPE	*PLATE SIZE (B)*	*EMBEDMENT RATIO (H/B)*	*BREAKOUT FACTOR*		
			EXPERIMENT	*NUMERICAL*	*DEVIATION (%)*
UR	50 X 50	1	2.76	3.56	28.9
		2	4.71	4.71	0
		3	5.67	5.67	0
UR	75 X 75	1	2.60	2.95	13.46
		2	3.42	3.95	15.5
	100 X 100	1	1.91	2.70	42.10
RE	50 X 50	1	3.46	3.96	14.45
		2	5.91	5.11	-13.53
		3	7.47	6.47	-13.38

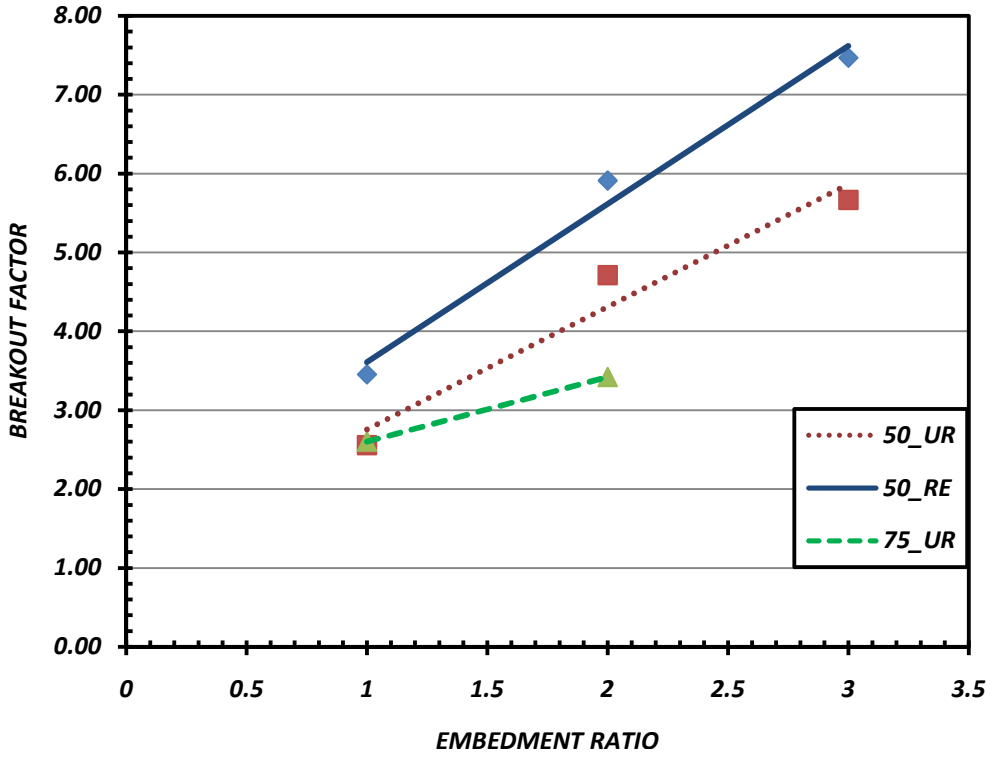

Fig 5.3(b): Breakout Factor vs Embedment Ratio (Experiemnt)

5.2.6 Stress Contour

Variation of stress contour obtained from numerical analysis is compared based on the following aspects a) Embedment ratio, b) Plate size, c) Reinforcement and d) Boundary effect

a) **Embedment Ratio:** Fig 4.6(a) to 4.6(l) presented in Chapter 4 shows that with increase in embedment depth for a certain plate size the maximum stressed zone doesn't reach up to the top surface, but for shallow embedment it may reach up to top surface. This happens due to the fact that for higher embedment ratios the soil around the anchor fails before the failure surface could reach to the top surface

b) **Plate Size:** Comparison of stress contour obtained for different plate sizes having same embedment depth exhibit higher maximum stressed zone for lower plate sizes. With increase in area of anchor plates the volume of soil resisting axial movement increases. Thus for higher plate sizes the maximum stress value obtained in soil mass decreases.

c) **Reinforcement:** With the inclusion of geotextile as a reinforcing material the maximum stress for a certain pullout is achieved in the reinforcement due to mobilization of tensile stress in geotextile. Further Stress contour indicate that with

bending of geotextile larger volume of soil gets associated in resisting the pullout load leading to increase in pullout capacity.

d) **Boundary Effect:** Stress contours obtained showed that the effect of boundary on pullout capacity will be negligible for all embedment ratios in cases of 50 mm and 75 mm plate with a 1.0 ^{m} X 1.0 ^{m} soil domain which provides the basis of choosing a foundation tank of plan dimension 1.0 ^{m} X 1.0 ^{m}. For the ongoing investigation maximum size of square plate considered is 100 mm with maximum embedment depth of 300 mm. Stress contour for 100 mm plate is shown in fig 4.6(j) to 4.6(l). It is observed that for 100 mm plate with embedment ratio 2 and 3, with a 1.0 ^{m} X 1.0 ^{m} domain the boundary effect influences the pullout capacity, although the same is not true for embedment ratio equal to 1 (Ref: fig 4.6(g) to 4.6(i)).

Chapter 6

SUMMARY,CONCLUSION & FUTURE SCOPE OF STUDY

6.1 General

The present study focuses to understand the behavior of square plate anchors in the reinforced soft clay. It was aimed to determine the pull-out capacity of the horizontal square anchor plates of sizes 50 mm, 75 mm, and 100 mm for different embedment ratios 1, 2 and 3, with and without geotextile under monotonic loading. Model anchor tests have been carried out to determine the effect of different aspects on pullout capacity of horizontal plate anchors. For reinforced condition geotextile, having a width of four times the width of plate, is placed at a position having a fixed ratio of 0.25 times the embedment depth from the bottom of anchor plate.

Numerical simulations have been carried out on same size square plates of 50 mm x 50 mm, 75 mm x 75 mm and 100 mm x 100 mm for same embedment ratios with and without geotextile, simulating the experimental condition.

6.2 Conclusions

The following conclusions may be drawn from the present study

1) The load vs Displacement behavior obtained from model tests and numerical investigations show excellent qualitative agreement and good quantitative agreement. Also the initial slope of the curve tends to decrease with increase in plate size and higher embedment ratio and with the inclusion of geosynthtics.
2) The pullout capacity of the anchor plates has been found to increase with increase in embedment ratio. For 50 mm square anchor plate the increase in pullout capacity has been found to be 33% when embedment ratio changed from 1 to 2, and the same has been found to be 61% when embedment ratio changed to 3. For 75 mm plate this

increase has been observed to be 47% and 66% when embedment ratio changed from 1 to 2 and 3 respectively.This increment of pullout capacity with higher embedment ratio was found to increase with increase in plate size.

3) The pullout capacity has been found to increase with increase in plate size. For 150 mm depth of embedmentthis increase was found to be 113% when the plate size changed from 50 mm to 75 mm.
4) Inclusion of geotextile as a reinforcing material increases pullout capacity for all plate sizes and embedment ratios. For 50 mm plate with embedment ratio equal to 1 the improvement has been found to be 25% and the same has been found to be 36% and 31% for embedment ratio 2 and 3 respectively. This improvement has been found to be higher for larger plate sizes.
5) Non-dimensional pullout capacity, expressed in the form of breakout factor has been found to increase in reinforced case than in unreinforced case and also for higher embedment ratios. But the same has been found to decrease with increase in plate size.
6) Stress contour obtained from numerical analyses supports all the above conclusions and show that the effect of boundary on pullout capacity is negligible for all embedment ratios of 50 mm and 75 mm plate with a 1.0^{m} X 1.0^{m} soil domain. It has also been observed that this domain is influenced by boundary effects for 100 mm plate with embedment ratio 2 and 3.

6.3 Future Scope of Further Study

Some recommendations for further research are made as follows:

1) The study may be extended for Circular and Strip anchors and also for anchor group.
2) Pullout capacity may be obtained for dynamic and seismic loading.
3) The Study may be extended for inclined anchors.

References

Balla, A. (1961). The resistance to breaking out of mushroom foundations for pylons. Proc. 5th Intl. Conf. on Soil Mechanics and Foundation Engineering, Paris, France: pp.569-576.

Bhattacharya, P., Debjit, B., Mukherjee, S.P., Chattopadhyay, B.C., (2008). Pullout Behaviour of Square Anchors in Reinforced Clay, *The 12th International Conference of International Association for Computer Methods and Advances in Geomechanics (IACMAG), Goa, India,* pp.3441-3447.

Bhattacharya, P., (2010). Pullout Behaviour of Anchor Plates in Soft Clay with Geosynthetic Reinforcement, *Ph.D Thesis, Jadhavpur University, Kolkata*, India.

Chattopadhyay, B.C. and Pise, P.J., (1986). Breakout resistance of horizontal anchors in sand, *Soils and Foundations, Japanese Society of Soil Mechanics and Foundation Engineering,* Volume 26, No.4, pp.16-22

Das, T. K., Chattopadhyay, B.C., Roy, S., (2013). Pull-out Capacity of Plate Anchors with Coaxial Geotextile Reinforcement, *Annals of Pure and Applied Mathematics,* Vol. 5, No.1, pp.53-63.

Das, B.M. (1978). Model tests for uplift capacity of foundations in clay. Soils and Foundations, 18(2): 17- 24.

Das, B. M. (1980). A procedure for estimation of ultimate uplift capacity of foundations in clay. Soils and Foundations, 20 (1): 77-82.

Das, B. M., Puri, V. K. (1989). Holding capacity of Inclined Square plate anchors in Clay, *Soils and Foundations, Japanese Society of Soil Mechanics and Foundation Engineering,* Volume 29, No.3, pp.138-144.

Ghaly. A, Hanna. A, Hanna. M, (1991), Uplift Behavior of Screw Anchors in Sand. I: Dry Sand, International Journal of Rock Mechanics & Mining Sciences & Geomechanics Abstracts 117(5).

Ilamparuthi, K., Dickin, E.A., Muthukrisnaiah, (2002).Experimental investigation of the uplift behaviour of circular plate anchors embedded in sand,*Canadian Geotechnical Journal* 39, pp.648-664.

Krishnaswamy, N.R. and Parashar, S.P., (1994). Uplift behavior of plate anchors with geosynthetics, *Geotextiles and Geomembranes* 13, pp.67-89.

Meyerhof, G.G (1973) and Adams, J.I.,(1968) " The ultimate uplift capacity of foundations,"Canadian Geotechnical Journal , vol 5, No.4, pp. 225-244.

Merifield, R.S., Sloan, S.W., Yu, H.S., (2001).Stability of plate anchors in undrained clay, *Geotechnique* 51, No.2, pp.141-153.

Merifield, R.S, Lyamin, A. V., Sloan, S.W., (2003), Three dimensional Lower Bound Solution for Stability of Plate Anchors in Clay, *Journal of Geotechnical & Geoenvironmental Engineering*, Volume 129, No.3, pp.243-253.

Makarchian, M., Gheitasi, M., Badkhasan, E.,(2012),Experimental & Numerical Study of Uplift Behavior of Anchorsembedded in Reinforced Sand, *5th Asian Regional Conference on Geosynthetics, Geosynthetics Asia*.

Mistri, B. and Singh, B., (2011). PulloutBehavior of Plate Anchors in Cohesive Soils, *Bund.K,EJGE*, Volume 16, pp.1173-1184

Nene, A.S., and Garg. S. (1991), 'Behaviour of shallow plate anchors in reinforced cohesive soils', Indian Geotechnical Journal, vol.21, No.4, pp.327-336.

Ravichandran, P. T. and Ilamparuthi, K. (2004). Behavior of rectangular plate anchors in reinforced and unreinforced sand beds. Proc. ICCGE Mumbai: 123-128.

Randolph, M. F., Wang, D.,Zohu, H., Hossain, M. S., and Hu, Y.,(2008), *Large deformation finite element analysis for offshore applications* , proc., 12th International Conference of the International Association for Computer methods and advances in geomechanics, Goa, India, pp. 3307-3318.

Ravichandran, P.T., Mohammed, T.M., Ilamparuthi K., (2008). Study on Uplift Behaviour of Plate Anchors under Monotonic and Cyclic Loading in Geo-grid Reinforced Sand Bed, *The 12th International Conference of International Association for Computer Methods and Advances in Geomechanics (IACMAG),Goa, India,* pp.3448-3455.

Rowe, R.K. and Davis, E.H., (1982).The behaviour of anchor plates in sand", *Geotechnique* 32, No.1, pp.25- 41.

Rowe, R.K. and Davis, E.H., (1982). The behaviour of anchor plates in clay, *Geotechnique* 32, No.1, pp.9-23.

Saran, S., Ranjan, G. and Nene, A. S. (1986): Soil anchors and constitutive laws. Journal of Geotechnical Engineering, 112(12), pp. 1084-1100.

Subbarao, C., Mukhopadhyay, S., and Sinha, J., (1988), "Geotextile ties to improve uplift resistance of anchors." Proc. of the first Indian Geotextile Conference on Reinforced soil and Geotextiles, Bombay, India, F3-F8.

Tagaya, K., Scott, R. F., and Aboshi, H., 1988, "Pull-out Resistance of Buried Anchors in Sand," Soils and Foundations Vol. 28, No. 3, pp. 114–130.

Thorne, C. P., Wang, C. X., Carter, J. P.,(2004), *Uplift Capacity of rapidly loaded strip anchors in uniform strength clay*, *Geotechnique* Volume 54, Issue 8, pp. 507-517.

Yu, L., Zhou, Q., Liu, L., (2015). Experimental study on the stability of plate anchors in clay under cyclic loading, *Theoretical and applied Mechanics, China*, Letter 5, pp.93-96